



Title	STUDIES ON NOVEL TRANSITION METAL COMPLEXES WITH N-HETEROCYCLIC MULTIDENTATE LIGANDS FOR EFFICIENT REDOX SYSTEMS
Author(s)	森内, 敏之
Citation	大阪大学, 1995, 博士論文
Version Type	VoR
URL	https://doi.org/10.11501/3106807
rights	
Note	

The University of Osaka Institutional Knowledge Archive : OUKA

<https://ir.library.osaka-u.ac.jp/>

The University of Osaka

**STUDIES ON NOVEL TRANSITION METAL COMPLEXES
WITH *N*-HETEROCYCLIC MULTIDENTATE LIGANDS
FOR EFFICIENT REDOX SYSTEMS**

TOSHIYUKI MORIUCHI

Department of Applied Chemistry
Faculty of Engineering
Osaka University

1995

**STUDIES ON NOVEL TRANSITION METAL COMPLEXES
WITH N-HETEROCYCLIC MULTIDENTATE LIGANDS
FOR EFFICIENT REDOX SYSTEMS**

（ 効率的なレドックス系を指向した
含窒素複素環系多座配位子からなる新規遷移金属錯体に関する研究 ）

TOSHIYUKI MORIUCHI

Department of Applied Chemistry
Faculty of Engineering
Osaka University

1995

Preface

The work presented in this thesis has been carried out under the guidance of Professor Isao Ikeda at Osaka University during 1993-1995 and Professor Yoshiki Ohshiro at Osaka University during 1991-1992.

The object of this thesis is to construct a synthetically versatile catalytic system consisting of transition metal complexes with multidentate *N*-heterocyclic podand ligands, and to investigate the complexation behavior of multidentate *N*-heterocyclic ligand with the redox center. The author hopes that this basic work described in this thesis contributes to the further development of the efficient catalytic system consisting of transition metal complexes.



Toshiyuki Moriuchi

Department of Applied Chemistry
Faculty of Engineering
Osaka University
Yamada-oka, Suita,
Osaka 565,
Japan

June, 1995

Contents

General Introduction	---	1
Chapter 1	Catalytic Oxygenation with Molecular Oxygen Catalyzed by Transition Metal Complex with Multidentate <i>N</i>-Heterocyclic Podand Ligand	 --- 8
Chapter 2	Complexation Behavior of Quinone Ligands Bearing <i>N</i>-Heterocyclic Coordination Sites	 --- 34
Chapter 3	Complexation Behavior of Ferrocene Ligands Bearing <i>N</i>-Heterocyclic Coordination Sites	 --- 66
Conclusion	---	97
List of Publications	---	99
Acknowledgement	---	101

General Introduction

A smooth redox process is one of the essential factors necessary to develop new systems for materials and catalytic redox reactions. Redox system based on reversible redox of transition metal complexes has been developed in this respect. Since ligand coordination greatly contributes to redox process, the ligand design is essential in the construction of a versatile catalytic system.

Catalytic oxygenation based on redox of transition metal complexes is of importance from synthetic and biological viewpoints. A variety of catalysts¹ and complex models² for cytochrome P-450 and other metalloenzymes including porphyrin, Schiff base, and polycyclic amine complexes have been investigated to elucidate the oxygenation mechanism and to develop an efficient system.³ Oxygen source for shunt path is hydrogen peroxide, *t*-butyl hydroperoxide, iodosylbenzene, sodium hypochlorite, and so on depending on the system. Our system for oxygenation has been addressed by the design of ligands; the coordination interaction between $\text{Mn}(\text{OAc})_2$ or $\text{VO}(\text{OEt})\text{Cl}_2$ and the *N*-heterocyclic multidentate podand ligand, *N,N'*-bis[2-(4-imidazolyl)ethyl]-2,6-pyridinedicarboxamide (BIPA), is revealed to play an important role in the oxygenation reactions of styrenes with iodosylbenzene or molecular oxygen in the presence of a co-reductant.⁴ The requisite complex is considered to be formed for the efficient epoxidation. Imidazoles are proven to serve as an axial *N*-ligand to increase the activity of porphyrin complex catalysts.^{2a, j} Effect of various additives has been intensely studied to attain the more efficient oxygenation. The rate acceleration is observed in the presence of lipophilic carboxylic acids and lipophilic

heterocyclic bases,^{3d} or aldehyde.^{3b} We have also demonstrated that *o*-quinones mediate the Mn(III)TPPCl-catalyzed epoxidation reaction with hydrogen peroxide.⁵ Monooxygenase model reactions with molecular oxygen are achieved by reductive activation with an electron donor.^{1, 2c} Only few systems without the need for a co-reductant have been reported in hydroxylation⁶ or epoxidation.⁷ From synthetic viewpoints, such an epoxidation reaction has quite recently been reported to be promoted by addition of excess amounts of cyclic ketones⁸ or methyl-2-oxocyclopentane carboxylate.⁹

Tyrosinase is a typical monooxygenase. A variety of tyrosinase models have been investigated so far to address its mechanism¹⁰ and a more efficient oxygenation system.¹¹ Since chelate Co(II) complexes are known to catalyze the oxygenation of phenols to *p*-benzoquinone, extensive studies have been focused on the complexes of Schiff bases,¹² porphyrines,¹³ and so on.¹⁴ However, these catalysts are not always synthetically useful partly due to the stability of these ligands. Construction of a more synthetically versatile oxygenation system consisting of transition metal and ligand is desired.

The quinone functional group is able to construct an efficient system including the possible preparation of switching materials.¹⁵ A variety of models consisting of porphyrin complexes and quinones have been investigated for electron transfer in photosynthesis.¹⁶ The redox interaction of quinones is performed using low valent transition metals.¹⁷ Its efficiency contributes to a catalytic system with synthetic potential.¹⁸ If ligands form a reversible redox cycle, the redox interaction between ligands and transition metals is envisaged to raise the catalytic efficiency. In a previous paper,¹⁹ the trimethyl ester of coenzyme PQQ has been revealed to serve as a ligand forming a reversible redox cycle under oxygen atmosphere in the palladium-catalyzed oxidation of an olefin and

α,β -epoxysilane. Further development of this concept is considered to require an investigation of the transition metal complexes with quinone ligands.

The molecular recognition of particular molecules²⁰ or ions²¹ by organometallic ligands containing one or more metallocene units has been an area of great interest in both organic and inorganic chemistry. Ferrocene receptors are envisaged to construct a specific molecular recognition site, since ferrocene has an easily reversible redox couple and the two coplanar cyclopentadienyl rings of ferrocene which can rotate with respect to each other. Extensive studies have been focused on ferrocene receptors so far.^{20, 21} Transition metal complexes with ferrocene ligands are expected to construct an efficient redox system. Investigation of complexation behavior of ferrocene ligands is required for construction of efficient system.

The redox interaction between ligands and transition metals is considered to play an important role in a smooth redox process. Since ligand coordination greatly contributes to redox process, the ligand design is essential in the construction of a versatile redox system. Flexible ligands permit us to construct the more efficient catalytic system rather than the rigid ligand such as porphyrin. Such a system is considered to be formed by use of multidentate ligands. The ligand should be stable under the redox reaction conditions. So *N*-heterocyclic multidentate ligands could be a candidate from these points of view. If the ligands possess a redox moiety, the redox interaction between transition metal and ligand contributes to the more smooth electron transfer. The interaction has not been investigated so far although it is expected to expand the catalytic system in oxidation reactions. We investigated the character of the multidentate *N*-heterocyclic podand ligand.

In Chapter 1, the catalytic oxygenation with molecular oxygen catalyzed by transition metal complex of multidentate *N*-heterocyclic podand ligand is described. In Chapter 2, the complexation behavior of quinone ligands bearing *N*-heterocyclic coordination sites are stated. Chapter 3 deals with the complexation behavior of ferrocene ligands bearing *N*-heterocyclic coordination sites.

References

1. (a) Yamada, T.; Takai, T.; Rhode, O.; Mukaiyama, T. *Bull. Chem. Soc. Jpn.* **1991**, *64*, 2109. (b) Takai, T.; Hata, E.; Yamada, T.; Mukaiyama, T. *Bull. Chem. Soc. Jpn.* **1991**, *64*, 2513. (c) Yamada, T.; Imagawa, K.; Nagata, T.; Mukaiyama, T. *Chem. Lett.* **1992**, 2231.
2. (a) Groves, J. T.; Nemo, T. E.; Myers, R. S. *J. Am. Chem. Soc.* **1979**, *101*, 1032. (b) Mansuy, D.; Bartoli, J. F.; Chottard, J. C.; Lange, M. *Angew. Chem., Int. Ed. Eng.* **1980**, *19*, 909. (c) Tabushi, I.; Yazaki, A. *J. Am. Chem. Soc.* **1981**, *103*, 7371. (d) Collman, J. P.; Brauman, J. I.; Meunier, B.; Hayashi, T.; Kodadek, T.; Raybuck, S. A. *J. Am. Chem. Soc.* **1985**, *107*, 2000. (e) Meunier, B. *Bull. Soc. Chim. Fr.* **1986**, 578. (f) Hecht, S. M. *Acc. Chem. Res.* **1986**, *19*, 383. (g) Stubbe, J.; Kozarich, J. W. *Chem. Rev.* **1987**, *87*, 1107. (h) Koola, J. D.; Kochi, J. K. *Inorg. Chem.* **1987**, *26*, 908. (i) Kinneary, J. F.; Albert, J. S.; Burrows, C. J. *J. Am. Chem. Soc.* **1988**, *110*, 6124. (j) Battioni, P.; Renaud, J. P.; Bartoli, J. F.; Reina-Artiles, M.; Fort, M.; Mansuy, D. *J. Am. Chem. Soc.* **1988**, *110*, 8462. (k) Nam, W.; Ho, R.; Valentine, J. S. *J. Am. Chem. Soc.* **1991**, *113*, 7052.
3. (a) "Metal-Catalyzed Oxidations of Organic Compounds," ed by Sheldon, R. A.; Kochi, J. K. Academic Press, New York (1981). (b)

- van der Made, A. W.; van Gerwen, M. J. P.; Drenth, W.; Nolte, R. J. *M. J. Chem. Soc., Chem. Commun.* **1987**, 888. (c) Kaku, Y.; Otsuka, M.; Ohno, M. *Chem. Lett.* **1989**, 611. (d) Banfi, S.; Maiocchi, A.; Moggi, A.; Montanari, F.; Quici, S. *J. Chem. Soc., Chem. Commun.* **1990**, 1794. (e) Yoon, H.; Wagler, T. R.; O'Connor, K. J.; Burrows, C. *J. J. Am. Chem. Soc.* **1990**, *112*, 4568.
4. Hirao, T.; Mikami, S.; Ohshiro, Y. *Synlett* **1990**, 541.
 5. Hirao, T.; Ohno, M.; Ohshiro, Y. *Tetrahedron Lett.* **1990**, *31*, 6039.
 6. (a) Ellis, Jr., P. E.; Lyons, J. E. *J. Chem. Soc., Chem. Commun.* **1989**, 1189, 1315. (b) Maldotti, A.; Bartocci, C.; Amadelli, R.; Polo, E.; Battioni, P.; Mansuy, D. *J. Chem. Soc., Chem. Commun.* **1991**, 1487.
 7. (a) Groves, J. T.; Quinn, R. *J. Am. Chem. Soc.* **1985**, *107* 5790. (b) Weber, L.; Haufe, G.; Rehorek, D.; Hennig, H. *J. Chem. Soc., Chem. Commun.* **1991**, 502.
 8. Takai, T.; Hata, E.; Yoroze, K.; Mukaiyama, T. *Chem. Lett.* **1992**, 2077.
 9. Punniyamurthy, T.; Bhatia, B.; Iqbal, J. *Tetrahedron Lett.* **1993**, *34*, 4657.
 10. (a) Capdevielle, P.; Maumy, M. *Tetrahedron Lett.* **1982**, *23*, 1573; **1983**, *24*, 5611. (b) Tyeklar, Z.; Karlin, K. D. *Acc. Chem. Res.* **1989**, *22*, 241. (c) Kitajima, N.; Fujisawa, K.; Moro-oka, Y. *J. Am. Chem. Soc.* **1989**, *111*, 8975. (d) Kitajima, N.; Koda, T.; Iwata, Y.; Moro-oka, Y. *J. Am. Chem. Soc.* **1990**, *112*, 8833. (e) Nasir, M. S.; Cohen, B. I.; Karlin, K. D. *J. Am. Chem. Soc.* **1992**, *114* 2482. (f) Casella, L.; Carugo, O.; Gullotti, M.; Garofani, S.; Zanello, P. *Inorg. Chem.* **1993**, *32*, 2056.
 11. (a) Réglér, M.; Jorand, C.; Waegell, B. *J. Chem. Soc., Chem. Commun.* **1990**, 1752. (b) Casella, L.; Gullotti, M.; Radaelli, R.; Di Gennaro, P. *J. Chem. Soc., Chem. Commun.* **1991**, 1611. (c) Rockcliffe, D. A.; Martell, A. E. *Inorg. Chem.* **1993**, *32*, 3143.

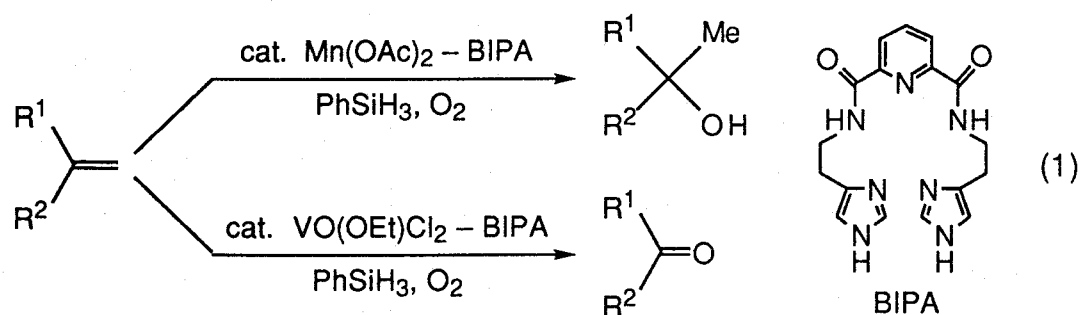
12. (a) Mckillop, A.; Ray, S. J. *Synthesis* **1977**, 847. (b) Nishinaga, A. In "Fundamental Research in Homogeneous Catalysis," ed by Ishii, Y.; Tsutsui, M. Plenum Press, New York (1978). (c) Nishinaga, A.; Tomita, H. *J. Mol. Catal.* **1980**, 7, 179. (d) Nishinaga, A.; Tomita, H.; Nishikawa, K.; Matsuura, T.; Ooi, S.; Hirotsu, K. *J. Chem. Soc., Dalton Trans.* **1981**, 1504. (e) Zombeck, A.; Drago, R. S.; Corden, B. B.; Gaul, J. H. *J. Am. Chem. Soc.*, **1981**, 103, 7580. (f) Corden, B. B.; Drago, R. S.; Perito, R. P. *J. Am. Chem. Soc.* **1985**, 107, 2903. (g) Yamada, M.; Araki, K.; Shiraishi, S. *J. Chem. Soc., Chem. Commun.* **1988**, 530; **1990**, 2687. (h) Ganeshpure, P. A.; Sudalai, A.; Sataish, S. *Tetrahedron Lett.* **1989**, 30, 5929.
13. (a) Wang, X.; Motekaitis, R. J.; Martell, A. E. *Inorg. Chem.* **1984**, 23, 271. (b) Frostin-Rio, M.; Pujol, D.; Bied-Charreton, C.; Perrée-Fauvet, M.; Gaudemer, A. *J. Chem. Soc., Perkin Trans. 1*, **1984**, 1971.
14. (a) Tada, M.; Katsu, T. *Bull. Chem. Soc. Jpn.* **1972**, 45, 2558 and references cited therein. (b) Bedell, S. A.; Martell, A. E. *Inorg. Chem.* **1983**, 22, 364; *J. Am. Chem. Soc.* **1985**, 107, 7909.
15. (a) Malkin, J.; Zelichenok, A.; Krongauz, V.; Dvornikov, A. S.; Rentzepis, P. M. *J. Am. Chem. Soc.* **1994**, 116, 1101. (b) DelMedico, A.; Auburn, P. R.; Dodsworth, E. S.; Lever, A. B. P.; Pietro, W. J. *Inorg. Chem.* **1994**, 33, 1583.
16. (a) Dalton, J.; Milgrom, L. R. *J. Chem. Soc., Chem. Commun.* **1979**, 609. (b) Nishitani, S.; Kurata, N.; Sakata, Y.; Misumi, S.; Migita, M.; Okada, T.; Mataga, N. *Tetrahedron Lett.* **1981**, 22, 2099. (c) Bergkamp, M. A.; Dalton, J.; Netzel, T. L. *J. Am. Chem. Soc.* **1982**, 104, 253. (d) Weiser, J.; Staab, H. A. *Angew. Chem., Int. Ed. Engl.* **1984**, 23, 623. (e) Staab, H. A.; Feurer, A.; Hauck, R. *Angew. Chem., Int. Ed. Engl.* **1994**, 33, 2428.

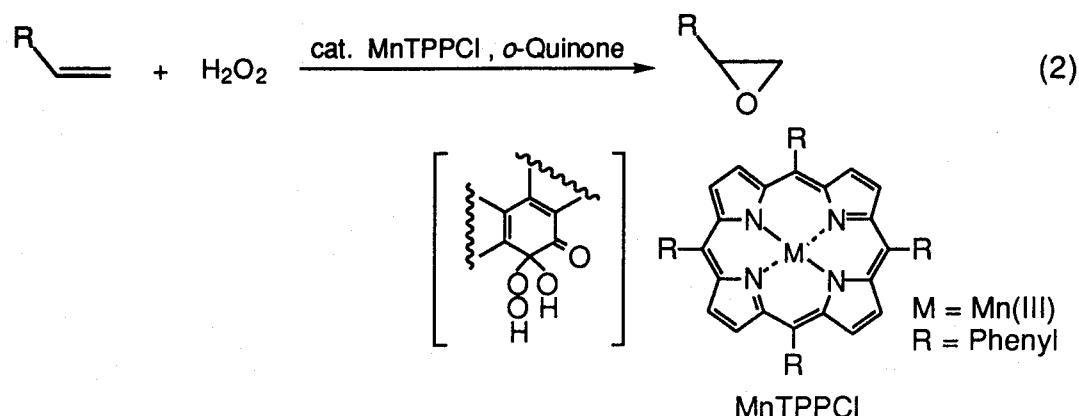
17. (a) Durfee, W. S.; Pierpont, C. G. *Inorg. Chem.* **1993**, *32*, 493. (b) Hilt, G.; Steckhan, E. *J. Chem. Soc., Chem. Commun.* **1993**, 1706. (c) Bäckvall, J. E.; Hopkins, R. B.; Grennberg, H.; Mader, M. M.; Awasthi, A. K. *J. Am. Chem. Soc.* **1990**, *112*, 5160.
18. Fox, G. A.; Pierpont, C. G. *J. Chem. Soc., Chem. Commun.* **1988**, 806.
19. Hirao, T.; Murakami, T.; Ohno, M.; Ohshiro, Y. *Chem. Lett.* **1989**, 785; **1991**, 299.
20. (a) J. C. Medina, C. Li, S. G. Bott, J. L. Atwood, and G. W. Gokel, *J. Am. Chem. Soc.* **113**, 366 (1991). (b) P. D. Beer, Z. Chen, A. J. Goulden, A. Graydon, S. E. Stokes, and T. Wear, *J. Chem. Soc., Chem. Commun.* **1993**, 1834.
21. (a) Beer, P. D.; *Chem. Rev.* **1989**, *18*, 409. (b) Butler, I. R.; *Organometallics* **1992**, *11*, 74. (c) Medina, J. C.; Goodnow, T. T.; Rojas, M. T.; Atwood, J. L.; Lynn, B. C.; Kaifer, A. E.; Gokel, G. W. *J. Am. Chem. Soc.* **1992**, *114*, 10583. (d) Beer, P. D.; Chen, Z.; Drew, M. G. B.; Kingston, J.; Ogden, M.; Spencer, P. *J. Chem. Soc., Chem. Commun.* **1993**, 1046. (e) Yamamoto, Y.; Tanase, T.; Mori, I.; Nakamura, Y. *J. Chem. Soc., Dalton Trans.* **1994**, 3191.

Chapter 1. Catalytic Oxygenation with Molecular Oxygen Catalyzed by Transition Metal Complex with Multidentate *N*-Heterocyclic Podand Ligand

1-1. Introduction

Smooth electron transfer based on reversible redox of transition metal complexes is required for efficient catalytic cycle. Since ligand coordination greatly contributes to redox process, the ligand design is essential for construction of a versatile catalytic system. Our system for oxygenation has been addressed by the design of multidentate flexible ligands; the coordination interaction between $\text{Mn}(\text{OAc})_2$ or $\text{VO}(\text{OEt})\text{Cl}_2$ and the *N*-heterocyclic podand ligand, *N,N'*-bis(2-(4-imidazolyl)ethyl)-2,6-pyridinedicarboxamide (BIPA), is revealed to play an important role in the oxygenation reactions of styrens with iodosylbenzene or molecular oxygen in the presence of a co-reductant (eq. 1).¹ The requisite complex catalyst is considered to be formed for the efficient epoxidation. We have also demonstrated that *o*-quinones mediate the $\text{Mn}(\text{III})\text{TPPCl}$ -catalyzed epoxidation reaction with hydrogen peroxide (eq. 2).²





Monooxygenase model reactions with molecular oxygen are achieved by reductive activation with an electron donor.³ Only few systems without need for a co-reductant have been reported in hydroxylation⁴ or epoxidation.⁵ This chapter describes a catalytic oxygenation with molecular oxygen catalyzed by the transition metal complexes of the multidentate *N*-heterocyclic podand ligand.

1-2. Results and Discussion

1-2-1. Oxygenation of Olefins

Treatment of 2-norbornene (**1**) with a catalytic amount of FeCl_2 and BIPA in DMF under molecular oxygen (1.0×10^3 kPa) led to the stereoselective formation of *exo*-2,3-epoxynorbornane (**2**, eq. 3). The *endo*-isomer was not detected by ^1H -NMR analysis. Catalyst turnover was more than 20 under the conditions employed here although not optimized. The results including other catalysts are listed in Table 1.

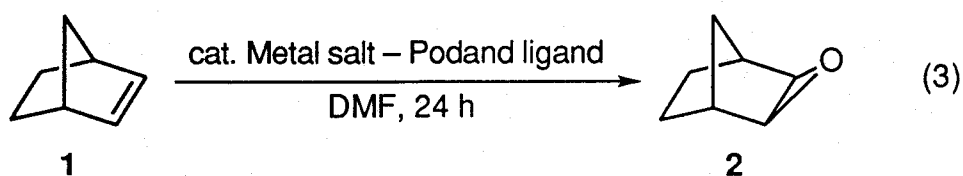
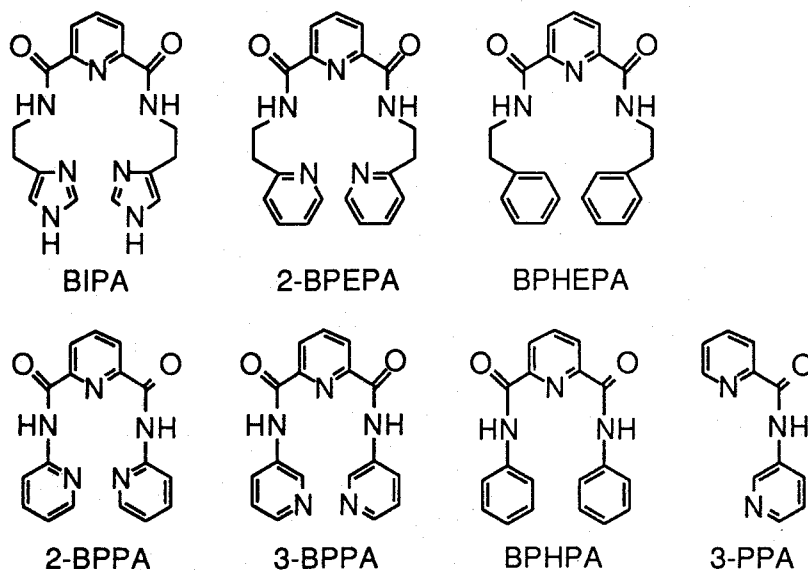


Table 1. Catalytic Epoxidation of 2-Norbornene ^a

Ligand	Metal salt	Temp. (°C)	Atmosphere (10 ³ kPa)	Turnover ^b
BIPA	FeCl ₂	70	O ₂ (1.0)	22
—	FeCl ₂	70	O ₂ (1.0)	4
BIPA	FeCl ₂	70	O ₂ (0.1)	trace
BIPA	FeCl ₂	70	Ar (1.0)	no reaction
BIPA	FeCl ₂	70	Air (1.0)	trace
BIPA	FeCl ₂	rt	O ₂ (1.0)	1
2-BPEPA	FeCl ₂	70	O ₂ (1.0)	17
BPHEPA	FeCl ₂	70	O ₂ (1.0)	5
2-BPPA	FeCl ₂	70	O ₂ (1.0)	17
3-BPPA	FeCl ₂	70	O ₂ (1.0)	18
BPHPA	FeCl ₂	70	O ₂ (1.0)	2
3-PPA	FeCl ₂	70	O ₂ (1.0)	13
BIPA	FeCl ₃	70	O ₂ (1.0)	6
—	FeCl ₃	70	O ₂ (1.0)	2
BIPA	Co(OAc) ₂	70	O ₂ (1.0)	24
—	Co(OAc) ₂	70	O ₂ (1.0)	4
BIPA	CoCl ₂	70	O ₂ (1.0)	13
—	CoCl ₂	70	O ₂ (1.0)	3
BIPA	CrCl ₂	70	O ₂ (1.0)	11
—	CrCl ₂	70	O ₂ (1.0)	5
BIPA	RhCl ₃	70	O ₂ (1.0)	6
BIPA	RuCl ₃	70	O ₂ (1.0)	4
BIPA	Ni(OAc) ₂	70	O ₂ (1.0)	1
BIPA	Mn(OAc) ₂	70	O ₂ (1.0)	trace
BIPA	Cu(OAc) ₂	70	O ₂ (1.0)	trace

^a Metal salt, 0.02 mmol; ligand, 0.02 mmol; 1, 2.0 mmol.^b Turnover was determined by GLC based on a catalyst.

The involvement of BIPA as a ligand is essential for the efficient epoxidation. The reaction under air (1.0×10^3 kPa) or atmospheric molecular oxygen gave only a trace amount of **2**. No oxidized product was obtained under argon and consumption of molecular oxygen was almost in accord with the amount of epoxide, suggesting the incorporation of molecular oxygen to **2**. On the basis of these observations, other podand ligands derived from 2,6-pyridinedicarboxylic acid were examined. With the podand ligand, 2-BPEPA, bearing 2-pyridyl group instead of 4-imidazolyl one the FeCl_2 -catalyzed epoxidation reaction of **1** was also performed although the yield was decreased a little. On the contrary, BPHEPA with the phenyl group was no more efficient ligand, indicating that the coordinating heterocyclic moieties of BIPA and 2-BPEPA are essential for epoxidation. 2-BPPA or 3-BPPA was also found to work not so efficiently as BIPA. The serious decrease in the yield of **2** was observed with BPHPA as predicted.

A combination with $\text{Co}(\text{OAc})_2$ was similarly efficient, but CoCl_2 was less active than $\text{Co}(\text{OAc})_2$. Use of RhCl_3 , RuCl_3 , $\text{Ni}(\text{OAc})_2$, $\text{Mn}(\text{OAc})_2$, or $\text{Cu}(\text{OAc})_2$ resulted in low yield even in the presence of BIPA.

The present epoxidation reaction did not formally require a co-reductant. If DMF worked as an electron donor,⁶ FeCl_3 should have worked similarly as FeCl_2 . The fatal decrease in the yield of **2** was observed with FeCl_3 -BIPA, which indicates the different reaction course rather than the reported monooxygenase mechanism.^{3a,4,5,7}

trans- β -Methylstyrene (**3**) also underwent the present epoxidation reaction although oxidative cleavage of the carbon-carbon double bond was accompanied to give benzaldehyde (**6**) as a byproduct (eq. 4). A trace amount of the diketone **5** was also obtained. The results including other catalysts are listed in Table 2. In this epoxidation reaction, the ligand effect of BIPA is also observed and the catalytic epoxidation reaction

proceeded in the absence of a co-reductant. The reaction under air (1.0×10^3 kPa) or atmospheric molecular oxygen gave only a trace amount of **4**. $\text{Co}(\text{OAc})_2$ was found to work almost similarly as FeCl_2 , but no efficient catalyst was formed with CoCl_2 .

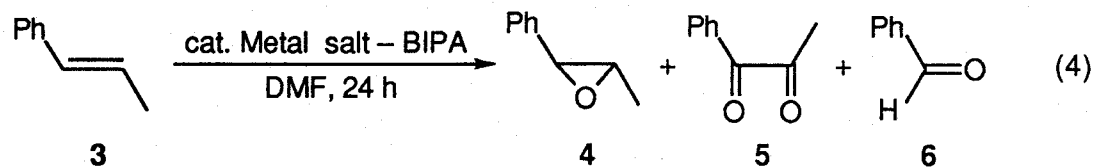


Table 2. Catalytic Epoxidation of *trans*- β -Methylstyrene ^a

Metal salt	Ligand	Temp. (°C)	Atmosphere (10^3 kPa)	Turnover ^b		
				4 ^c	5	6
FeCl_2	BIPA	70	O_2 (1.0)	16	3	40
FeCl_2	—	70	O_2 (1.0)	7	1	28
FeCl_2	BIPA	70	O_2 (0.1)	0.2	—	1
FeCl_2	—	70	O_2 (0.1)	—	—	1
FeCl_2	BIPA	rt	O_2 (1.0)	5	5	39
FeCl_2	—	rt	O_2 (1.0)	0.2	0.1	6
$\text{Co}(\text{OAc})_2$	BIPA	70	O_2 (1.0)	14	7	36
$\text{Co}(\text{OAc})_2$	—	70	O_2 (1.0)	9	7	28
CoCl_2	BIPA	70	O_2 (1.0)	0.4	0.3	5
CoCl_2	—	70	O_2 (1.0)	0.8	0.3	6

^a Metal salt, 0.02 mmol; BIPA, 0.02 mmol; **3**, 2.0 mmol.

^b Turnover was determined by GLC based on a catalyst.

^c Only *trans*-isomer.

A combination of podand ligands and transition metals is important in the efficient epoxidation reaction (eq. 5 and Table 3). Use of 2-BPEPA and $\text{Co}(\text{OAc})_2$ gave a poor result in the epoxidation reaction of **1** possibly due to the difference of the coordination interaction. The decrease in the yield of the epoxide was also observed with FeCl_2 -2-BPEPA in the case of **3** or *trans*-stilbene (**7**). DMAC and NMP were more suitable in the epoxidation reaction, but *trans*-stilbene oxide (**8**) was not obtained in

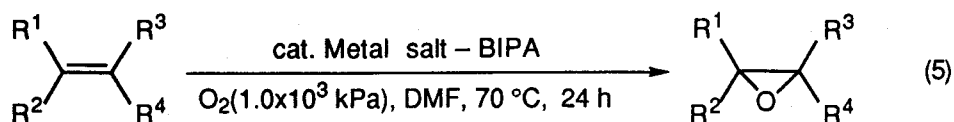

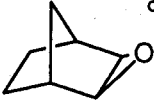
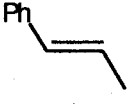
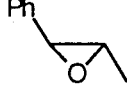
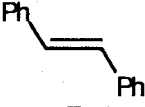
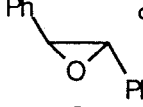

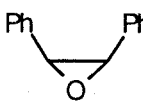

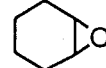


Table 3. Catalytic Epoxidation of Olefins ^a

Olefin	Metal salt	Ligand	Solvent	Product	Turnover ^b
 1	Co(OAc) ₂	BIPA	DMF	 2	24
	Co(OAc) ₂	2-BPEPA	DMF		7
	Co(OAc) ₂	BPHEPA	DMF		5
	Co(OAc) ₂	—	DMF		4
	CoCl ₂	BIPA	DMF		13
	CoCl ₂	2-BPEPA	DMF		2
	CoCl ₂	BPHEPA	DMF		6
	CoCl ₂	—	DMF		3
 3	FeCl ₂	BIPA	DMF	 4	16 (40)
	FeCl ₂	2-BPEPA	DMF		9 (35)
	FeCl ₂	BPHEPA	DMF		5 (23)
	FeCl ₂	—	DMF		7 (28)
 7	FeCl ₂	BIPA	DMF	 8	21 (23)
	FeCl ₂	BIPA	DMAC ^e		23 (32)
	FeCl ₂	BIPA	NMP ^f		31 (20)
	FeCl ₂	BIPA	pyridine		0 (0)
	FeCl ₂	2-BPEPA	DMF		3 (5)
	FeCl ₂	BPHEPA	DMF		1 (3)
	FeCl ₂	—	DMF		1 (2)
	Co(OAc) ₂	BIPA	DMF		2 (5)
	Co(OAc) ₂	—	DMF		trace(1)
 9	FeCl ₂	BIPA	DMF	 10	0 (0)
	FeCl ₂	—	DMF		0 (0)
	Co(OAc) ₂	BIPA	DMF		0 (0)
	Co(OAc) ₂	—	DMF		0 (0)
 11	FeCl ₂	BIPA	DMF	 12	0.3 (7) ^g
	FeCl ₂	—	DMF		0.3 (6) ^g

^a Metal salt, 0.02 mmol; ligand, 0.02 mmol; olefin, 2.0 mmol.

^b Based on a catalyst. The number in parentheses is turnover for the preparation of benzaldehyde.

^c Only *exo*-isomer.

^d Only *trans*-isomer.

^e DMAC = *N,N*-dimethylacetamide.

^f NMP = 1-methyl-2-pyrrolidinone.

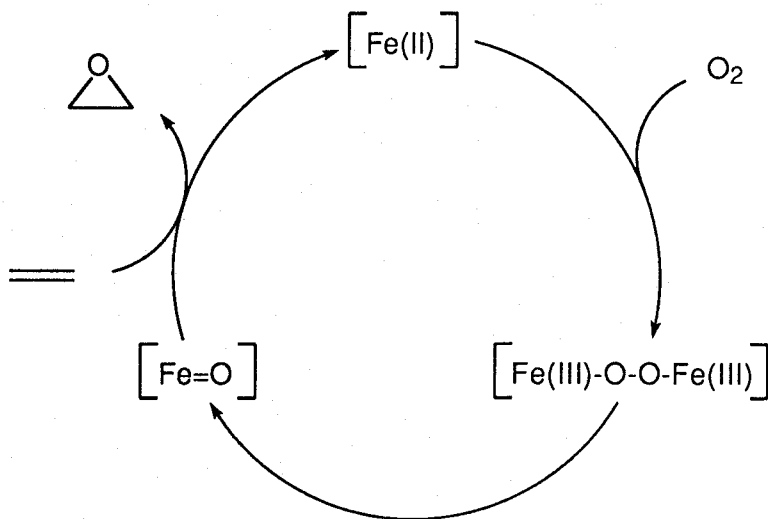
^g The number in parentheses is turnover for the preparation of cyclohexenone.

pyridine as a solvent. Although *cis*-stilbene (**9**) is known to be more reactive than **7** in the epoxidation reaction, the oxidation reaction of **9** did not proceed under the conditions employed here. Cyclohexene also showed the lower susceptibility to epoxidation.

Cyclic voltammetry verified that BIPA forms a complex with an equimolar amount of FeCl_2 in methanol, leading to the shift of the iron reduction wave from +0.35 to -0.35 V. A facile reduction of molecular oxygen was observed with the more electron-rich iron species when it was introduced into the solution. The similar activation was attained with BIPA in the presence of $\text{Co}(\text{OAc})_2$, but not with 2-BPEPA. These findings are consistent with the above-mentioned results.

The μ -peroxodiiron intermediate seems to be involved in this system as reported in the aromatic hydroxylation (Scheme 1).⁸ Although the iron

Scheme 1



complex with BIPA has not been isolated yet, the flexible heterocyclic multidentate ligand is considered to contribute to an efficient non-heme system for oxygenation. In the presumed octahedral geometry with two iron-nitrogen (amide) bonds, four nitrogen atoms of BIPA appear to exist

approximately on the same plane as iron does. The optimized geometry based on ZINDO calculation (CACHe system) also refers to this structure. The second 4-imidazolyl group is capable of behaving as an anchored axial ligand to facilitate the oxidation process. The presence of excess amounts of the imidazole ligand has been reported to increase the activity of P-450 model catalysts.^{7c,i}

1-2-2. Additive Effect on Epoxidation of Olefins

As described above, complexation of FeCl₂ with the flexible multidentate podand ligand, BIPA, has been revealed to permit the epoxidation reaction with molecular oxygen even in the absence of a co-reductant. An intramolecular coordination interaction of the axial *N*-ligand is considered to participate in forming an efficient catalytic system. These findings prompted us to develop an oxygenation method under milder conditions. An additive effect has been investigated in the catalytic epoxidation reaction with molecular oxygen (eq. 6).

The presence of 4-ethoxycarbonyl-3-methyl-2-cyclohexen-1-one (**13**) in the reaction of **7** with molecular oxygen catalyzed by FeCl₂ and BIPA in DMF led to the facile oxidation to **8** under the mild conditions. The reaction proceeded even at room temperature under molecular oxygen (1.0 x 10³ kPa). Furthermore, **8** was obtained under an atmospheric pressure of molecular oxygen when the reaction temperature was raised to 50 °C. The results are listed in Table 4. The involvement of BIPA is essential for the efficient epoxidation as described above. The similar effect of **13** was observed in the case of **3**. The *cis*-olefin **9** showed the lower susceptibility to oxidation under the conditions employed here than **7** to give only the *trans*-isomer **8** in a lower yield. This finding suggests that a simple radical mechanism is not operating here.

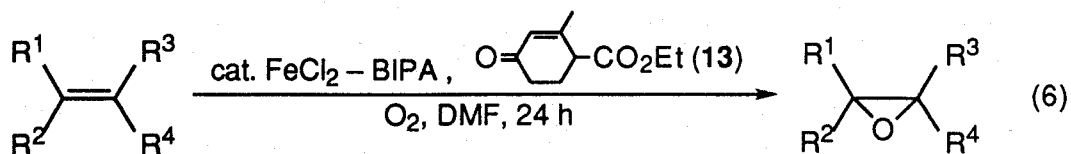
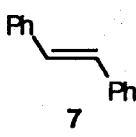
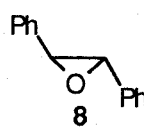
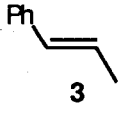
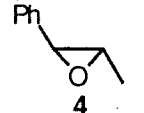
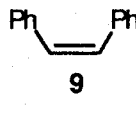
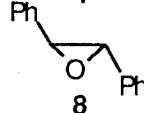


Table 4. Effect of **13** on the Catalytic Epoxidation of Olefin ^a

Olefin	Ligand	Temp. (°C)	O ₂ (10 ³ kPa)	13	Product	Turnover ^c
				Molar equiv. ^b		
 7	BIPA	rt	1.0	10	 8	9 (14)
	—	rt	1.0	10		0 (0)
	BIPA	rt	1.0	20		12 (15)
	BIPA	rt	1.0	100		11 (17)
	BIPA	50	0.1	10		10 (3)
	—	50	0.1	10		trace (0)
	BIPA	50	0.1	20		22 (5)
	BIPA	50	0.1	50		30 (7)
	BIPA ^e	50	0.1	50		11 (3)
	BIPA	50	0.1	100		10 (4)
 3	BIPA	50	0.1	20	 4	10 (10)
	BMEIPA	50	0.1	20		13 ^f (14)
	—	50	0.1	20		1 (6)
 9	BIPA	rt	1.0	10	 8	4 (4) ^g

^a FeCl₂, 0.01 mmol; BIPA, 0.01 mmol; olefin, 1.0 mmol.

^b Based on a catalyst.

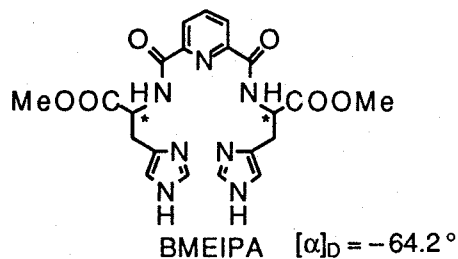
^c Based on a catalyst. The number in parentheses is turnover for the formation of benzaldehyde.

^d Only *trans*-isomer.

^e FeCl₃ was used instead of FeCl₂.

^f ee ≈ 0

^g The *cis*-epoxide **2c** and the isomerized olefin **1a** were not detected by ¹H-NMR.



The formation of **8** is dependent on the amount of **13** as shown in Figure 1. When the reaction was carried out under an atmospheric pressure of molecular oxygen, the epoxidation yield was raised by the increase of **13**, but lowered by addition of more than 70 molar equiv. of **13**.

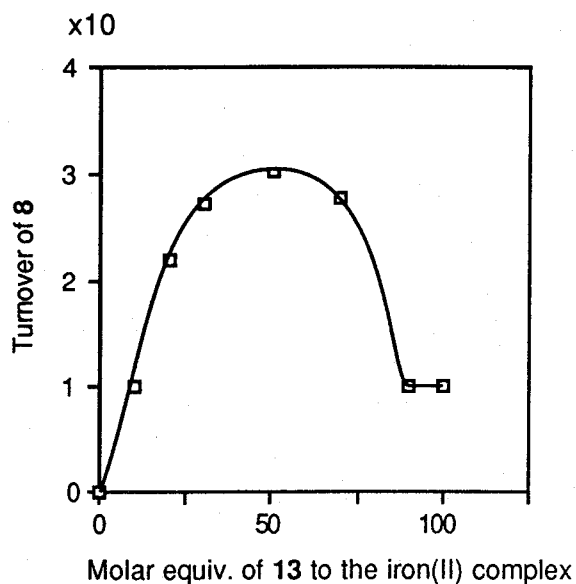


Figure 1. Effect of **13** on the epoxidation at 50 °C under an atmospheric pressure of molecular oxygen.

It remains obscure why **13** facilitates the epoxidation reaction, but there must exist an electrical interaction between the iron species and **13**. The peak at 530 nm in the UV-vis. spectra attributable to the iron complex with BIPA in DMF disappeared on the addition of **13** (5 molar equiv.) as shown Figure 2. Such an interaction is assumed to enhance one of the catalytic cycle steps. On the contrary, the epoxidation reaction was disturbed by excess amounts of **13** to prevent an olefin from coordination. Use of dimethyl maleate or 2-cyclohexen-1-one instead of **13** resulted in no epoxidation, indicating that the role of **13** is not simply based on the characteristic of an electron-deficient olefin.

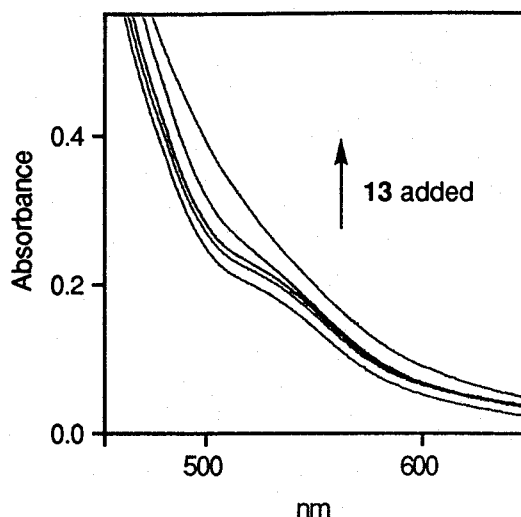


Figure 2. UV - vis. spectra of FeCl_2 - BIPA with **13**.

$[\text{FeCl}_2 - \text{BIPA}] = 1.0 \times 10^{-3} \text{ M};$
 $[\mathbf{13}] = 0, 1.0, 2.0, 3.0, 5.0 \times 10^{-3} \text{ M};$
 solv. DMF; under nitrogen.

Another possibility to be checked is that **13** serves as an electron donor. If so, FeCl_3 could be used as a catalyst with equal ease. The serious decrease in the yield of **8** was, however, observed with FeCl_3 -BIPA. The dehydrogenation product, 4-ethoxycarbonyl-3-methylphenol, was not detected in the reaction mixture, suggesting that the contribution of **13** only as an electron donor is not always reasonable. 2-Cyclohexen-1-one was not oxidized to phenol under the similar conditions without formation of the epoxide (*vide supra*). Since **13** is found to be oxidized to 4-ethoxycarbonyl-4-hydroxy-3-methyl-2-cyclohexen-1-one with molecular oxygen,⁹ molecular oxygen is assumed to be activated in the presence of **13** to afford a peroxide at the α -position of the ethoxycarbonyl group. Although almost half amounts of **13** or 2-cyclohexen-1-one (50 molar equiv. were used in each case) were only recovered, a small amount of the oxygenated alcohol was observed as a sole detectable product by GLC and ^1H -NMR.

These findings imply that only one of the interaction and paths mentioned above is not necessarily the case operating here. It is not deniable that these roles are considered to cooperate each other to construct a real catalytic oxygenation system.

Although the mechanism on the additive effect of **13** has to wait for further studies, the iron(II) complex with the multidentate *N*-heterocyclic podand ligand forms an efficient catalyst for epoxidation in cooperation with the cyclohexenone **13**.

1-2-3. Oxygenation of Phenols

We examined the catalytic phenolase and catecholase properties of the cobalt(II) complex with the multidentate *N*-heterocyclic podand ligand. Treatment of 2, 6-di-*t*-butylphenol (**14a**) with 5 mol% of Co(OAc)₂ and 2-BPEPA in DMF under an atmospheric pressure of molecular oxygen resulted in the selective formation of the corresponding *p*-benzoquinone **15a** in a good yield with a small amount of the dehydrogenative coupling product **16a** (eq. 7). DMF was superior to *N,N*-dimethylacetamide and 1-methyl-2-pyrrolidinone as a solvent (Table 5). Cu(OAc)₂¹¹ did not induce the oxygenation reaction only giving the diphenquinone **16a** even in the presence of 2-BPEPA.

It should be noted that the oxygenation depends on the podand ligands. Use of BIPA bearing the 4-imidazolyl group, which is effective in the FeCl₂- or Co(OAc)₂-catalyzed epoxidation reaction with molecular oxygen, drastically decreased the conversion to **14a** with the predominant formation of **15a**. A combination of 2-BPEPA and Co(OAc)₂ gives a poor result in the epoxidation. Taking them into consideration, the 4-imidazolyl and 2-pyridyl groups are considered to play a respective important role in each oxygenation possibly due to the difference of the coordination interaction. It is consistent with the observation that

BPHEPA bearing the phenyl group instead was no more efficient ligand for the oxygenation. The pendant length is also a key factor as exemplified by a combination of 2-BPMPA or 2-BPPA and Co(OAc)₂ giving a poor result in the oxygenation reaction of **14a**.

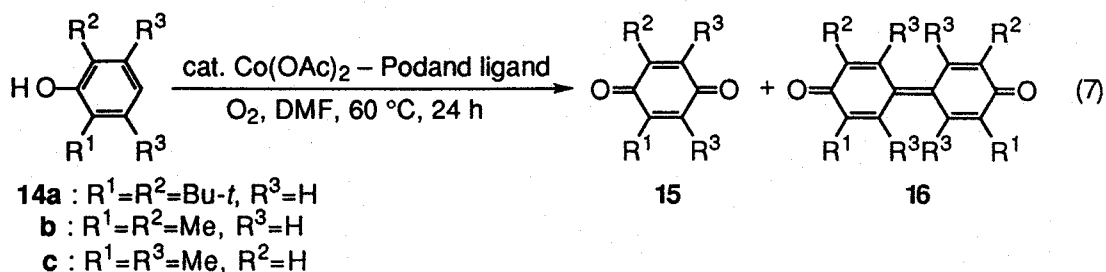
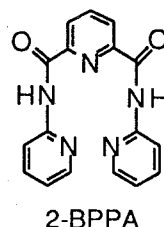
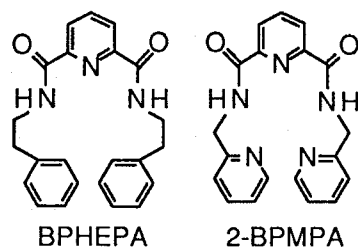
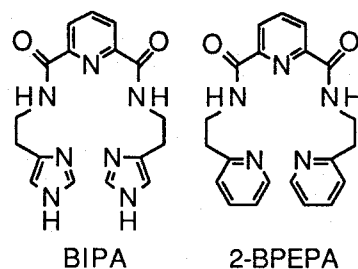


Table 5. Catalytic Oxidation of Phenols ^a

14	Ligand	Solvent	Yield (%) ^b	
			15	16
a	BIPA	DMF	10	41
	2-BPEPA	DMF	86, 82 ^c	9
	2-BPEPA ^d	DMF	92	6
	BPHEPA	DMF	0	38
	2-BPMPA	DMF	3	3
	2-BPPA	DMF	0	0
	—	DMF	0	45
	2-BPEPA	DMAC ^e	54	10
	2-BPEPA	NMP ^f	76	7
b	BIPA	DMF	1	0
	2-BPEPA	DMF	77, 71 ^c	1
	BPHEPA	DMF	0	0
	—	DMF	0	0
c	BIPA	DMF	0	0
	2-BPEPA	DMF	70	0
	BPHEPA	DMF	0	0
	—	DMF	0	0



^a Co(OAc)₂, 0.01 mmol; ligand, 0.01 mmol; **14**, 0.20 mmol.

^b GLC yields based on **14**.

^c Isolated yield.

^d Use of the isolated complex.

^e DMAC = *N,N*-dimethylacetamide.

^f NMP = 1-methyl-2-pyrrolidinone.

A substituent on a phenol ring is known to markedly influence the rate of oxidation due to redox potential. More distinct efficiency of the podand ligand 2-BPEPA was observed in the oxygenation of 2,6-dimethylphenol (**14b**) to the quinone **15b**. Furthermore, the $\text{Co}(\text{OAc})_2$ -catalyzed oxygenation of 2,3,5-trimethylphenol (**14c**) to **15c** was almost quantitatively accomplished by 2-BPEPA. A combination of $\text{Co}(\text{OAc})_2$ and 2-BPEPA is only effective. In contrast, with BIPA or BPHEPA, the oxygenation reaction did not proceed under the conditions employed here.

The phenol **14d** blocked at the para position underwent the selective catalytic oxygenation to the *o*-benzoquinone **15d** in the presence of $\text{Co}(\text{OAc})_2$ and 2-BPEPA. The activity difference of the podand ligands was huge only giving poor results with BIPA and BPHEPA as shown in Table 6.

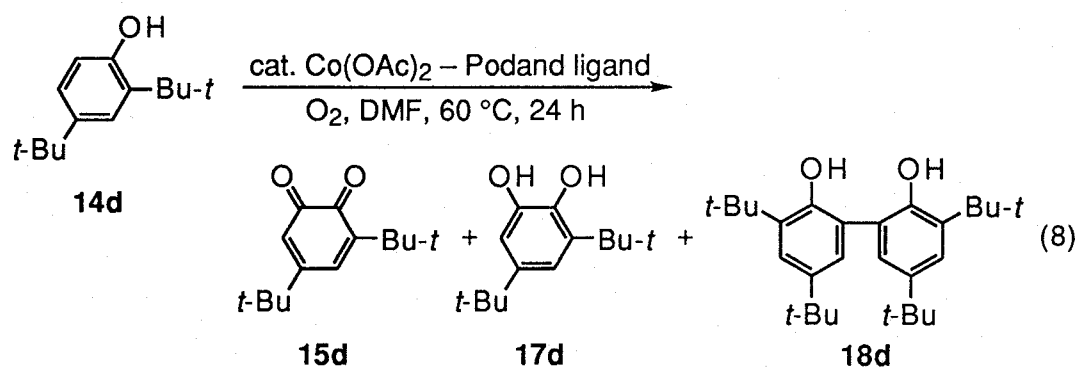


Table 6. Catalytic Oxidation 2,4-Di-*t*-butylphenol ^a

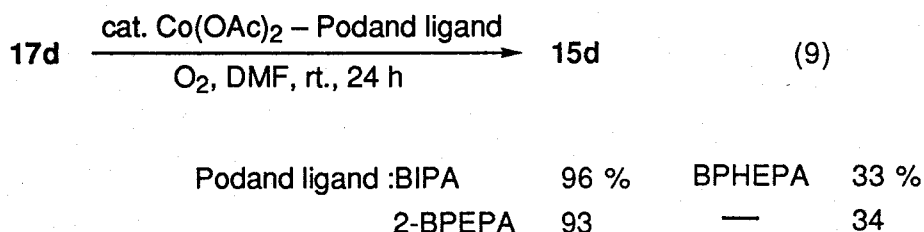
Ligand	Yield (%) ^b		
	15d	17d	18d
BIPA	0	0	9
2-BPEPA	72, 69 ^c	5	trace
BPHEPA	0	0	0
2-BMPA	0	0	0
2-BPPA	0	0	0
—	0	0	0

^a $\text{Co}(\text{OAc})_2$, 0.01 mmol; ligand, 0.01 mmol; **14d**, 0.20 mmol.

^b GLC yields based on **14d**.

^c Isolated yield.

Facile dehydrogenation of 3, 5-di-*t*-butylcatechol (**17d**) to **15d** was achieved by the catalytic system consisting of Co(OAc)₂ and 2-BPEPA or BIPA under the milder conditions (eq. 9). This finding suggests that the introduction of the hydroxyl group is the rate determining step in the oxygenation reaction of **14d**.



A substituent on a pyridyl ring of podand ligands is expected to influence the efficiency of the catalyst. A substituent effect on a pyridyl ring of 2-BPEPA in the oxygenation of phenols was investigated. The 4-substituted derivatives of 2-BPEPA were easily prepared as follows.¹² Treatment of chelidamic acid chloride with two equivalents of 2-(2-aminoethyl)pyridine in the presence of triethylamine afforded *N,N'*-bis[2-(2-pyridyl)ethyl]-4-hydroxy-2, 6-pyridinedicarboxamide (2-BPEHPA) in 22% yield and *N,N'*-bis[2-(2-pyridyl)ethyl]-4-chloro-2, 6-pyridinedicarboxamide (2-BPECPA) in 16% yield. We could obtain *N,N'*-bis[2-(2-pyridyl)ethyl]-4-methoxy-2, 6-pyridinedicarboxamide (2-BPEMPA) in 59% yield by displacement of 2-BPEPA with methanol-sodium hydroxide (Scheme 2).

2-BPEMPA, which bears an electron-releasing methoxyl group, gave a better result than 2-BPEPA (Table 7). 2-BPEHPA bearing a hydroxyl group was found to be the less efficient ligand.

Scheme 2

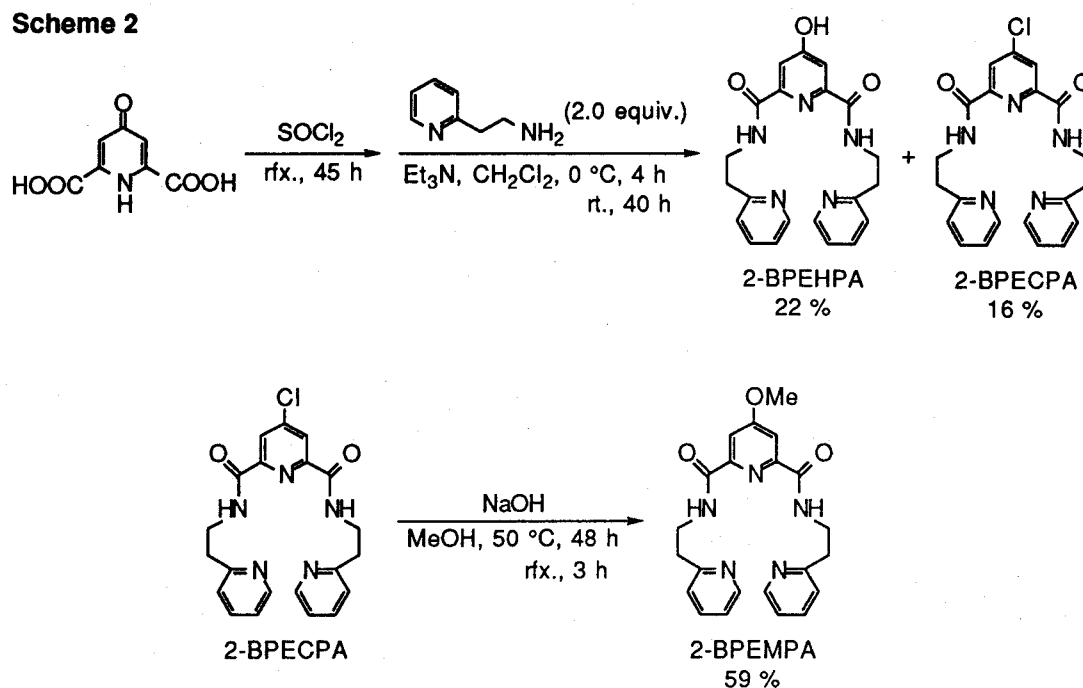


Table 7. Catalytic Oxidation of Phenols ^a

14	Ligand	Yield (%) ^b	
		15	16
b	2-BPEPA	77	1
	2-BPEMPA	82	0
	2-BPEHPA	60	trace
	2-BPECPA	78	trace
c	2-BPEPA	70	0
	2-BPEMPA	69	0
	2-BPEHPA	23	0
	2-BPECPA	59	0

^a $\text{Co}(\text{OAc})_2$, 0.01 mmol; ligand, 0.01 mmol; **14**, 0.20 mmol.

^b GLC yields based on **14**.

1-Naphthol (**14e**) underwent the catalytic oxygenation to the *p*-quinone **15e** in the presence of $\text{Co}(\text{OAc})_2$ and 2-BPEPA derivatives although yields were not so good (eq. 10 and Table 8).

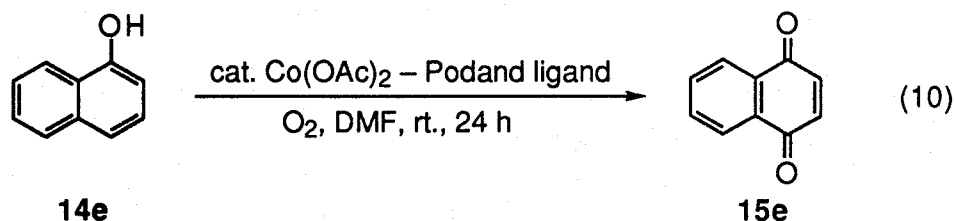


Table 8. Catalytic Oxidation of 1-Naphthol ^a

Ligand	Yield (%) ^b
2-BPEPA	36
2-BPEMPA	45
2-BPEHPA	36
2-BPECPA	37
—	0

^a Co(OAc)₂, 0.01 mmol; ligand, 0.01 mmol;
14e, 0.20 mmol.

^b GLC yields based on **14e**.

The complexation of Co(OAc)₂ with 2-BPEPA was verified by the following observations. Cyclic voltammetry of Co(OAc)₂ with an equimolar amount of 2-BPEPA in methanol gave the new cobalt reversible reduction wave at -0.07 V. This potential is reasonable for the efficient catalyst of tyrosinase model.¹³ The reduction potentials of the cobalt(II) complexes depend on the podand ligands possibly due to the difference of the coordination interaction, other podand ligands did not give the reversible reduction wave as 2-BPEPA. These findings are consistent with the above-mentioned results. A new absorption at 317 nm also appeared in the UV-vis. spectrum of Co(OAc)₂ and 2-BPEPA in DMF. The cobalt complex was isolated by treatment of Co(OAc)₂ with an equimolar amount of 2-BPEPA in methanol. The spectral data showed the substitution of cobalt with two amide moieties and the different coordination sites of two podand 2-pyridyl groups. One of them is assumed to serve as an intramolecular axial ligand as proposed in the

Fe(II)–BIPA complex. This coordination mode is likely to contribute to the efficiency of the catalyst. The higher catalytic activity was attained by use of thus isolated complex in the oxygenation of **14a** to **15a** (Table 5).

1-3. Conclusion

The complexation of FeCl₂ with the flexible multidentate podand ligand, BIPA, is revealed to permit the epoxidation reaction with molecular oxygen even in the absence of a co-reductant. Furthermore, the addition of 4-ethoxycarbonyl-3-methyl-2-cyclohexen-1-one (**13**) results in the facile epoxidation reaction with molecular oxygen under the milder conditions. The cobalt(II) complex with 2-BPEPA serves as an efficient catalyst for the selective oxygenation of phenols to the corresponding quinones. A combination of podand ligands and transition metals is a key factor for the construction of efficient non-heme systems of oxygenation, possibly due to the difference of the multidentate coordination interaction.

1-4. Experimental

General

Melting points were measured using Yanagimoto micromelting point apparatus and are uncorrected. Infrared spectra were recorded on a Perkin-Elmer FT-IR 1605 infrared. ¹H-NMR spectra were recorded on a Bruker AM-600 (600MHz) spectrometer and a JEOL JNM-GSX-400 (400MHz) spectrometer with tetramethylsilane as an internal standard. UV-vis. spectra were recorded using a Hitachi U-3000. The X-ray crystallography was made on Rigaku AFC5R diffractometer. The fast

atom bombardment mass spectra were run on a JEOL JMS-DX303HF spectrometer. Recycling preparative HPLC analysis was performed on a JAI LC-908. The standard electrochemical instrumentation consisted of a Hokuto Denko potentiostat / galvanostat HA-301S and a Hokuto Denko function generator HB-104S with a three-electrode system consisting of a glassy carbon working electrode, a platinum auxiliary electrode, and a KCl-saturated calomel reference electrode. Cyclic voltammograms were recorded with Graphtec WX 1000.

BIPA, 2-BPEPA, BPHEPA, 2-BPMPA, 2-BPPA, 3-BPPA, BPHPA, 3-PPA, and BMEIPA were prepared according to the method reported in a previous paper.¹

Synthesis of *N*, *N'*-Bis[2-(2-pyridyl)ethyl]-4-hydroxy-2,6-pyridinedicarboxamide (2-BPEHPA) and *N*, *N'*-Bis[2-(2-pyridyl)ethyl]-4-chloro-2,6-pyridinedicarboxamide (2-BPECPA). Chelidamic acid (2.197 g, 12.0 mmol) was treated with thionyl chloride (58 mL) at reflux temperature for 48 h. Excess thionyl chloride was removed under the reduced pressure to give the corresponding acid chloride as a white solid. To a solution of 2-(2-aminoethyl)pyridine (2.8 mL, 24.0 mmol) and triethylamine (7.0 mL, 50.0 mmol) in dichloromethane (15 mL) was slowly added a solution of the acid chloride in dichloromethane (35 mL) at 0 °C. The mixture was stirred at 0 °C for 4 h and at room temperature for 40 h. The resulting mixture was diluted with dichloromethane (30 mL), washed with saturated NaHCO₃ aqueous solution and brine, and dried over MgSO₄. White solid was obtained by evaporation of the dichloromethane solution in vacuo. 2-BPEHPA and 2-BPECPA were isolated by recycling preparative HPLC and recrystallized from dichloromethane.

2-BPEHPA: Mp 101-103 °C (uncorrected); R_f = 0.45 (ethyl acetate-methanol v/v 5:1); IR (KBr, cm⁻¹) 3312 (NH), 1661 (C=O); ¹H NMR (400 MHz, CDCl₃) δ

8.86 (br, 2H, NH), 8.45 (ddd, 2H, $J = 5.0, 1.8, 1.0$ Hz, Py), 7.61 (s, 2H, Py), 7.59 (dt, 2H, $J = 7.7, 1.8$ Hz), 7.21 (dt, 2H, $J = 7.8, 1.0$ Hz, Py), 7.11 (ddd, 2H, $J = 7.8, 5.0, 1.0$ Hz, Py), 3.81 (q, 4H, $J = 6.4$ Hz, CH₂), 3.13 (t, 4H, $J = 6.4$ Hz, CH₂); MS (EI) m/z 391 (M⁺).

2-BPECPA: Mp 164-166 °C (uncorrected); $R_f = 0.47$ (ethyl acetate-methanol v/v 5:1); IR (KBr, cm⁻¹) 3259 (NH), 1664 (C=O); ¹H NMR (400 MHz, CDCl₃) δ 8.78 (br, 2H, NH), 8.49 (ddd, 2H, $J = 5.0, 1.8, 0.9$ Hz, Py), 8.30 (s, 2H, Py), 7.63 (dt, 2H, $J = 7.7, 1.8$ Hz), 7.22 (dt, 2H, $J = 7.7, 0.9$ Hz, Py), 7.16 (ddd, 2H, $J = 7.7, 5.0, 0.9$ Hz, Py), 3.93 (q, 4H, $J = 6.5$ Hz, CH₂), 3.15 (t, 4H, $J = 6.5$ Hz, CH₂); MS (EI) m/z 409 (M⁺).

Synthesis of *N, N'*-Bis[2-(2-pyridyl)ethyl]-4-methoxy-2,6-pyridinedicarboxamide (2-BPEMPA). To a solution of 2-BPECPA (0.408, 1.0 mmol) in methanol (50 mL) was added a solution of NaOH (0.623 g, 15.0 mmol) in methanol at room temperature. The mixture was stirred at 50 °C for 48 h and at reflux temperature for 3 h. After evaporation of the solution, the mixture was extracted with dichloromethane (20 mL) and dried over MgSO₄. White solid was obtained by evaporation of the dichloromethane solution in vacuo. 2-BPEMPA was isolated by recycling preparative HPLC and recrystallized from dichloromethane.

2-BPEMPA: Mp 95-97 °C (uncorrected); $R_f = 0.38$ (ethyl acetate-methanol v/v 5:1); IR (KBr, cm⁻¹) 3296 (NH), 1656 (C=O); ¹H NMR (400 MHz, CDCl₃) δ 8.71 (br, 2H, NH), 8.51 (ddd, 2H, $J = 4.9, 1.8, 1.1$ Hz, Py), 7.82 (s, 2H, Py), 7.62 (dt, 2H, $J = 7.7, 1.8$ Hz), 7.22 (dt, 2H, $J = 7.7, 1.1$ Hz, Py), 7.16 (ddd, 2H, $J = 7.7, 4.9, 1.1$ Hz, Py), 3.96 (s, 3H, OMe), 3.92 (q, 4H, $J = 6.4$ Hz, CH₂), 3.15 (t, 4H, $J = 6.4$ Hz, CH₂); MS (EI) m/z 405 (M⁺).

General Procedure for the Epoxidation of Olefins. Metal salt (0.02 mmol) was treated with the podand ligand (0.02 mmol) in DMF (0.8 mL) in a glass vessel under nitrogen for 24 h. After the addition of olefin (2.0 mmol) in DMF (0.2 mL) to the resulting solution, the vessel was put in a

stainless steel autoclave. The epoxidation reaction was carried out under molecular oxygen (1.0×10^3 kPa) at 70 °C for 24 h. The mixture was diluted with ether (30 mL), washed with 1.5 M HCl solution and brine, dried over MgSO_4 , and concentrated. The formation of products was detected by ^1H -NMR and GLC. Mp and spectral data for all products were identical with those of authentic samples.

1-Phenyl-1,2-propanedione (5): ^1H NMR (270 MHz, CDCl_3) δ 8.02 (d, 2H, J = 7.6 Hz, Ph), 7.65 (t, 1H, J = 7.6 Hz, Ph), 7.50 (t, 2H, J = 7.6 Hz, Ph), 2.53 (s, 3H, CH_3).

Epoxidation of Olefins in the Presence of 4-Ethoxycarbonyl-3-methyl-2-cyclohexen-1-one. To a mixture of olefin (1.0 mmol) and BIPA (0.01 mmol) was added FeCl_2 (0.01 mmol) in DMF (0.8 mL). The resulting mixture was stirred under nitrogen at room temperature for 24 h. 4-Ethoxycarbonyl-3-methyl-2-cyclohexen-1-one (13) was added to the resultant mixture. After the reaction vessel was substituted with molecular oxygen, the mixture was stirred under an atmospheric pressure of molecular oxygen at 50 °C for 24 h. The mixture was diluted with ether (30 mL), washed with 1.5 M HCl solution and brine, dried over MgSO_4 , and concentrated. The formation of products was detected by ^1H -NMR and GLC. Mp and spectral data for all products were identical with those of authentic samples.

General Procedure for the Oxygenation of Phenols. To a mixture of the phenol 14 (0.2 mmol) and the podand ligand (0.01 mmol) was added $\text{Co}(\text{OAc})_2$ (0.01 mmol) in DMF (0.2 mL). The resulting mixture was stirred under an atmospheric pressure of molecular oxygen at 60 °C for 24 h. The mixture was diluted with ether (30 mL), washed with 1.5 M HCl solution and brine, and dried over MgSO_4 . GLC analysis (1.0 m 10% SE-30 column, 50-250 °C) of the concentrated residue showed the formation of 15-18 (eq.5, eq. 6, Tables 5, and 6). The quinone 15 was isolated by

chromatography on a silica gel column. Mp and spectral data for all products were identical with those of authentic samples.¹⁴

2,6-Di-*t*-butyl-1,4-benzoquinone (15a): mp 65-66 °C (uncorrected); R_f = 0.40 (hexane-chloroform v/v 1:1); IR (KBr, cm^{-1}) 1654 (C=O); ^1H NMR (600 MHz, $(\text{CD}_3)_2\text{CO}$) δ 6.49 (s, 2H, CH), 1.29 (s, 18H, CH_3); MS (EI) m/z 220 (M^+).^{14a}

3,3',5,5'-Tetra-*t*-butyldiphenoquinone (16a): mp 242-243 °C (uncorrected); R_f = 0.55 (hexane-chloroform v/v 1:1); IR (KBr, cm^{-1}) 1608 (C=O); ^1H NMR (600 MHz, $(\text{CD}_3)_2\text{CO}$) δ 7.87 (s, 4H, CH), 1.34 (s, 36H, CH_3); MS (EI) m/z 408 (M^+).^{15a}

2,6-Dimethyl-1,4-benzoquinone (15b): mp 70-72 °C (uncorrected); R_f = 0.25 (hexane-chloroform v/v 1:4); IR (KBr, cm^{-1}) 1656 (C=O); ^1H NMR (600 MHz, $(\text{CD}_3)_2\text{CO}$) δ 6.59 (s, 2H, CH), 2.02 (s, 6H, CH_3); MS (EI) m/z 136 (M^+).^{14a}

3,3',5,5'-Tetramethyldiphenoquinone (16b): mp 208-210 °C (uncorrected); R_f = 0.10 (hexane-chloroform v/v 1:4); IR (KBr, cm^{-1}) 1594 (C=O); ^1H NMR (600 MHz, $(\text{CD}_3)_2\text{CO}$) δ 8.09 (s, 4H, CH), 2.08 (s, 12H, CH_3); MS (EI) m/z 240 (M^+).^{14a}

2,3,5-Trimethyl-1,4-benzoquinone (15c): mp 29-30 °C (uncorrected); R_f = 0.40 (chloroform); IR (KBr, cm^{-1}) 1650 (C=O); ^1H NMR (600 MHz, CDCl_3) δ 6.56 (s, 1H, CH), 2.04 (s, 3H, CH_3), 2.03 (s, 3H, CH_3), 2.01 (s, 3H, CH_3); MS (EI) m/z 150 (M^+).^{15a}

3,5-Di-*t*-butyl-1,2-benzoquinone (15d): mp 113-114 °C (uncorrected); R_f = 0.35 (chloroform); IR (KBr, cm^{-1}) 1656 (C=O); ^1H NMR (600 MHz, $(\text{CD}_3)_2\text{CO}$) δ 7.10 (d, 1H, J = 2.3 Hz, CH), 6.14 (d, 1H, J = 2.3 Hz, CH), 1.27 (s, 9H, CH_3), 1.25 (s, 9H, CH_3); MS (EI) m/z 222 (M^++2).^{14b}

3,3',5,5'-Tetra-*t*-butyl-2,2'-dihydroxybiphenyl (18d): mp 188-190 °C (uncorrected); R_f = 0.75 (chloroform); IR (KBr, cm^{-1}) 3540 (OH); ^1H NMR

(600 MHz, $(\text{CD}_3)_2\text{CO}$) δ 7.38 (d, 2H, $J = 2.4$ Hz, CH), 7.09 (d, 2H, $J = 2.4$ Hz, CH), 1.46 (s, 18H, CH_3), 1.32 (s, 18H, CH_3); MS (EI) m/z 410 (M^+).^{14b}

Dehydrogenation of 3,5-Di-*t*-butylcatechol 17d. To a mixture of the 3,5-di-*t*-butylcatechol (**17d**, 0.2 mmol) and the podand ligand (0.01 mmol) was added $\text{Co}(\text{OAc})_2$ (0.01 mmol) in DMF (0.2 mL). The resulting mixture was stirred under an atmospheric pressure of molecular oxygen at room temperature for 24 h. The mixture was diluted with ether (30 mL), washed with 1.5 M HCl solution and brine, and dried over MgSO_4 . GLC analysis (1.0 m 10% SE-30 column, 50-250 °C) of the concentrated residue showed the formation of **15d** (eq 7). The quinone **15d** was isolated by chromatography on a silica gel column.

Oxygenation of 1-Naphthol 14e. To a mixture of the 1-naphthol (**14e**, 0.2 mmol) and the podand ligand (0.01 mmol) was added $\text{Co}(\text{OAc})_2$ (0.01 mmol) in DMF (0.2 mL). The resulting mixture was stirred under an atmospheric pressure of molecular oxygen at at room temperature for 24 h. The mixture was diluted with ether (30 mL), washed with 1.5 M HCl solution and brine, and dried over MgSO_4 . GLC analysis (1.0 m 10% OV-17 column, 50-250 °C) of the concentrated residue showed the formation of **15e** (eq. 7 and Table 8). The quinone **15e** was isolated by chromatography on a silica gel column. Mp and spectral data were identical with the authentic samples.¹⁵

1,4-Naphthoquinone (15e): mp 120-121 °C (uncorrected); $R_f = 0.45$ (chloroform); IR (KBr, cm^{-1}) 1661 ($\text{C}=\text{O}$); ^1H NMR (600 MHz, CDCl_3) δ 8.11 (dd, 2H, $J = 5.8, 3.4$ Hz), 7.78 (dd, 2H, $J = 5.8, 3.4$ Hz), 7.63 (s, 2H); MS (EI) m/z 158 (M^+).¹⁵

Isolation of Co-2-BPEPA Complex. A mixture of 2-BPEPA (0.1 mmol) and $\text{Co}(\text{OAc})_2$ (0.1 mmol) in methanol (1.0 mL) was stirred under nitrogen at room temperature for 24 h. After evaporation of the methanol

solution in vacuo, the complex was separated by chromatography on a silica gel column.

Co-2-BPEPA Complex: mp 205-207 °C (uncorrected); $R_f = 0.08$ (chloroform-methanol v/v 1:1); IR (KBr, cm^{-1}) 1594 (C=O); ^1H NMR (600 MHz, CD_3OD) δ 9.57 (dd, 1H, $J = 5.9, 1.5$ Hz, Py), 8.33 (t, 1H, $J = 7.8$ Hz, Py), 8.15 (dd, 1H, $J = 7.8, 0.9$ Hz, Py), 8.11 (dt, 1H, $J = 7.7, 1.5$ Hz, Py), 8.01 (dd, 1H, $J = 5.9, 1.5$ Hz, Py), 7.90 (dd, 1H, $J = 7.8, 0.9$ Hz, Py), 7.72 (ddd, 1H, $J = 7.7, 5.9, 0.9$ Hz, Py), 7.71 (dt, 1H, $J = 7.7, 1.5$ Hz, Py), 7.56 (dd, 1H, $J = 7.7, 0.9$ Hz, Py), 7.25 (dd, 1H, $J = 7.7, 0.9$ Hz, Py), 7.14 (ddd, 1H, $J = 7.7, 5.9, 0.9$ Hz, Py), 4.2-4.1 (m, 2H, CH_2), 4.07 (dd, 1H, $J = 13.1, 9.0$ Hz, CH_2), 3.27 (dt, 1H, $J = 14.3, 2.6$ Hz, CH_2), 3.16 (dt, 1H, $J = 14.3, 2.6$ Hz, CH_2), 3.00 (dd, 1H, $J = 15.0, 6.4$ Hz, CH_2), 2.47 (ddd, 1H, $J = 15.0, 11.9, 9.0$ Hz, CH_2), 2.18 (dt, 1H, $J = 14.3, 4.0$ Hz, CH_2); ^{13}C NMR (150 MHz, CD_3OD) δ 172.0 (C=O), 171.7 (C=O), 165.1 (Py), 163.1 (Py), 158.2 (Py), 157.0 (Py), 151.7 (Py), 142.0 (Py), 141.5 (Py), 141.1 (Py), 128.9 (Py), 127.2 (Py), 125.4 (Py), 125.2 (Py), 125.0 (Py), 124.5 (Py), 41.5 (CH_2), 40.5 (CH_2), 37.4 (CH_2), 36.7 (CH_2); MS (FAB) m/z 433; UV-vis. 317nm ($[\text{Co-2-BPEPA complex}] = 4.0 \times 10^{-4}$ M, solv. DMF, under nitrogen); Cyclic voltammetry $E_p = -0.07$ V vs. SCE ($[\text{Co-2-BPEPA complex}] = 2.0 \times 10^{-3}$ M, $[\text{Bu}_4\text{NClO}_4] = 0.1$ M, solv. MeOH, scan rate = 50 mV/s, glassy carbon working electrode).

UV-vis. Spectra Measurements. UV-vis. spectra were taken under nitrogen atmosphere at 30 °C after keeping the DMF solutions of the metal salt and the podand ligands.

Electrochemical Experiments. Cyclic voltammograms were obtained in MeOH solution containing 0.1 M Bu_4NClO_4 as a supporting electrolyte (2×10^{-3} M). Potentials were determined with reference to a KCl saturated calomel electrode at 50 mVs^{-1} scan rate.

1-5. References and Notes

1. Hirao, T.; Mikami, S.; Ohshiro, Y. *Synlett* **1990**, 541.
2. Hirao, T.; Ohno, M.; Ohshiro, Y. *Tetrahedron Lett.* **1990**, 31, 6039.
3. (a) Tabushi, I.; Yazaki, A. *J. Am. Chem. Soc.* **1981**, 103, 7371. (b) Yamada, T.; Takai, T.; Rhode, O.; Mukaiyama, T. *Bull. Chem. Soc. Jpn.* **1991**, 64, 2109. (c) Takai, T.; Hata, E.; Yamada, T.; Mukaiyama, T. *Bull. Chem. Soc. Jpn.* **1991**, 64, 2513. (d) Yamada, T.; Imagawa, K.; Nagata, T.; Mukaiyama, T. *Chem. Lett.* **1992**, 2231.
4. (a) Ellis, Jr., P. E.; Lyons, J. E. *J. Chem. Soc., Chem. Commun.* **1989**, 1189, 1315. (b) Maldotti, A.; Bartocci, C.; Amadelli, R.; Polo, E.; Battioni, P.; Mansuy, D. *J. Chem. Soc., Chem. Commun.* **1991**, 1487.
5. (a) Groves, J. T.; Quinn, R. *J. Am. Chem. Soc.* **1985**, 107, 5790. (b) Weber, L.; Haufe, G.; Rehorek, D.; Hennig, H. *J. Chem. Soc., Chem. Commun.* **1991**, 502.
6. Epoxidation of *trans*-stilbene was observed in acetonitrile although BIPA is less soluble in acetonitrile.
7. (a) Groves, J. T.; Nemo, T. E.; Myers, R. S. *J. Am. Chem. Soc.* **1979**, 101, 1032. (b) Mansuy, D.; Bartoli, J. F.; Chottard, J. C.; Lange, M. *Angew. Chem., Int. Ed. Eng.* **1980**, 19, 909. (c) Collman, J. P.; Brauman, J. I.; Meunier, B.; Hayashi, T.; Kodadek, T.; Raybuck, S. A. *J. Am. Chem. Soc.* **1985**, 107, 2000. (d) Meunier, B. *Bull. Soc. Chim. Fr.* **1986**, 578. (e) Hecht, S. M. *Acc. Chem. Res.* **1986**, 19, 383. (f) Stubbe, J.; Kozarich, J. W. *Chem. Rev.* **1987**, 87, 1107. (g) Koola, J. D.; Kochi, J. K. *Inorg. Chem.* **1987**, 26, 908. (h) Kinneary, J. F.; Albert, J. S.; Burrows, C. J. *J. Am. Chem. Soc.* **1988**, 110, 6124. (i) Battioni, P.; Renaud, J. P.; Bartoli, J. F.; Reina-Artiles, M.; Fort, M.; Mansuy, D. *J. Am. Chem. Soc.* **1988**, 110, 8462. (j) Nam, W.; Ho, R.; Valentine, J. S. *J. Am. Chem. Soc.* **1991**, 113, 7052.

8. (a) Duprat, A. F.; Capdevielle, P.; Maumy, M. *J. Chem. Soc., Chem. Commun.* **1991**, 464. (b) Tolman, W. B.; Liu, S.; Bentsen, J. B.; Lippard, S. J. *J. Am. Chem. Soc.* **1991**, *113*, 152.
9. Hirao, T.; Ikeda, I. unpublished result. Treatment of 4-ethoxycarbonyl-3-methyl-2-cyclohexen-1-one with a catalytic amount of polyaniline as a synthetic metal catalyst¹⁰ under an atmospheric pressure of molecular oxygen resulted in hydroxylation to 4-ethoxycarbonyl-4-hydroxy-3-methyl-2-cyclohexen-1-one.
10. Hirao, T.; Higuchi, M.; Ikeda, I.; Ohshiro, Y. *J. Chem. Soc., Chem. Commun.* **1993**, 194.
11. (a) Capdevielle, P.; Maumy, M. *Tetrahedron Lett.* **1982**, *23*, 1573; **1983**, *24*, 5611. (b) Kitajima, N.; Koda, T.; Iwata, Y.; Moro-oka, Y. *J. Am. Chem. Soc.* **1990**, *112*, 8833. (c) Réglier, M.; Jorand, C.; Waegell, B. *J. Chem. Soc., Chem. Commun.* **1990**, 1752. (d) Casella, L.; Gullotti, M.; Radaelli, R.; Di Gennaro, P. *J. Chem. Soc., Chem. Commun.* **1991**, 1611. (e) Rockcliffe, D. A.; Martell, A. E. *Inorg. Chem.* **1993**, *32*, 3143.
12. Nishiyama, H.; Yamaguchi, S.; Kondo, M.; Itoh, K. *J. Org. Chem.* **1992**, *57*, 4306.
13. (a) Araki, K.; Kuboki, T.; Otohata, M.; Kishimoto, N.; Yamada, M.; Shiraishi, S. *J. Chem. Soc., Dalton Trans.* **1993**, 3647. (b) Malachowski, M. R.; Huynh, H. B.; Tomlinson, L. J.; Kelly, R. S.; Furbee jun, J. W. *J. Chem. Soc., Dalton Trans.* **1995**, 31.
14. (a) Mckillop, A.; Ray, S. J. *Synthesis* **1977**, 847. (b) Tada, M.; Katsu, T. *Bull. Chem. Soc. Jpn.* **1972**, *45*, 2558 and references cited therein.
15. Frostin-Rio, M.; Pujol, D.; Bied-Charreton, C.; Perrée-Fauvet, M.; Gaudemer, A. *J. Chem. Soc., Perkin Trans. 1* **1984**, 1971.

Chapter 2. Complexation Behavior of Quinone Ligands Bearing *N*-Heterocyclic Coordination Sites

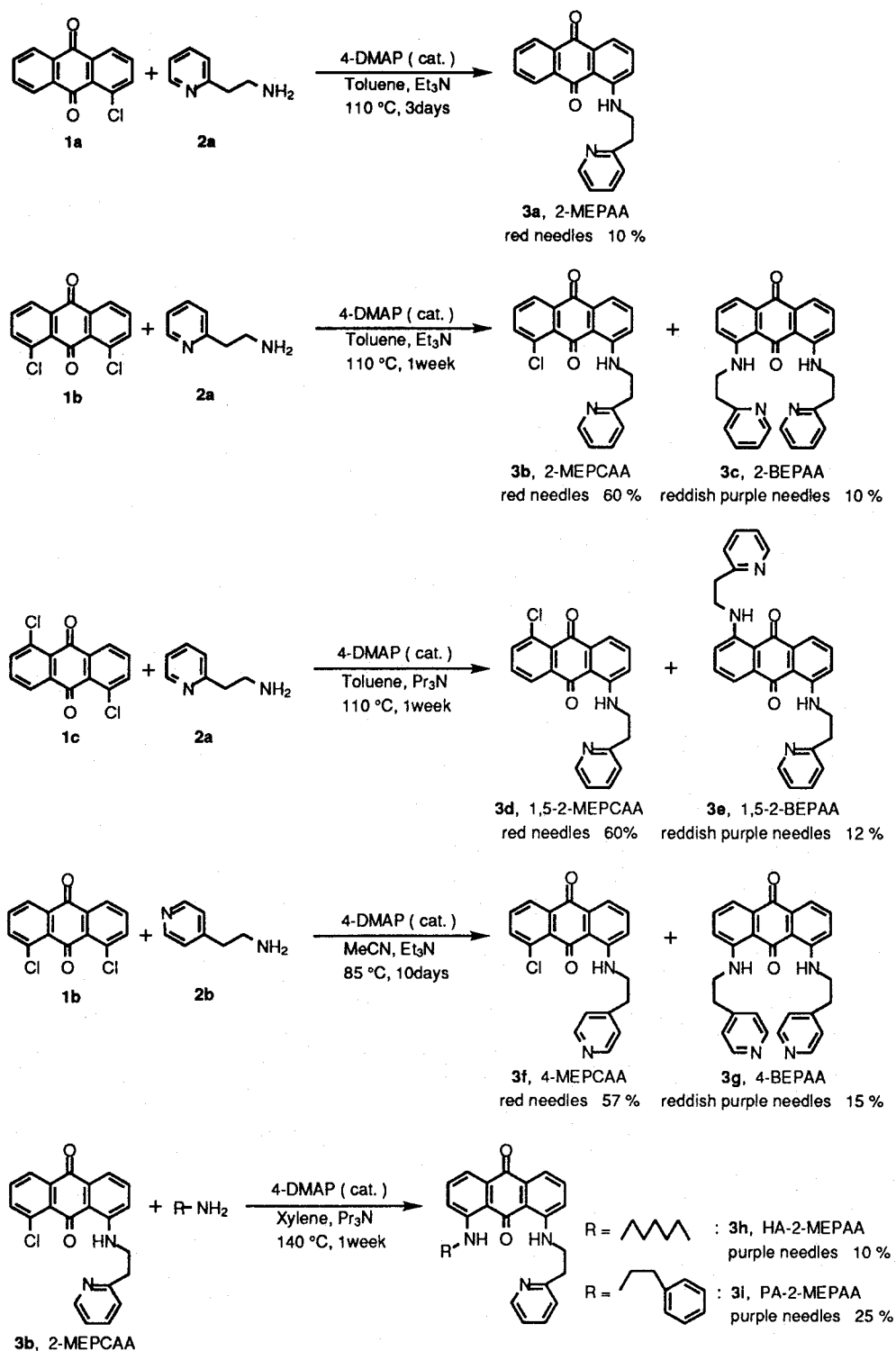
2-1. Introduction

In a previous chapter, the coordination interaction between transition metals and the *N*-heterocyclic multidentate podand ligands is revealed to play an important role in the oxygenation reaction with molecular oxygen. A facile reversible redox process of transition metals is required to realize efficient catalytic redox reactions. In a previous paper,¹ the trimethyl ester of coenzyme PQQ, a novel coenzyme involved in a variety of dehydrogenases,² has been revealed to serve as a ligand forming a reversible redox cycle under oxygen atmosphere in the palladium-catalyzed oxidation of an olefin and α,β -epoxysilane. Further development of this concept is considered to require an investigation of the transition metal complexes with quinone ligands. This chapter describes the complexation behavior of quinone ligands bearing *N*-heterocyclic coordination sites.

2-2. Results and Discussion

The quinones **3** were prepared from the corresponding chloroanthraquinones (**1**) and amines (**2**) as shown in Scheme 1.³

Scheme 1



Complexation of **3b** with palladium(II) acetate in acetonitrile afforded the 1:1 blue palladium(II) complex **4b** (eq. 1). The formation of **4b**

was supported by spectrophotometric titration. A new absorption at 647 nm increased with isosbestic points up to the 1:1 ratio of **3b** / $[\text{Pd}(\text{OAc})_2]$, being accompanied by the disappearance of the absorption of **3b** at 505 nm (Figure 1). The saturated titration curve indicates that the 1:1 complex **4b** was formed (Figure 2). A similar spectral change was observed when **3a** was employed, **3a** was also found to form the 1:1 complex **4a** with palladium(II) acetate in acetonitrile (eq. 1, Figures 3, and 4).

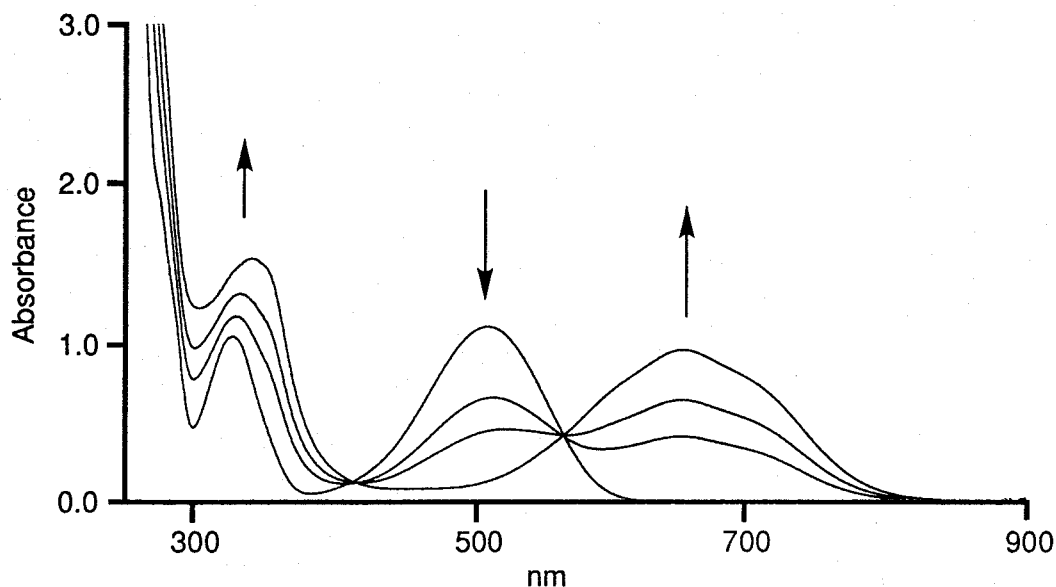
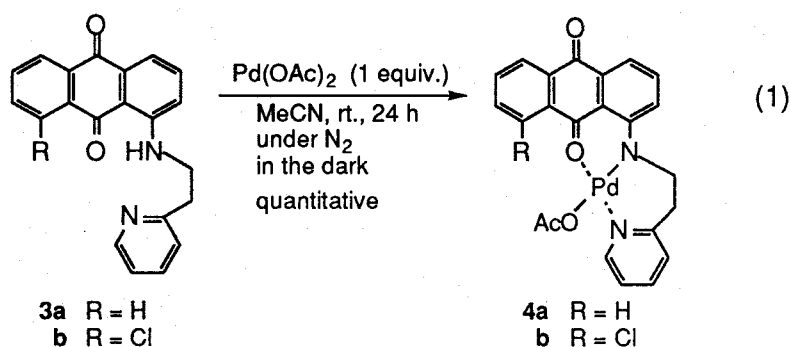


Figure 1. UV-vis. spectra of **4b** on treatment of **3b** with $\text{Pd}(\text{OAc})_2$. $[\text{3b}] = 1.0 \times 10^{-4} \text{ M}$; $[\text{Pd}(\text{OAc})_2] = 0, 0.4, 0.6, 1.0 \times 10^{-4} \text{ M}$; solv. MeCN; under nitrogen atmosphere.

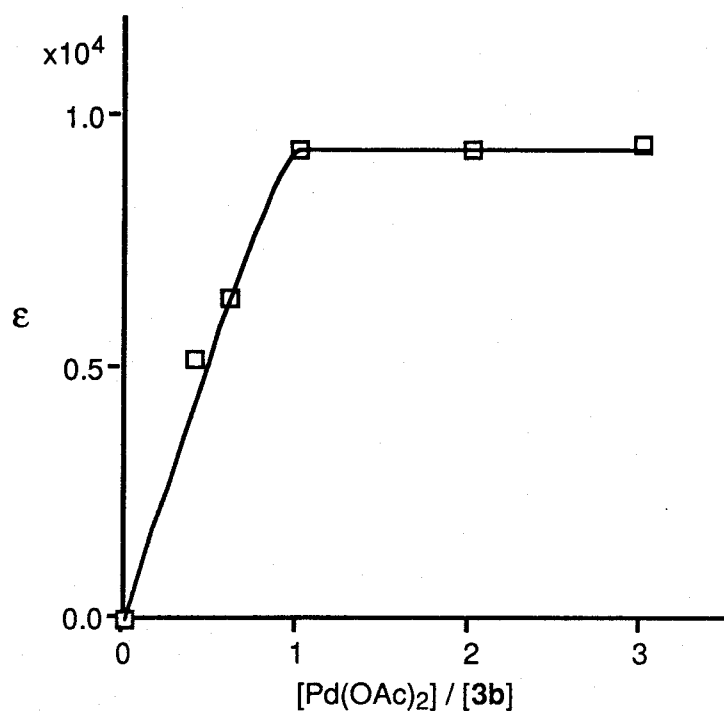


Figure 2. Spectrophotometric titration of **4b** at 647 nm.

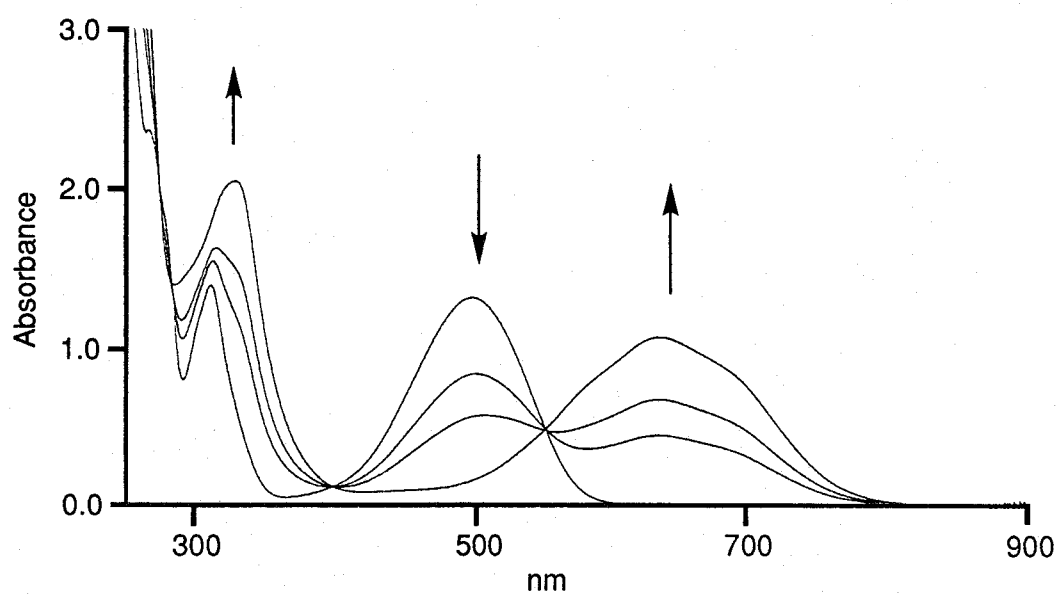


Figure 3. UV-vis. spectra of **4a** on treatment of **3a** with Pd(OAc)₂.
 [3a] = 1.0 × 10⁻⁴ M; [Pd(OAc)₂] = 0, 0.4, 0.6, 1.0 × 10⁻⁴ M; solv. MeCN; under nitrogen atmosphere.

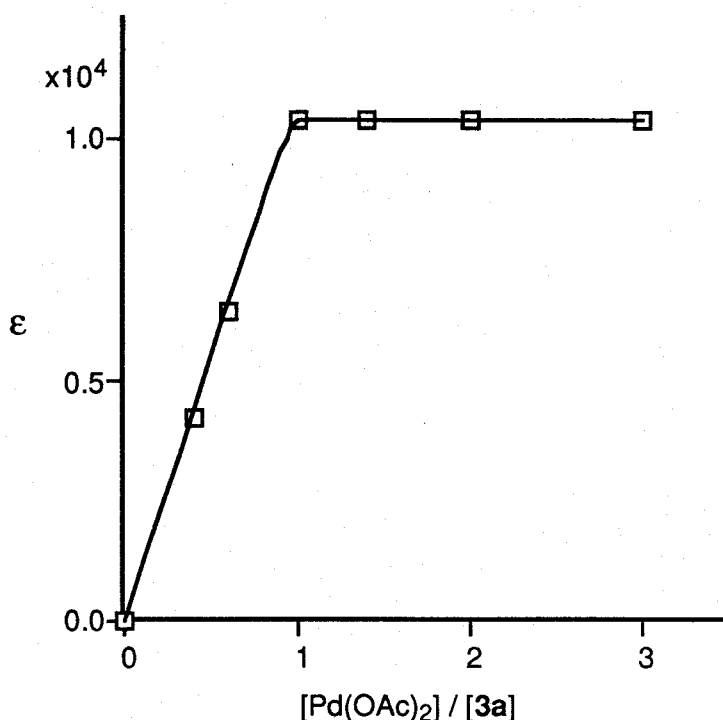


Figure 4. Spectrophotometric titration of **4a** at 638 nm.

The structure of the isolated complex **4a** and **4b** were elucidated by ¹H-NMR. Only one acetoxyl group was detected, indicating the displacement of palladium(II) acetate with the amino nitrogen of quinone ligands. The down-field shift of the pyridyl protons implies the coordination of the pyridyl nitrogen to palladium.

Further structural information of **4b** was obtained by X-ray crystal structure determination (Figure 5 and Table 1). The quinone oxygen and pyridyl nitrogen coordinate *trans* to the palladium. The coordination geometry is a nearly square planar with the palladium-bonded amino nitrogen in a position *trans* to the acetoxyl group. Another interesting feature is the bent anthraquinone skeleton of **4b**, being in sharp contrast with the planar one of **3b** (Figure 6 and Table 1).

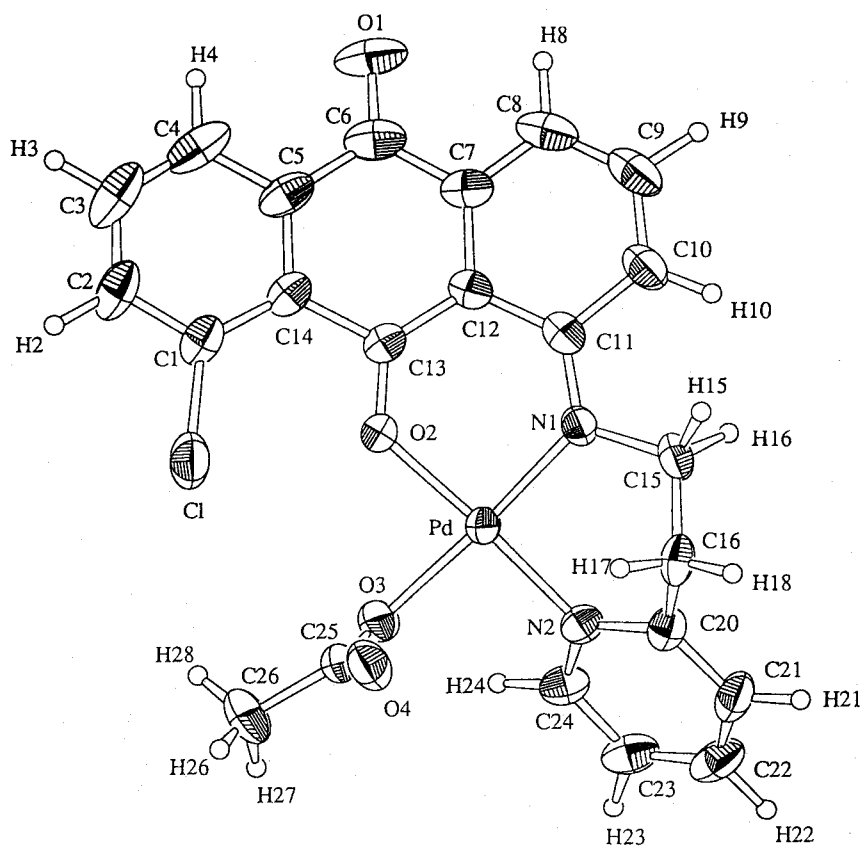


Figure 5. ORTEP view of the X-ray crystal structure of **4b** (40% probability ellipsoids). H₂O is omitted for clarity.

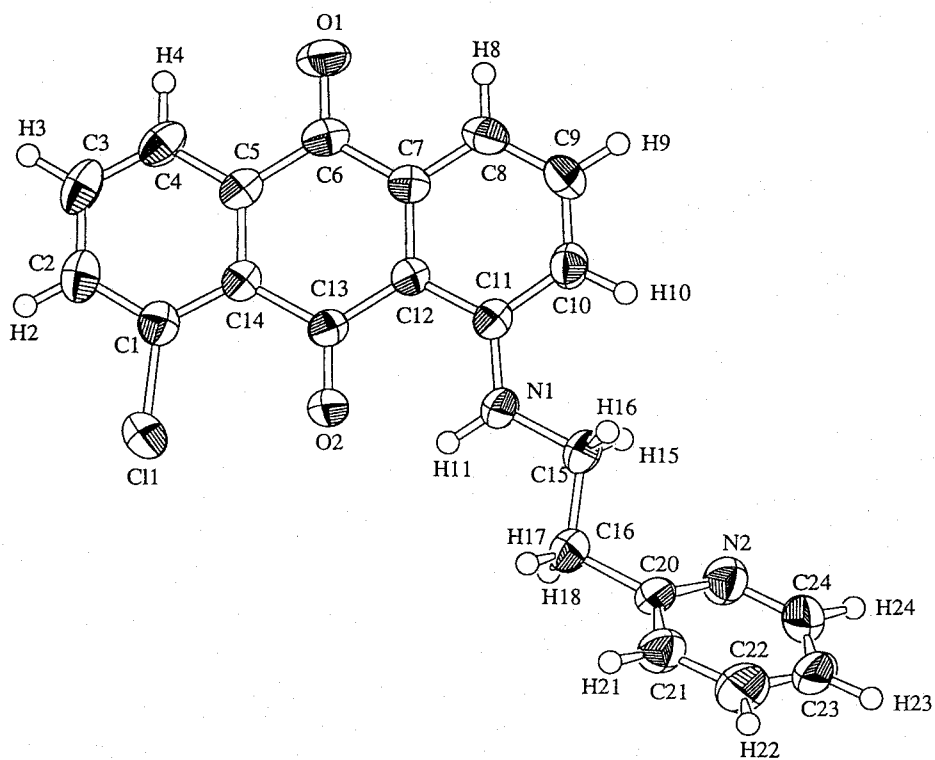


Figure 6. ORTEP view of the X-ray crystal structure of **3b** (40% probability ellipsoids).

Table 1. Crystallographic Data for **3b**, **4b**, and **4l**

	3b	4b	4l
formula	C ₂₁ H ₁₅ N ₂ O ₂ Cl	C ₂₃ H ₁₉ N ₂ O ₅ ClPd	C ₃₁ H ₂₇ N ₃ O ₄ Pd
mol wt	362.81	545.27	611.97
cryst system	monoclinic	monoclinic	monoclinic
space group	<i>P</i> 2 ₁ / <i>n</i>	<i>P</i> 2 ₁ / <i>c</i>	<i>P</i> 2 ₁ / <i>a</i>
<i>a</i> , Å	7.054(3)	10.212(9)	11.000(7)
<i>b</i> , Å	10.605(3)	8.004(4)	14.747(10)
<i>c</i> , Å	22.582(2)	26.005(3)	31.89(1)
β , deg	94.02(2)	93.91(2)	90.36(5)
<i>V</i> , Å ³	1685.0(7)	2120(1)	5172(4)
<i>Z</i>	4	4	8
<i>D</i> _{calcd} , g cm ⁻³	1.430	1.708	1.572
μ (Mo K α), cm ⁻¹	2.45	10.41	7.62
<i>T</i> , °C	23	23	23
λ (Mo K α), Å	0.71069	0.71069	0.71069
<i>R</i>	0.068	0.043	0.078
<i>R</i> _w	0.108	0.030	0.068

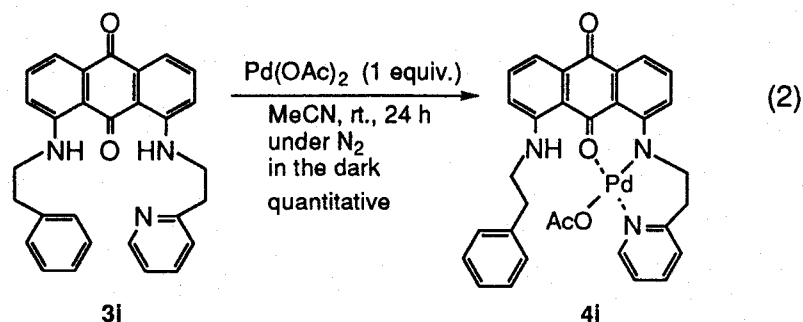
Selected bond distances and angles of **3b** and **4b** are summarized in Table 2. The bond angle C(13)–O(2)–Pd is 127.7(3)°. No typical difference was observed in the O(1)–C(6) bonds of **3b** and **4b**, but the coordinated carbonyl bond distance of **4b** is 0.04 Å longer than the non-coordinated one. These findings are supported by the IR spectral difference ($\nu_{\text{C=O}}$ **3b**: 1659, 1635 cm⁻¹; **4b**: 1654, 1624 cm⁻¹). In this connection, the bond distances of both N(1)–C(11) and C(12)–C(13) are shortened upon complexation, which is correlated to the conjugated 6-membered palladacycle.

Table 2. Selected Bond Distances (Å) and Bond Angles (deg)
for **3b**, **4b**, and **4l**

	3b	4b	4l
Bond Distances			
Pd–O(2)	-----	1.970(3)	1.964(9)
Pd–O(3)	-----	2.030(3)	2.050(2)
Pd–N(1)	-----	1.974(3)	1.940(2)
Pd–N(2)	-----	2.009(4)	1.990(1)
O(1)–C(6)	1.214(7)	1.216(6)	1.220(2)
O(2)–C(13)	1.222(7)	1.263(5)	1.300(2)
N(1)–C(11)	1.363(8)	1.327(5)	1.350(2)
C(10)–C(11)	1.421(9)	1.447(6)	1.420(3)
C(11)–C(12)	1.425(9)	1.457(6)	1.440(2)
C(12)–C(13)	1.476(8)	1.414(6)	1.420(3)
C(13)–C(14)	1.507(8)	1.504(6)	1.450(2)
Bond Angles			
O(2)–Pd–O(3)	-----	85.6(1)	90.8(5)
O(2)–Pd–N(1)	-----	90.8(1)	88.5(5)
O(3)–Pd–N(2)	-----	89.3(2)	85.0(5)
N(1)–Pd–N(2)	-----	94.3(2)	95.6(6)
O(2)–Pd–N(2)	-----	172.6(2)	175.1(4)
O(3)–Pd–N(1)	-----	176.3(1)	176.9(8)
C(13)–O(2)–Pd	-----	127.7(3)	128.0(1)
C(11)–N(1)–Pd	-----	124.1(3)	124.0(1)
O(2)–C(13)–C(12)	121.5(5)	125.3(4)	122.0(1)
C(11)–C(12)–C(13)	120.5(5)	122.3(4)	122.0(1)
C(12)–C(11)–N(1)	122.3(5)	124.9(4)	122.0(2)
C(10)–C(11)–N(1)	120.0(6)	119.8(4)	121.0(1)
C(11)–N(1)–C(15)	123.3(5)	117.4(4)	114.0(1)
O(2)–C(13)–C(14)	119.6(5)	113.8(5)	114.0(1)

On the basis of these observations, the effect of the pendant moiety at the 8-position was examined. The quinone ligand **3i** bearing the

phenethyl group at the 8-position was also found to form the 1:1 complex **4i** with palladium(II) acetate in acetonitrile (eq. 2).



The formation of **4i** was checked by spectrophotometric titration as observed with **4b**. The spectral change with isosbestic points was observed up to the 1:1 ratio of $[3i] / [Pd(OAc)_2]$ (Figures 7 and 8). In the 1H -NMR spectra of the isolated complex **4i**, the down-field shift of the pyridyl protons and no shift of the phenethyl group indicated that the amino nitrogen of the phenethylamino group does not contribute to the coordination.

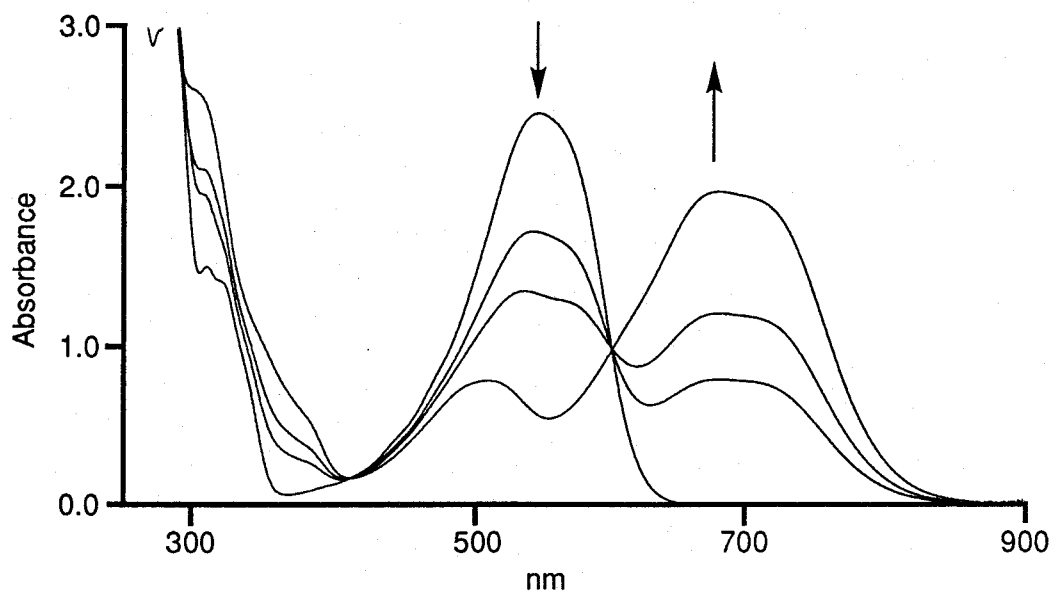


Figure 7. UV-vis. spectra of **4i** on treatment of **3i** with $Pd(OAc)_2$. $[3i] = 1.0 \times 10^{-4} M$; $[Pd(OAc)_2] = 0, 0.4, 0.6, 1.0 \times 10^{-4} M$; solv. MeCN; under nitrogen atmosphere.

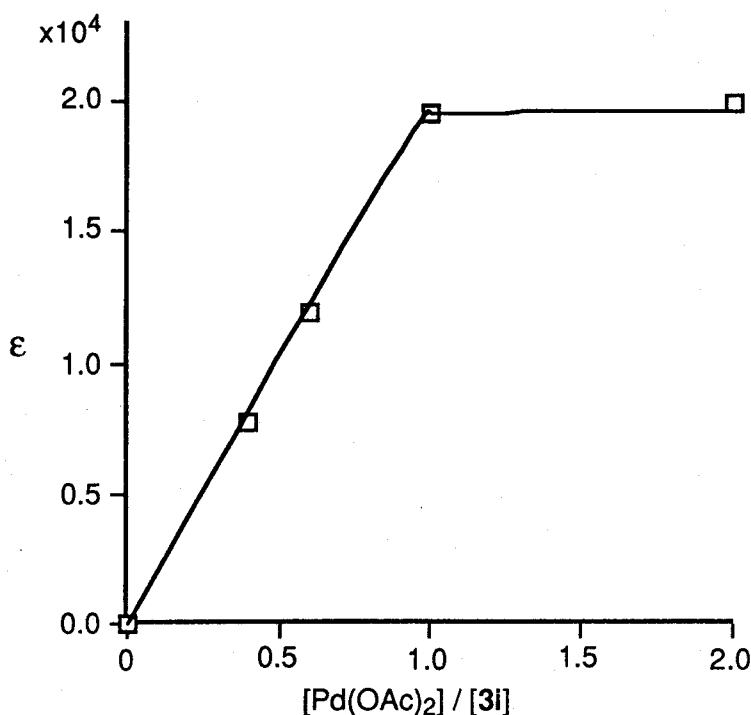


Figure 8. Spectrophotometric titration of **4i** at 675 nm.

X-ray crystal structure determination of **4i** also showed the same conformation as **4b** (Figure 9, Tables 1, and 2). It should, however, be noted that the calculated position of the *para* phenyl hydrogen atom is located almost facing the π -electrons of the pyridyl ring of the neighboring molecule in the crystal structure of **4i** (Figure 10). The distance between the hydrogen and the center of the pyridyl ring is 2.78 Å, which suggests the existence of a π hydrogen bond⁴ (edge-to-face interaction) between the phenyl hydrogen and pyridyl ring of the other molecule in the crystal structure. The dihedral angle between the least-square planes of the phenyl and pyridyl groups is 76.3°. These distance and angle values are reasonable for the edge-to-face interaction.

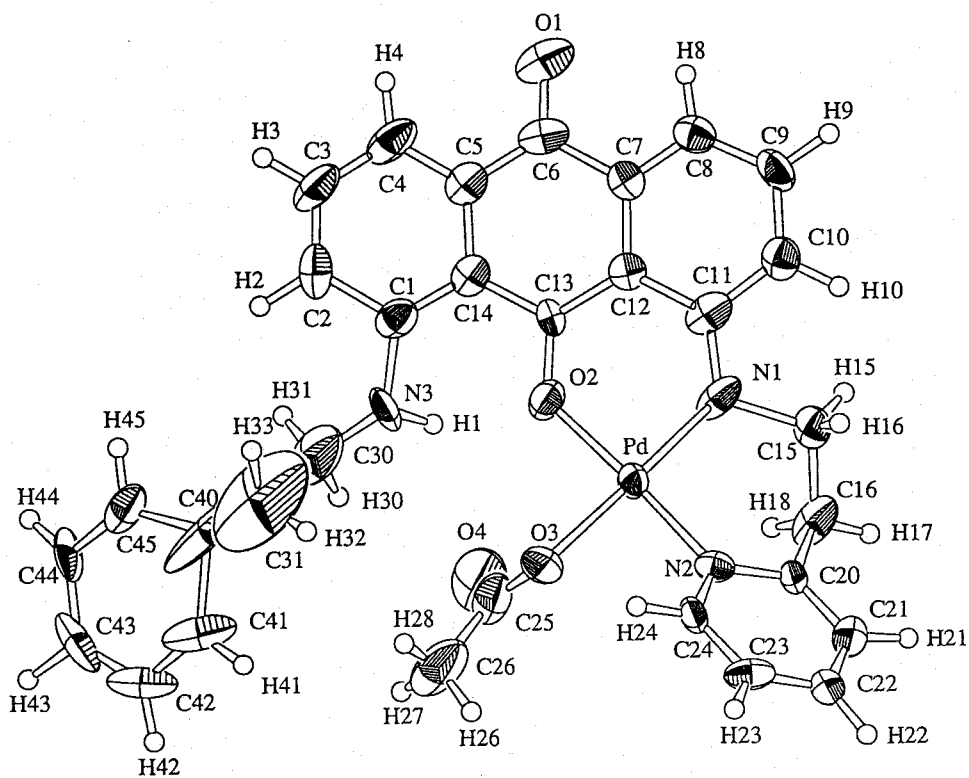


Figure 9. ORTEP view of the X-ray crystal structure of **4i** (40% probability ellipsoids).

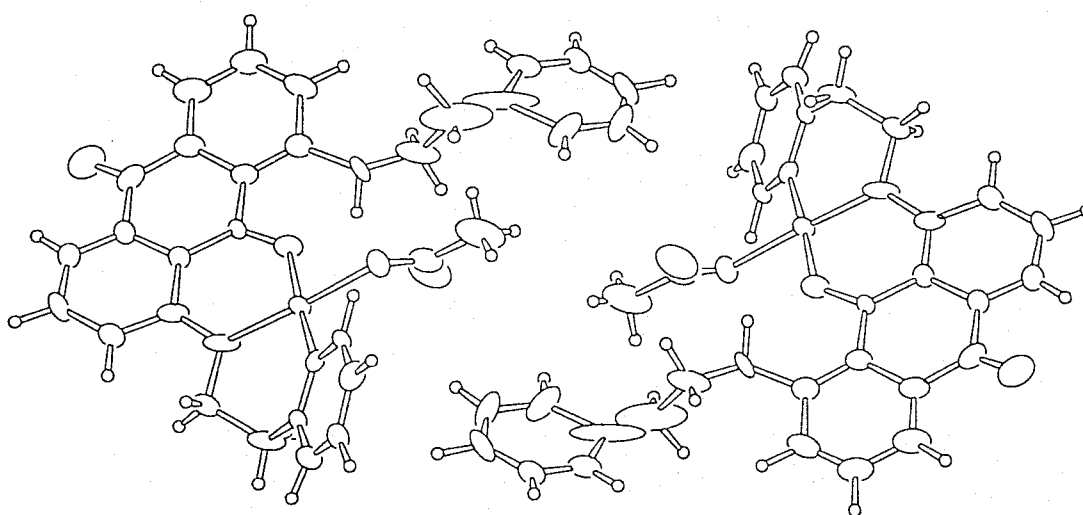
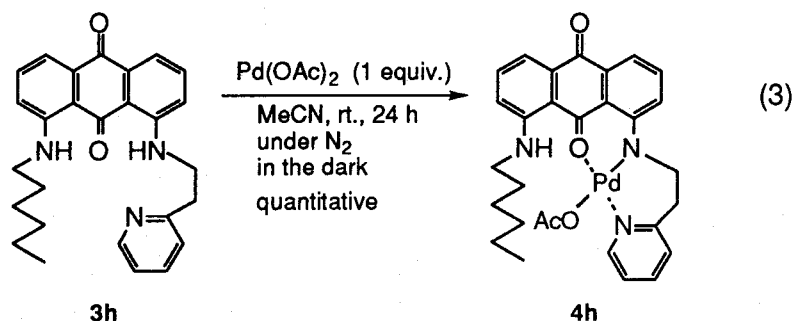
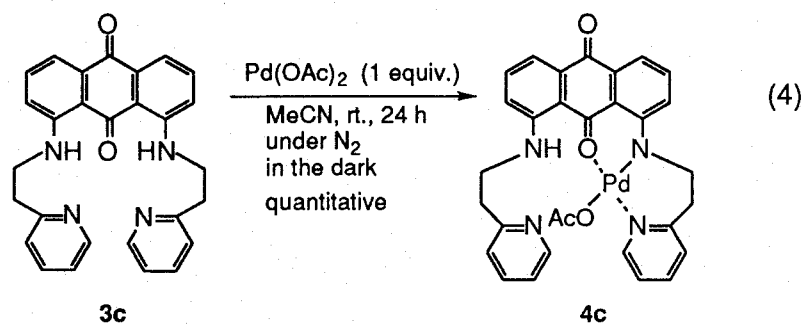


Figure 10. Unit cell of **4i**.

A similar spectral change based on such a complexation was observed to give the complex **4h** when **3h** was employed (eq. 3).



Although **3c** bearing two 2-pyridyl groups was expected to form the 1:2 complex, **3c** was also found to form the 1:1 complex **4c** with palladium(II) acetate in acetonitrile (eq. 4). The formation of **4c** was checked by spectrophotometric titration as observed with **4b**. The spectral change with isosbestic points was observed up to the 1:1 ratio of $[\mathbf{3c}] / [\text{Pd}(\text{OAc})_2]$ (Figure 11).



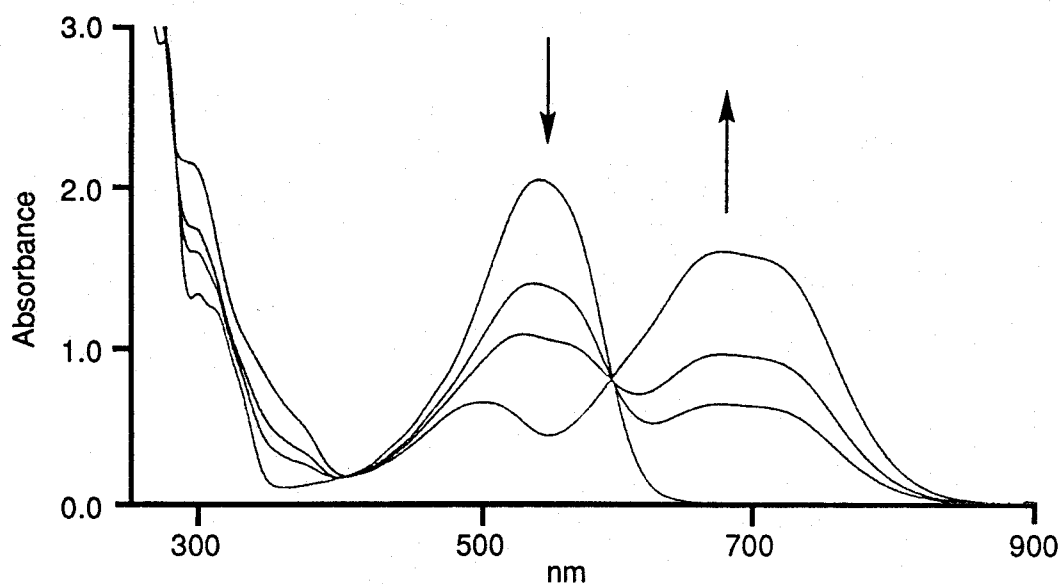
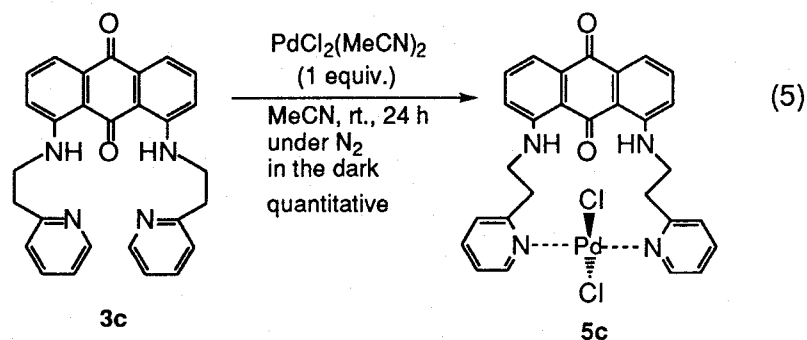


Figure 11. UV-vis. spectra of **4c** on treatment of **3c** with $\text{Pd}(\text{OAc})_2$. $[\mathbf{3c}] = 1.0 \times 10^{-4} \text{ M}$; $[\text{Pd}(\text{OAc})_2] = 0, 0.4, 0.6, 1.0 \times 10^{-4} \text{ M}$; solv. MeCN; under nitrogen atmosphere.

The quinone **3c** showed the different complexation behavior with palladium(II) chloride as shown in eq. 5. Only the pyridyl nitrogens coordinated to the palladium.



The formation of **5c** was checked by spectrophotometric titration. The spectral change with isosbestic points was observed up to the 1:1 ratio of $[\mathbf{4c}] / [\text{PdCl}_2]$ (Figure 12).

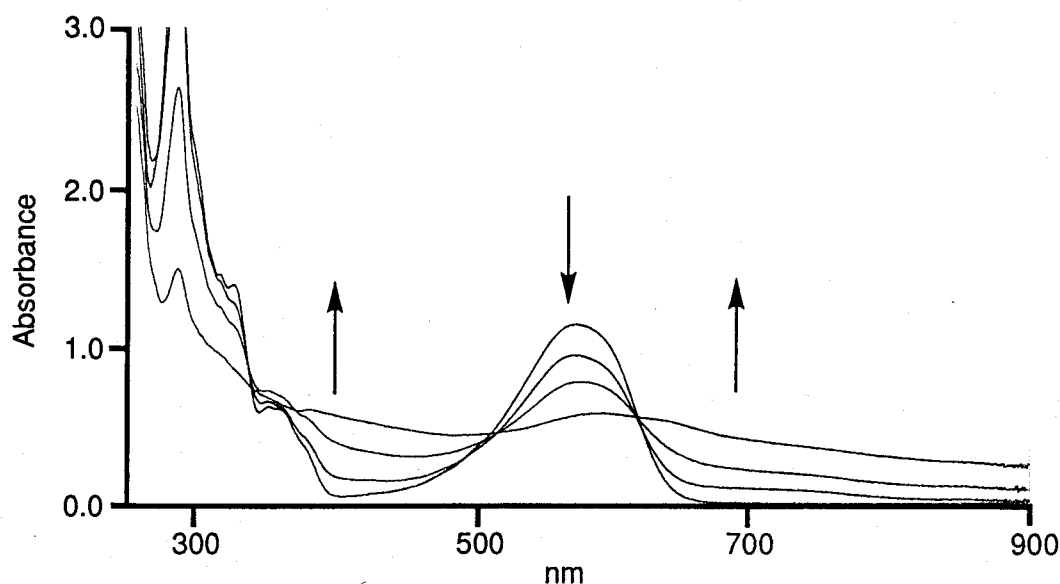
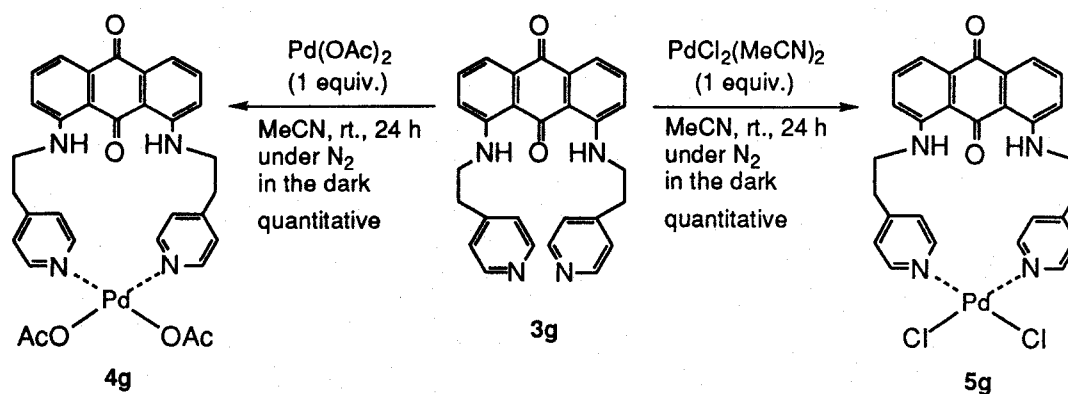


Figure 12. UV-vis. spectra of **5c** on treatment of **3c** with PdCl_2 . $[\mathbf{3c}] = 1.0 \times 10^{-4} \text{ M}$; $[\text{PdCl}_2] = 0, 0.4, 0.6, 1.0 \times 10^{-4} \text{ M}$; solv. MeCN; under nitrogen atmosphere.

The structure of the isolated complex **5c** was elucidated by ^1H -NMR. The down-field shift of the pyridyl protons implies the coordination of the pyridyl nitrogen to palladium. The down-field shift of the pyridyl protons and no remarkable shift of the anthraquinone group indicated that the quinone oxygen does not contribute to coordination and only the pyridyl nitrogens coordinate to palladium. IR spectra also showed that the pyridyl nitrogens coordinate *trans* to palladium.

In comparison with **3c**, the quinone oxygen of **3g** bearing two 4-pyridyl groups did not coordinate and only the pyridyl nitrogens coordinate to palladium of both palladium(II) acetate or palladium(II) chloride (Scheme 2). Complexation behavior of quinone ligands depends on the coordination site, the *cis* complex **3g** was formed with palladium(II) chloride.

Scheme 2



Further structural information of **5g** was obtained by X-ray crystal structure determination (Figure 13, Tables 3, and 4). Only the pyridyl nitrogens coordinate *cis* to the palladium, being in sharp contrast with **4b**. The coordination geometry is a nearly square planar with the palladium-bonded amino nitrogen in a position *trans* to the acetoxyl group.

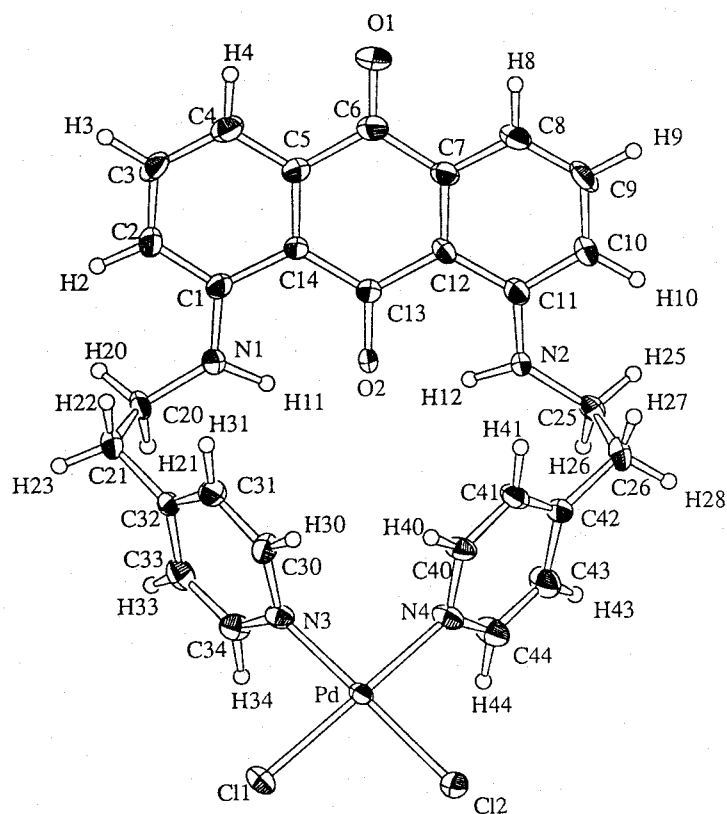


Figure 13. ORTEP view of the X-ray crystal structure of **5g** (40% probability ellipsoids). CH_3CN is omitted for clarity.

Table 3. Crystallographic Data for **5g**

5g	
formula	C ₃₀ H ₂₇ N ₅ O ₂ Cl ₂ Pd
mol wt	666.90
cryst system	triclinic
space group	$P\bar{1}$
<i>a</i> , Å	11.384(7)
<i>b</i> , Å	16.766(4)
<i>c</i> , Å	8.100(2)
α , deg	102.59(2)
β , deg	105.01(1)
γ , deg	76.23(2)
<i>V</i> , Å ³	1430.0(5)
<i>Z</i>	2
<i>D</i> _{calcd} , g cm ⁻³	1.453
μ (Mo K α), cm ⁻¹	8.58
<i>T</i> , °C	23
λ (Mo K α), Å	0.71069
<i>R</i>	0.071
<i>R</i> _w	0.063

Table 4. Selected Bond Distances (Å) and Bond Angles (deg) for **5g**

5g	
Bond Distances	
Pd–Cl(1)	2.300(2)
Pd–Cl(2)	2.291(3)
Pd–N(3)	1.992(8)
Pd–N(4)	2.061(7)
O(1)–C(6)	1.21(1)
O(2)–C(13)	1.243(10)
N(1)–C(1)	1.37(1)
N(2)–C(11)	1.35(1)
Bond Angles	
Cl(1)–Pd–Cl(2)	92.17(9)
Cl(1)–Pd–N(3)	87.8(2)
Cl(2)–Pd–N(4)	89.3(2)
N(3)–Pd–N(4)	90.6(3)
Cl(1)–Pd–N(4)	176.1(3)
Cl(2)–Pd–N(3)	177.4(2)
C(15)–N(4)–Pd	122.5(6)
C(19)–N(4)–Pd	120.4(6)
C(20)–N(3)–Pd	125.0(7)
C(24)–N(3)–Pd	121.0(7)

On the basis of these observations, the quinone ligand bearing the pendant moieties at both the 1- and 5-position was examined. The quinone ligand **3e** bearing two 2-(2-pyridyl)ethyl groups at the 1- and 5-positions was found to form the 1:1 complex **5e** and the 1:2 complex **6e** with palladium(II) acetate in acetonitrile (Scheme 3). The formation of **5e** and **6e** was supported by spectrophotometric titration. The spectral change with isosbestic points was observed up to the 1:1 ratio and up to the 1:2 ratio of [**3i**] / [Pd(OAc)₂] (Figures 14 and 15).

Scheme 3

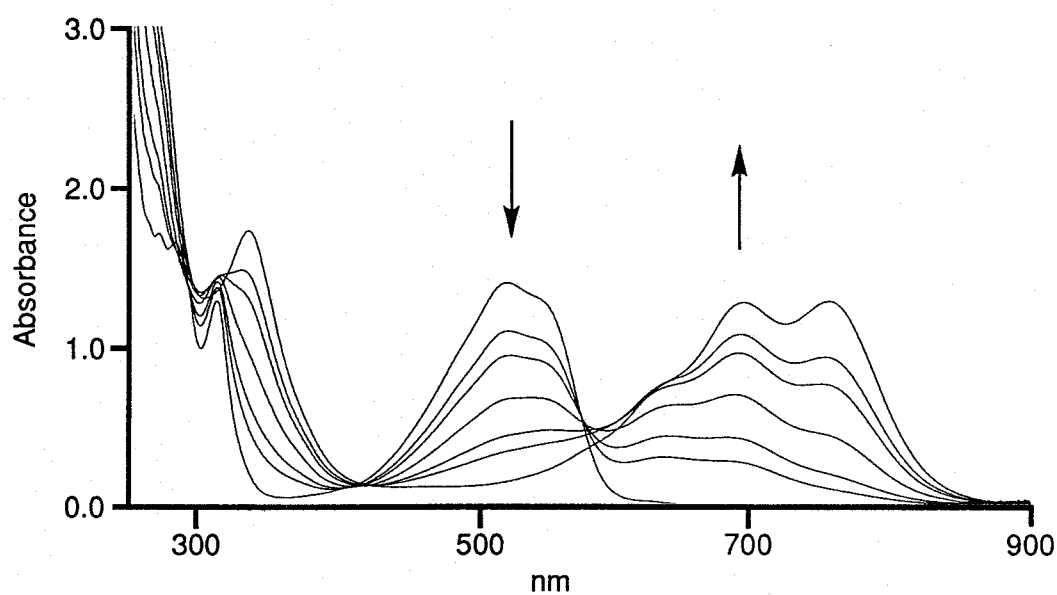
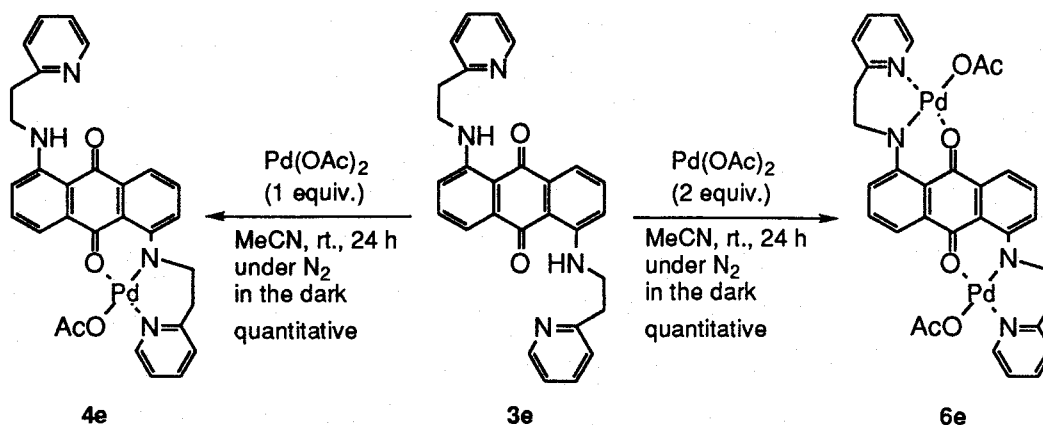


Figure 14. UV-vis. spectra of **4e** and **6e** on treatment of **3e** with $\text{Pd}(\text{OAc})_2$. $[\text{3e}] = 1.0 \times 10^{-4}$ M; $[\text{Pd}(\text{OAc})_2] = 0, 0.4, 0.6, 1.0, 1.4, 1.6, 2.0 \times 10^{-4}$ M; solv. CH_2Cl_2 ; under nitrogen atmosphere.

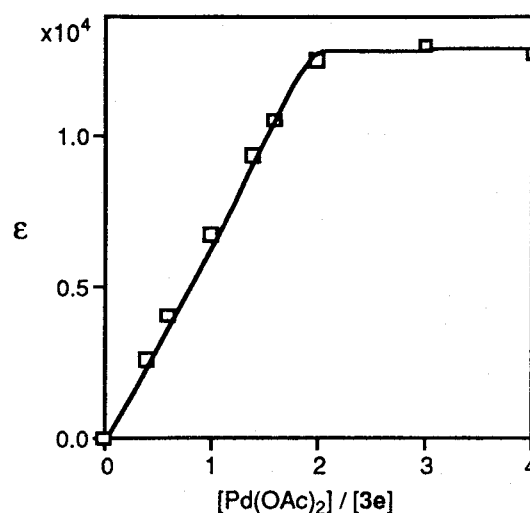


Figure 15. Spectrophotometric titration at 691nm.

The redox properties of **4** were investigated by cyclic voltammetry using 0.1 M Bu₄NClO₄ as a supporting electrolyte in acetonitrile at a 50 mVs⁻¹ scan rate (Table 5). Four separate reversible redox couples were observed depending on the palladium and quinone redox, indicating the smooth redox interaction between them. These results are also consistent with the structures of **4**. On the contrary, **5** only showed two separate reversible redox couples depending on the quinone redox.

Table 5. Redox Potential

Ligand and Complex		E _{1/2} ^a			
3a		-0.98		-1.43	
4a	-0.83	-1.00	-1.28	-1.49	
3b		-0.93		-1.42	
4b	-0.79	-0.93	-1.21	-1.42	
3c		-1.06		-1.55	
4c	-0.90	-1.04	-1.28	-1.47	
3e		-1.05		-1.58	
4e	-0.87	-1.05	-1.31	-1.57	
3h		-1.07		-1.59	
4h	-0.91	-1.05	-1.37	-1.60	
3i		-1.05		-1.59	
4i	-0.91	-1.05	-1.33	-1.55	

^a V vs. SCE

2-3. Conclusion

Synthesis and characterization of the Pd(II)-quinone complexes bearing a heterocyclic pendant functional group are presented here. The complexation behavior of quinone ligands is disclosed to depend on the coordination sites or gegen ions. In the case of palladium(II) complexes in which the quinone oxygen coordinates to palladium, four separate reversible redox couples based on the smooth redox interaction between palladium and quinone are observed. Both these complexes and the Pd(0)-quinone complexes⁵ are indispensable to each other for elucidating the redox interaction via electron transfer.

2-4. Experimental

General

Melting points were measured using Yanagimoto micromelting point apparatus and are uncorrected. Infrared spectra were recorded on a Perkin-Elmer FT-IR 1605 infrared. ¹H-NMR spectra were recorded on a Bruker AM-600 (600MHz) spectrometer and a JEOL JNM-GSX-400 (400MHz) spectrometer with tetramethylsilane as an internal standard. UV-vis. spectra were recorded using a Hitachi U-3000. The X-ray crystallography was made on Rigaku AFC5R diffractometer. The fast atom bombardment mass spectra were run on a JEOL JMS-DX303HF spectrometer. Recycling preparative HPLC analysis was performed on a JAI LC-908. The standard electrochemical instrumentation consisted of a Hokuto Denko potentiostat / galvanostat HA-301S and a Hokuto Denko function generator HB-104S with a three-electrode system consisting of a glassy carbon working electrode, a platinum auxiliary electrode, and a

KCl-saturated calomel reference electrode. Cyclic voltammograms were recorded with Graphtec WX 1000.

Synthesis of 1-(2-(2-Pyridyl)ethylamino)anthraquinone (3a). A mixture of 1-chloroanthraquinone (**1a**, 2.43 g, 10.0 mmol), 2-(2-aminoethyl)pyridine (**2a**, 3.05 g, 25.0 mmol), and a catalytic amount of 4-dimethylaminopyridine (49 mg, 0.40 mmol) in the presence of triethylamine (10.1 g, 100 mmol) was stirred in toluene (100 mL) at 110 °C for 3 days. After evaporation of the toluene solution in vacuo, the resulting mixture was diluted with chloroform (60 mL), washed with saturated NaHCO₃ aqueous solution and brine, and dried over MgSO₄. Red solid was obtained by evaporation of the chloroform solution in vacuo. The quinone **3a** was isolated in 43 % yield by silica-gel column chromatography eluting with ethyl acetate and purified as a red needle by recrystallization from chloroform-hexane (1:3 v/v).

3a: Mp 119-120 °C (uncorrected); R_f = 0.45 (ethyl acetate); IR (KBr, cm⁻¹) 1664, 1629 (C=O); ¹H-NMR (400 MHz, CD₃CN) δ 9.77 (br, 1H), 8.55 (dd, 1H, J = 4.9, 1.9 Hz), 8.22 (dd, 1H, J = 7.6, 1.5 Hz), 8.16 (dd, 1H, J = 7.6, 1.5 Hz), 7.82 (dt, 1H, J = 7.6, 1.5 Hz), 7.76 (dt, 1H, J = 7.6, 1.5 Hz), 7.68 (dt, 1H, J = 7.7, 1.8 Hz), 7.60 (dd, 1H, J = 8.6, 7.3 Hz), 7.51 (dd, 1H, J = 7.3, 1.2 Hz), 7.32 (dd, 1H, J = 7.8, 1.2 Hz), 7.26 (dd, 1H, J = 8.6, 1.2 Hz), 7.20 (ddd, 1H, J = 7.7, 4.9, 1.2 Hz), 3.80 (q, 2H, J = 6.9 Hz), 3.19 (t, 2H, J = 6.9 Hz); MS (EI) m/z 328 (M⁺); Anal. Calcd. for C₂₁H₁₆N₂O₂: C, 76.81; H, 4.91; N, 8.53. Found: C, 76.69; H, 4.90; N, 8.43.

Synthesis of 1-(2-(2-Pyridyl)ethylamino)-8-chloroanthraquinone (3b) and 1,8-Bis[2-(2-pyridyl)ethylamino]chloroanthraquinone (3c). A mixture of 1,8-dichloroanthraquinone (**1b**, 0.554 g, 2.0 mmol), 2-(2-aminoethyl)pyridine (**2a**, 1.22 g, 10.0 mmol) and a catalytic amount of 4-dimethylaminopyridine (2 mg, 0.16 mmol) in the presence of triethylamine (2.05 g, 40 mmol) was stirred in toluene (30 mL) at 110 °C

for 2 weeks. After evaporation of the toluene solution in vacuo, the resulting mixture was diluted with chloroform (30 mL), washed with saturated NaHCO₃ aqueous solution and brine, and dried over MgSO₄. The quinone **3b** (red needles) and **3c** (reddish purple needles) were isolated in 60 % and 10 % yield, respectively, by silica-gel column chromatography and purified by recrystallization from chloroform-hexane (1:3 v/v).

3b: Mp 168-170 °C (uncorrected); R_f = 0.45 (ethyl acetate-chloroform 1:1 v/v); IR (KBr, cm⁻¹) 1659, 1635 (C=O); ¹H-NMR (400 MHz, CD₃CN) δ 9.60 (br, 1H), 8.55 (dd, 1H, J = 4.9, 1.9 Hz), 8.18 (dd, 1H, J = 7.8, 1.4 Hz), 7.82 (dd, 1H, J = 7.8, 1.4 Hz), 7.68 (ddd, 1H, J = 7.8, 7.6, 1.9 Hz), 7.66 (t, 1H, J = 7.8 Hz), 7.58 (dd, 1H, J = 8.7, 7.4 Hz), 7.46 (dd, 1H, J = 7.4, 1.0 Hz), 7.32 (dd, 1H, J = 7.8, 1.1 Hz), 7.27 (dd, 1H, J = 8.7, 1.0 Hz), 7.20 (ddd, 1H, J = 7.6, 4.9, 1.1 Hz), 3.79 (q, 2H, J = 6.8 Hz), 3.18 (t, 2H, J = 6.8 Hz); MS (EI) m/z 362 (M⁺); Anal. Calcd. for C₂₁H₁₅N₂O₂Cl: C, 69.52; H, 4.17; N, 7.72; Cl, 9.77. Found: C, 69.26; H, 4.09; N, 7.64; Cl, 9.86.

3c: Mp 178-180 °C (uncorrected); R_f = 0.19 (ethyl acetate); IR (KBr, cm⁻¹) 1661, 1624 (C=O); ¹H-NMR (400 MHz, CD₃CN) δ 9.61 (br, 2H), 8.56 (dd, 2H, J = 4.9, 1.8 Hz), 7.68 (dt, 2H, J = 7.7, 1.8 Hz), 7.51 (dd, 2H, J = 8.6, 7.9 Hz), 7.42 (dd, 2H, J = 7.9, 1.1 Hz), 7.33 (dd, 2H, J = 7.7, 1.2 Hz), 7.21 (ddd, 2H, J = 7.7, 4.9, 1.2 Hz), 7.19 (dd, 2H, J = 8.6, 1.1 Hz), 3.75 (q, 4H, J = 6.7 Hz), 3.18 (t, 4H, J = 6.7 Hz); MS (EI) m/z 448 (M⁺); Anal. Calcd. for C₂₈H₂₄N₄O₂·H₂O: C, 72.09; H, 5.62; N, 12.01. Found: C, 72.29; H, 5.25; N, 11.65.

Synthesis of 1-[2-(2-Pyridyl)ethylamino]-5-chloroanthraquinone (3d) and 1,5-Bis[2-(2-pyridyl)ethylamino]chloroanthraquinone (3e). A mixture of 1,5-dichloroanthraquinone (**1c**, 1.39 g, 5.0 mmol), 2-(2-aminoethyl)pyridine (**2a**, 3.05 g, 25 mmol) and a catalytic amount of 4-dimethylaminopyridine (0.05 g, 0.40 mmol) in the presence of tripropylamine (7.16 g, 50 mmol) was stirred in toluene (70 mL) at 110 °C for 1 weeks. After evaporation of the toluene solution in vacuo, the

resulting mixture was diluted with chloroform (30 mL), washed with saturated NaHCO₃ aqueous solution and brine, and dried over MgSO₄. The quinone **3d** (red needles) and **3e** (reddish purple needles) were isolated in 60 % and 12 % yield, respectively, by silica-gel column chromatography and purified by recrystallization from chloroform-hexane (1:3 v/v).

3d: Mp 166-167 °C (uncorrected); R_f = 0.45 (ethyl acetate); IR (KBr, cm⁻¹) 1664, 1626 (C=O); ¹H-NMR (600 MHz, CDCl₃) δ 9.73 (br, 1H), 8.61 (dd, 1H, J = 4.8, 0.9 Hz), 8.28 (dd, 1H, J = 7.7, 1.1 Hz), 7.69 (dd, 1H, J = 8.1, 1.1 Hz), 7.64-7.60 (m, 2H), 7.55-7.53 (m, 2H), 7.26 (dd, 1H, J = 7.6, 1.1 Hz), 7.17 (ddd, 1H, J = 7.5, 4.8, 1.1 Hz), 7.10 (dd, 1H, J = 6.3, 6.0 Hz), 3.79 (q, 2H, J = 7.0 Hz), 3.22 (t, 2H, J = 7.0 Hz); MS (EI) m/z 362 (M⁺); Anal. Calcd. for C₂₁H₁₅N₂O₂Cl: C, 69.52; H, 4.17; N, 7.72; Cl, 9.77. Found: C, 69.18; H, 4.23; N, 7.84; Cl, 9.69.

3e: Mp 169-170 °C (uncorrected); R_f = 0.30 (ethyl acetate); IR (KBr, cm⁻¹) 1611 (C=O); ¹H-NMR (400 MHz, CD₃CN) δ 9.70 (br, 2H), 8.54 (dd, 2H, J = 4.9, 1.8 Hz), 7.69 (dt, 2H, J = 7.7, 1.8 Hz), 7.55 (dd, 2H, J = 7.7, 7.5 Hz), 7.45 (dd, 2H, J = 7.5, 1.0 Hz), 7.31 (dd, 2H, J = 7.7, 0.9 Hz), 7.21 (ddd, 2H, J = 7.7, 4.9, 0.9 Hz), 7.15 (dd, 2H, J = 7.7, 1.0 Hz), 3.76 (q, 4H, J = 6.9 Hz), 3.17 (t, 4H, J = 6.9 Hz); MS (EI) m/z 448 (M⁺); Anal. Calcd. for C₂₈H₂₄N₄O₂·0.5H₂O: C, 74.98; H, 5.39; N, 12.49. Found: C, 73.29; H, 5.33; N, 12.15.

Synthesis of 1-[2-(4-Pyridyl)ethylamino]-8-chloroanthraquinone (3f) and 1,8-Bis{2-(4-pyridyl)ethylamino}chloroanthraquinone (3g). A mixture of 1,8-dichloroanthraquinone (**1b**, 1.39 g, 5.0 mmol), 4-(2-aminoethyl)pyridine (**2b**, 2.44 g, 20.0 mmol) and a catalytic amount of 4-dimethylaminopyridine (0.05 g, 0.40 mmol) in the presence of triethylamine (5.06 g, 50 mmol) was stirred in acetonitrile (50 mL) at 85 °C for 10 days. After evaporation of the acetonitrile solution in vacuo, the resulting mixture was diluted with chloroform (30 mL), washed with

saturated NaHCO₃ aqueous solution and brine, and dried over MgSO₄. The quinone **3f** (red needles) and **3g** (reddish purple needles) were isolated in 57 % and 15 % yield, respectively, by silica-gel column chromatography and purified by recrystallization from chloroform-hexane (1:3 v/v).

3f: Mp 155-156 °C (uncorrected); *R_f* = 0.23 (ethyl acetate); IR (KBr, cm⁻¹) 1661, 1626 (C=O); ¹H-NMR (400 MHz, CD₃CN) δ 9.52 (br, 1H), 8.51 (d, 2H, *J* = 5.9 Hz), 8.18 (dd, 1H, *J* = 7.8, 1.2 Hz), 7.82 (dd, 1H, *J* = 8.1, 1.2 Hz), 7.66 (dd, 1H, *J* = 8.1, 7.8 Hz), 7.59 (dd, 1H, *J* = 8.5, 7.7 Hz), 7.48 (dd, 1H, *J* = 7.7, 1.0 Hz), 7.30 (d, 1H, *J* = 5.9 Hz), 7.25 (dd, 1H, *J* = 8.5, 1.0 Hz), 3.68 (q, 2H, *J* = 7.1 Hz), 3.05 (t, 2H, *J* = 7.1 Hz); MS (EI) *m/z* 362 (M⁺).

3g: Mp 184-185 °C (uncorrected); *R_f* = 0.53 (methanol); IR (KBr, cm⁻¹) 1655, 1616 (C=O); ¹H-NMR (600 MHz, CDCl₃) δ 9.60 (br, 2H), 8.56 (d, 4H, *J* = 5.3 Hz), 7.58 (dd, 2H, *J* = 7.6, 1.0 Hz), 7.50 (dd, 2H, *J* = 8.4, 7.6 Hz), 7.23 (d, 4H, *J* = 5.3 Hz), 7.04 (dd, 2H, *J* = 8.4, 1.0 Hz), 3.62 (q, 4H, *J* = 7.1 Hz), 3.05 (t, 4H, *J* = 7.1 Hz); MS (EI) *m/z* 448 (M⁺).

Synthesis of 1-{2-(2-Pyridyl)ethylamino}-8-(hexylamino)anthraquinone (3h). The quinone **3h** was prepared by treatment of **3b** (0.36 g, 1.0 mmol) with hexylamine (**2c**, 0.25 g, 2.5 mmol) in the presence of tripropylamine (1.43 g, 10 mmol) and a catalytic amount of 4-dimethylaminopyridine (0.01 g, 0.10 mmol) in xylene (20 mL) at 140 °C for 1 weeks. The quinone **3h** was isolated in 53 % yield by silica-gel column chromatography eluting with ethyl acetate-chloroform (3:1 v/v) and purified as a purple needle by recrystallization from chloroform-hexane (1:1 v/v).

3h: Mp 117-118 °C (uncorrected); *R_f* = 0.50 (ethyl acetate); IR (KBr, cm⁻¹) 1659, 1619 (C=O); ¹H-NMR (600 MHz, CD₂Cl₂) δ 9.71 (t, 1H, *J* = 5.4 Hz), 9.54 (t, 1H, *J* = 5.1 Hz), 8.55 (br, 1H), 7.60 (dt, 1H, *J* = 7.6, 1.8 Hz), 7.47-7.42 (m, 4H), 7.24 (dd, 1H, *J* = 7.6, 0.7 Hz), 7.15 (ddd, 1H, *J* = 7.6, 5.7, 0.7 Hz), 7.10 (dd, 1H, *J* = 6.6, 1.9 Hz), 7.00 (dd, 1H, *J* = 7.7, 1.9 Hz), 3.73 (dt, 2H, *J* = 7.0,

5.4 Hz), 3.28 (td, 2H, $J = 7.1, 5.1$ Hz), 3.18 (t, 2H, $J = 7.0$ Hz), 1.77-1.72 (m, 2H), 1.51-1.46 (m, 2H), 1.40-1.35 (m, 4H), 0.92 (t, 3H, $J = 7.1$ Hz); MS (EI) m/z 427 (M^+); Anal. Calcd. for $C_{27}H_{29}N_3O_2$: C, 75.85; H, 6.84; N, 9.83. Found: C, 75.25; H, 6.76; N, 9.69.

Synthesis of 1-{2-(2-Pyridyl)ethylamino}-8-(2-phenylethylamino)anthraquinone (3i). The quinone **3i** was prepared by treatment of **3b** (0.36 g, 1.0 mmol) with 2-phenethylamine (**5**, 0.30 g, 2.5 mmol) in the presence of tripropylamine (1.43 g, 10 mmol) and a catalytic amount of 4-dimethylaminopyridine (0.01 g, 0.10 mmol) in xylene (20 mL) at 140 °C for 1 week. The quinone **3i** was isolated in 53 % yield by silica-gel column chromatography eluting with ethyl acetate-chloroform (3:1 v/v) and purified as a purple needle by recrystallization from chloroform-hexane (1:1 v/v).

3i: Mp 183-184 °C (uncorrected); $R_f = 0.44$ (ethyl acetate-chloroform 3:1 v/v); IR (KBr, cm^{-1}) 1663, 1622 (C=O); 1H -NMR (600 MHz, $CDCl_3$) δ 9.73 (br, 1H), 9.69 (br, 1H), 8.62 (dd, 1H, $J = 4.7, 1.7$ Hz), 7.63 (dt, 1H, $J = 7.5, 1.7$ Hz), 7.54 (dd, 2H, $J = 7.6, 0.7$ Hz), 7.49-7.46 (m, 2H), 7.37-7.32 (m, 4H), 7.29-7.26 (m, 2H), 7.19 (dd, 1H, $J = 7.5, 4.7$ Hz), 7.10 (dd, 1H, $J = 8.5, 0.8$ Hz), 7.03 (dd, 1H, $J = 8.5, 0.8$ Hz), 3.77 (q, 2H, $J = 7.0$ Hz), 3.58 (q, 2H, $J = 7.3$ Hz), 3.25 (t, 2H, $J = 7.0$ Hz), 3.08 (t, 2H, $J = 7.3$ Hz); MS (EI) m/z 447 (M^+); Anal. Calcd. for $C_{29}H_{25}N_3O_2 \cdot 1/4H_2O$: C, 77.06; H, 5.69; N, 9.30. Found: C, 77.04; H, 5.57; N, 9.29.

Preparation of the Complex 4a. To **3a** (9.9 mg, 0.03 mmol) in acetonitrile (9 mL) was added palladium(II) acetate (6.8 mg, 0.03 mmol) in acetonitrile (1.2 mL) under nitrogen atmosphere. Stirring at room temperature for 24 h in the dark afforded a blue solution. After evaporation of the solution, the complex **4a** (blue needles) was isolated almost quantitatively by recrystallization from acetonitrile.

4a: Mp 123-127 °C (decomp.); IR (KBr, cm^{-1}) 1658, 1615 (C=O); ^1H -NMR (400 MHz, CD_3CN) δ 8.51 (dd, 1H, J = 5.8, 1.5 Hz), 8.13 (dd, 2H, J = 7.7, 1.4 Hz), 7.93 (dt, 1H, J = 7.8, 1.5 Hz), 7.78 (dt, 1H, J = 7.7, 1.4 Hz), 7.73 (dt, 1H, J = 7.7, 1.4 Hz), 7.53 (dd, 1H, J = 7.8, 1.2 Hz), 7.40 (dd, 1H, J = 6.7, 1.1 Hz), 7.33 (ddd, 1H, J = 7.8, 5.8, 1.2 Hz), 7.31 (dd, 1H, J = 9.2, 6.7 Hz), 7.24 (dd, 1H, J = 9.2, 1.1 Hz), 3.57 (t, 2H, J = 5.2 Hz), 3.28 (t, 2H, J = 5.2 Hz); MS (FAB) m/z 433 (M^+ -OAc); Anal. Calcd. for $\text{C}_{23}\text{H}_{18}\text{N}_2\text{O}_4\text{Pd}\cdot\text{H}_2\text{O}$: C, 54.08; H, 3.95; N, 5.48. Found: C, 54.07; H, 3.88; N, 5.65.

Preparation of the Complex 4b. To **3b** (10.9 mg, 0.03 mmol) in acetonitrile (9 mL) was added palladium(II) acetate (6.8 mg, 0.03 mmol) in acetonitrile (1.2 mL) under nitrogen atmosphere. Stirring at room temperature for 24 h in the dark afforded a blue solution. After evaporation of the solution, the complex **4b** (blue plates) was isolated almost quantitatively by recrystallization from acetonitrile.

4b: Mp 234-235 °C (decomp.); IR (KBr, cm^{-1}) 1654, 1624 (C=O); ^1H -NMR (400 MHz, CD_3CN) δ 8.49 (dd, 1H, J = 5.8, 1.6 Hz), 8.14 (dd, 1H, J = 7.8, 1.4 Hz), 7.93 (dt, 1H, J = 7.7, 1.6 Hz), 7.79 (dd, 1H, J = 8.0, 1.4 Hz), 7.63 (dd, 1H, J = 8.0, 7.8 Hz), 7.53 (d, 1H, J = 7.7 Hz), 7.36-7.30 (m, 3H), 7.27 (dd, 1H, J = 8.8, 1.8 Hz), 3.57 (t, 2H, J = 5.4 Hz), 3.30-3.26 (m, 2H); MS (FAB) m/z 469 (M^+ -OAc); Anal. Calcd. for $\text{C}_{23}\text{H}_{17}\text{N}_2\text{O}_4\text{ClPd}\cdot\text{H}_2\text{O}$: C, 50.66; H, 3.51; N, 5.14; Cl, 6.50. Found: C, 50.74; H, 3.51; N, 5.38; Cl, 6.55.

Preparation of the Complex 4c. To **3c** (112 mg, 0.25 mmol) in acetonitrile (70 mL) was added palladium(II) acetate (56.1 mg, 0.25 mmol) in acetonitrile (10 mL) under nitrogen atmosphere. Stirring at room temperature for 48 h in the dark afforded a blue solution. After evaporation of the solution, the complex **4c** (blue plates) was isolated almost quantitatively by recrystallization from acetonitrile.

4c: Mp 215-220 °C (decomp.); IR (KBr, cm^{-1}) 1654, 1598 (C=O); ^1H -NMR (400 MHz, CD_3CN) δ 8.71 (br, 1H), 8.53 (dd, 1H, J = 4.5, 1.8 Hz), 8.52 (dd, 1H, J =

4.9, 1.5 Hz), 7.93 (dt, 1H, $J = 7.7, 1.5$ Hz), 7.67 (dt, 1H, $J = 7.6, 1.8$ Hz), 7.52 (dd, 1H, $J = 7.7, 1.0$ Hz), 7.47 (dd, 1H, $J = 8.5, 7.3$ Hz), 7.40 (dd, 1H, $J = 7.3, 1.4$ Hz), 7.37-7.32 (m, 2H), 7.29 (dd, 1H, $J = 6.8, 1.5$ Hz), 7.25 (dd, 1H, $J = 8.7, 6.8$ Hz), 7.21-7.15 (m, 3H), 3.74-3.68 (m, 2H), 3.53 (t, 2H, $J = 5.5$ Hz), 3.16 (t, 2H, $J = 5.5$ Hz), 3.11-3.07 (m, 2H); MS (FAB) m/z 553 (M^+ -OAc).

Preparation of the Complex 4e. To **3e** (44.9 mg, 0.10 mmol) in dichloromethane (55 mL) was added slowly palladium(II) acetate (22.5 mg, 0.10 mmol) in dichloromethane (25 mL) under nitrogen atmosphere. Stirring at room temperature for 24 h in the dark afforded a purple solution. After evaporation of the solution, the complex **4e** (purple needles) was isolated almost quantitatively by recrystallization from acetonitrile.

4e: Mp 118-123 °C (decomp.); IR (KBr, cm^{-1}) 1620, 1596 (C=O); ^1H -NMR (600 MHz, CD_3CN) δ 9.70 (br, 1H), 8.54 (dd, 1H, $J = 4.6, 1.6$ Hz), 8.51 (dd, 1H, $J = 5.1, 1.8$ Hz), 7.91 (ddd, 1H, $J = 7.7, 5.3, 1.8$ Hz), 7.67 (ddd, 1H, $J = 7.6, 6.8, 1.6$ Hz), 7.54-7.48 (m, 2H), 7.43 (d, 1H, $J = 7.2$ Hz), 7.35-7.29 (m, 3H), 7.27-7.17 (m, 2H), 7.11 (d, 1H, $J = 8.4$ Hz), 7.10-7.07 (m, 1H), 3.74 (q, 2H, $J = 6.8$ Hz), 3.53-3.48 (m, 2H), 3.21-3.13 (m, 4H); MS (FAB) m/z 553 (M^+ -OAc).

Preparation of the Complex 4g. To **3g** (2.24 mg, 0.005 mmol) in acetonitrile (0.5 mL) was added palladium(II) acetate (1.12 mg, 0.005 mmol) in acetonitrile (0.1 mL) under nitrogen atmosphere. The stirring was stopped after 1 h and the mixture was allowed to stand for 1 h under nitrogen atmosphere. Then, purple solid **4g** precipitated out. The purple solid **4g** was filtrated and washed with ether.

4g: Mp > 300 °C (decomp.); IR (KBr, cm^{-1}) 1657, 1613 (C=O); ^1H -NMR (600 MHz, CD_3CN) δ 9.06 (br, 2H), 8.41 (d, 4H, $J = 6.0$ Hz), 7.57 (dd, 2H, $J = 8.5, 7.2$ Hz), 7.49 (d, 2H, $J = 7.2$ Hz), 7.22 (d, 2H, $J = 8.5$ Hz), 7.17 (d, 4H, $J = 6.0$ Hz), 3.70-3.63 (m, 4H), 3.03-2.98 (m, 4H); MS (FAB) m/z 554 (M^+ -2OAc).

Preparation of the Complex 4h. To **3h** (8.97 mg, 0.02 mmol) in dichloromethane (16 mL) was added palladium(II) acetate (8.98 mg, 0.04 mmol) in dichloromethane (4 mL) under nitrogen atmosphere. Stirring at room temperature for 48 h in the dark afforded a blue solution. After evaporation of the solution, the complex **4h** (blue needles) was isolated almost quantitatively by recrystallization from acetonitrile.

4h: Mp 100-105 °C (decomp.); IR (KBr, cm^{-1}) 1651, 1600 (C=O); ^1H -NMR (400 MHz, CD_3CN) δ 8.60 (br, 1H), 8.50 (dd, 1H, $J = 5.8, 1.6$ Hz), 7.92 (dt, 1H, $J = 7.7, 1.6$ Hz), 7.52 (dd, 1H, $J = 7.7, 1.4$ Hz), 7.47 (dd, 1H, $J = 8.6, 7.4$ Hz), 7.40 (dd, 1H, $J = 7.4, 1.2$ Hz), 7.33 (ddd, 1H, $J = 7.7, 5.8, 1.4$ Hz), 7.28 (dd, 1H, $J = 6.8, 1.5$ Hz), 7.25 (dd, 1H, $J = 8.7, 6.8$ Hz), 7.16 (dd, 1H, $J = 8.7, 1.5$ Hz), 7.11 (dd, 1H, $J = 8.6, 1.2$ Hz), 3.52 (t, 2H, $J = 5.5$ Hz), 3.33-3.27 (m, 2H), 3.15 (t, 2H, $J = 5.5$ Hz), 1.91-1.80 (m, 2H), 1.67-1.62 (m, 2H), 1.42-1.32 (m, 4H), 0.90 (t, 3H, $J = 7.0$ Hz); MS (FAB) m/z 532 (M^+ -OAc).

Preparation of the Complex 4i. To **3i** (22.4 mg, 0.05 mmol) in acetonitrile (20 mL) was added palladium(II) acetate (11.2 mg, 0.05 mmol) in acetonitrile (5 mL) under nitrogen atmosphere. Stirring at room temperature for 24 h in the dark afforded a blue solution. After evaporation of the solution, the complex **4i** (blue plates) was isolated almost quantitatively by recrystallization from acetonitrile.

4i: Mp 243-248 °C (decomp.); IR (KBr, cm^{-1}) 1646, 1620 (C=O); ^1H -NMR (400 MHz, CD_2Cl_2) δ 8.73 (br, 1H), 8.58 (ddd, 2H, $J = 5.9, 1.5, 0.8$ Hz), 7.83 (ddd, 1H, $J = 7.6, 7.4, 1.5$ Hz), 7.46-7.43 (m, 2H), 7.41 (dd, 1H, $J = 7.6, 1.4$ Hz), 7.32 (dd, 1H, $J = 6.9, 1.1$ Hz), 7.31-7.20 (m, 7H), 7.08 (dd, 1H, $J = 9.1, 1.1$ Hz), 7.05 (t, 1H, $J = 6.0$ Hz), 3.56-3.51 (m, 4H), 3.16-3.14 (m, 2H), 2.98-2.94 (m, 2H); MS (FAB) m/z 522 (M^+ -OAc); Anal. Calcd. for $\text{C}_{31}\text{H}_{27}\text{N}_3\text{O}_4\text{Pd}$: C, 60.84; H, 4.45; N, 6.87. Found: C, 60.22; H, 4.55; N, 7.04.

Preparation of the Complex 5c. To **3c** (22.4 mg, 0.05 mmol) in acetonitrile (35 mL) was added (acetonitrile)₂palladium(II) chloride (13.0

mg, 0.05 mmol) in acetonitrile (5 mL) under nitrogen atmosphere. The stirring was stopped after 1 h and the mixture was allowed to stand for 1 h under nitrogen atmosphere. Then, the purple solid **5c** precipitated out and was filtrated and washed with ether.

5c: Mp 250-260 °C (decomp.); IR (KBr, cm^{-1}) 1660, 1614 (C=O); ^1H -NMR (600 MHz, d_6 -DMSO) δ 9.88 (br, 2H), 9.24 (d, 2H, $J = 5.8$ Hz), 8.03 (dd, 2H, $J = 7.2, 6.7$ Hz), 7.83 (d, 2H, $J = 7.2$ Hz), 7.54 (dd, 2H, $J = 8.4, 7.2$ Hz), 7.47 (d, 2H, $J = 8.4$ Hz), 7.34 (dd, 2H, $J = 6.7, 5.8$ Hz), 7.00 (d, 2H, $J = 7.2$ Hz), 3.74-3.71 (m, 4H), 3.16-3.12 (m, 4H); MS (FAB) m/z 590 ($\text{M}^+ - \text{Cl}$).

Preparation of the Complex 5g. To **3g** (22.4 mg, 0.05 mmol) in acetonitrile (35 mL) was added (acetonitrile)₂palladium(II) chloride (13.0 mg, 0.05 mmol) in acetonitrile (5 mL) under nitrogen atmosphere. The stirring was stopped after 1 h and the mixture was allowed to stand for 1 h under nitrogen atmosphere. Then, the purple solid **5g** precipitated out and was filtrated and washed with ether. The complex **5g** (purple plates) was isolated almost quantitatively by recrystallization from acetonitrile.

5g: Mp > 300 °C (decomp.); IR (KBr, cm^{-1}) 1659, 1613 (C=O); ^1H -NMR (600 MHz, d_6 -DMSO) δ 9.04 (br, 2H), 8.61 (d, 4H, $J = 6.0$ Hz), 7.62 (dd, 2H, $J = 8.5, 7.2$ Hz), 7.41 (d, 2H, $J = 7.2$ Hz), 7.34 (d, 2H, $J = 8.5$ Hz), 7.29 (d, 4H, $J = 6.0$ Hz), 3.77-3.70 (m, 4H), 3.00-2.96 (m, 4H); MS (FAB) m/z 590 ($\text{M}^+ - \text{Cl}$).

Preparation of the Complex 6e. To **3e** (22.4 mg, 0.05 mmol) in acetonitrile (40 mL) was added palladium(II) acetate (56.1 mg, 0.25 mmol) in acetonitrile (10 mL) under nitrogen atmosphere. Stirring at room temperature for 24 h in the dark afforded a blue solution. After evaporation of the solution, the complex **6e** (blue plates) was isolated almost quantitatively by recrystallization from acetonitrile.

6e: Mp 242-249 °C (decomp.); IR (KBr, cm^{-1}) 1618 (C=O); ^1H -NMR (400 MHz, CD_2Cl_2) δ 8.57 (dd, 1H, $J = 5.9, 1.5$ Hz), 7.81 (ddd, 1H, $J = 7.7, 7.5, 1.5$ Hz), 7.39 (dd, 1H, $J = 7.5, 1.3$ Hz), 7.35 (d, 1H, $J = 6.9$ Hz), 7.26-7.20 (m, 2H),

7.01 (d, 1H, $J = 8.8$ Hz), 3.57-3.53 (m, 2H), 3.24-3.19 (m, 2H); MS (FAB) m/z 658 ($M^+ - 2OAc$).

UV-vis. Spectra Measurements. UV-vis. spectra were taken under nitrogen atmosphere at 30 °C after keeping the acetonitrile solutions of the quinone ligands and palladium(II) salt in the dark for 24 h.

Electrochemical Experiments. All electrochemical measurements were carried out at 25 °C under an atmospheric pressure of nitrogen, which was previously passed through a solution of the same composition as the electrolysis solution. Cyclic voltammograms were obtained in acetonitrile solution containing 0.1 M Bu_4NClO_4 as the supporting electrolyte (2×10^{-3} M). Potentials were determined with reference to a KCl saturated calomel electrode at 50 mVs⁻¹ scan rate.

X-ray Structure Determination of 3b. A red prismatic crystal of **3b** with approximate dimensions of 0.50 x 0.50 x 0.50 mm was mounted on a glass fiber. The measurement was made on Rigaku AFC5R diffractometer with graphite-monochromated Mo-K α radiation and a 12kW rotating anode generator. Cell constants and an orientation matrix for data collection were obtained from a least-square refinement using the setting angles of 25 carefully centered reflections in the range $26.99 < 2\theta < 27.48^\circ$ corresponded to a primitive monoclinic cell with dimensions. The data were collected at a temperature of $23 \pm 1^\circ\text{C}$ using the ω - 2θ scan technique to a maximum 2θ value of 55.0° . Totals of 4417 independent reflections were obtained and 4094 were unique ($R_{\text{int}} = 0.089$). The structure was solved by direct methods and expanded using Fourier techniques. The non-hydrogen atoms were refined anisotropically. The final cycle of full-matrix least-squares refinement was based on 3438 observed reflections ($I > 3.00\sigma(I)$) and 235 variable parameters. $R = 0.068$, $R_w = 0.108$. Crystallographic details appear in Table 1.

X-ray Structure Determination of 4b. A blue plate crystal of **4b** with approximate dimensions of 0.50 x 0.40 x 0.10 mm was mounted on a glass fiber. All measurement were made on Rigaku AFC5R diffractometer with graphite-monochromated Mo-K α radiation and a 12kW rotating anode generator. Cell constants and an orientation matrix for data collection were obtained from a least-square refinement using the setting angles of 25 carefully centered reflections in the range $27.12 < 2\theta < 27.50^\circ$ corresponded to a primitive monoclinic cell with dimensions. The data were collected at a temperature of $23 \pm 1^\circ\text{C}$ using the ω - 2θ scan technique to a maximum 2θ value of 55.0° . Totals of 5520 independent reflections were obtained and 5234 were unique ($R_{\text{int}} = 0.018$). The structure was solved by direct methods and expanded using Fourier techniques. The non-hydrogen atoms were refined anisotropically. The final cycle of full-matrix least-squares refinement was based on 3007 observed reflections ($I > 3.00\sigma(I)$) and 289 variable parameters. $R = 0.043$, $R_w = 0.030$. Crystallographic details appear in Table 1.

X-ray Structure Determination of 4i. A blue plate crystal of **4i** with approximate dimensions of 0.05 x 0.50 x 0.30 mm was mounted on a glass fiber. The measurement was made on Rigaku AFC5R diffractometer with graphite-monochromated Mo-K α radiation and a 12kW rotating anode generator. Cell constants and an orientation matrix for data collection were obtained from a least-square refinement using the setting angles of 25 carefully centered reflections in the range $25.77 < 2\theta < 27.36^\circ$ corresponded to a primitive monoclinic cell with dimensions. The data were collected at a temperature of $23 \pm 1^\circ\text{C}$ using the ω - 2θ scan technique to a maximum 2θ value of 55.2° . Totals of 10768 independent reflections were obtained and 7898 were unique ($R_{\text{int}} = 0.003$). The structure was solved by direct methods and expanded using Fourier techniques. The non-hydrogen atoms were refined anisotropically. The final cycle of full-

matrix least-squares refinement was based on 2265 observed reflections ($I > 3.00\sigma(I)$) and 352 variable parameters. $R = 0.078$, $R_w = 0.068$. Crystallographic details appear in Table 1.

X-ray Structure Determination of 5g. A blue plate crystal of 5g with approximate dimensions of 0.20 x 0.20 x 0.10 mm was mounted on a glass fiber. The measurement was made on Rigaku AFC5R diffractometer with graphite-monochromated Mo-K α radiation and a 12kW rotating anode generator. Cell constants and an orientation matrix for data collection were obtained from a least-square refinement using the setting angles of 25 carefully centered reflections in the range $26.91 < 2\theta < 27.51^\circ$ corresponded to a primitive monoclinic cell with dimensions. The data were collected at a temperature of $23 \pm 1^\circ\text{C}$ using the ω - 2θ scan technique to a maximum 2θ value of 55.0° . Totals of 6909 independent reflections were obtained and 6578 were unique ($R_{\text{int}} = 0.046$). The structure was solved by direct methods and expanded using Fourier techniques. The non-hydrogen atoms were refined anisotropically. The final cycle of full-matrix least-squares refinement was based on 4275 observed reflections ($I > 3.00\sigma(I)$) and 362 variable parameters. $R = 0.071$, $R_w = 0.063$. Crystallographic details appear in Table 1.

2-5. References

1. Hirao, T.; Murakami, T.; Ohno, M.; Ohshiro, Y. *Chem. Lett.* **1989**, 785; **1991**, 299.
2. (a) Duine, J. A.; Frank, J.; Jongejan, J. A. *Adv. Enzymol.* **1987**, 59, 170. (b) Hartmann, C.; Klinman, J. P. *BioFactors* **1988**, 1, 41. (c) Ohshiro, Y.; Ito, S.; Kurokawa, K.; Kato, J.; Hirao, T.; Agawa, T.

- Chem. Lett.* **1988**, 777. (d) Schwederski, B.; Kasack, V.; Kaim, W.; Roth, E.; Jordanov, J. *Angew. Chem., Int. Ed. Engl.* **1990**, *29*, 78.
3. Takenaka, S.; Nishihara, S.; Tahara, K.; Kondo, H.; Takagi, M. *Supramol. Chem.* **1993**, *2*, 41.
4. (a) Burley, S. K.; Petsko, G. A. *Science* **1985**, *229*, 23. (b) Nishio, M.; Hirota, M. *Tetrahedron* **1989**, *45*, 7201. (c) Jorgensen, W. L.; Severance, D. L. *J. Am. Chem. Soc.* **1990**, *112*, 4768. (d) Atwood, J. L.; Hamada, F.; Robinson, K. D.; Orr, G. W.; Vincent, R. L. *Nature* **1991**, *349*, 683. (e) Suzuki, S.; Green, P. G.; Bumgarner, R. E.; Dasgupta, S.; Goddard III, W. A.; Blake, G. A. *Science* **1992**, *257*, 942. (f) Cochran, J. E.; Parrott, T. J.; Whitlock, H. W. *J. Am. Chem. Soc.* **1992**, *114*, 2269. (g) Subramanian, S.; Wang, L.; Zaworotko, M. J. *Organometallics* **1993**, *12*, 310. (h) Sakaki, S.; Kato, K.; Miyazaki, T.; Musashi, Y.; Ohkubo, K.; Ihara, H.; Hirayama, C. *J. Chem. Soc., Faraday Trans.* **1993**, *89*, 659.
5. (a) Hiramatsu, M.; Shiozaki, K.; Fujinami, T.; Sasaki, S. *J. Organometal. Chem.* **1983**, *246*, 203. (b) Grennberg, H.; Gogoll, A.; Bäckvall, J. E. *Organometallics* **1993**, *12*, 1790.

Chapter 3. Complexation Behavior of Ferrocene Ligands Bearing *N*-Heterocyclic Coordination Sites

3-1. Introduction

In a previous chapter, quinone ligands bearing *N*-heterocyclic coordination sites is revealed to show a specific complexation behavior. Complexation of particular molecules¹ or ions² by organometallic ligands containing one or more metallocene units has become a great interest area in both organic and inorganic chemistry. For this purpose, the design and synthesis of ligands having redox center are considered to be a convinced approach. Ferrocene receptors are considered to construct a specific molecular recognition site based on redox couple and two rotatory coplanar cyclopentadienyl rings. A variety of ferrocene receptors have been investigated to develop an efficient system.^{1, 2}

This chapter describes the synthesis and the complexation behavior of ferrocene ligands bearing *N*-heterocyclic coordination sites.

3-2. Results and Discussion

3-2-1. Synthesis of Ferrocene Ligands

The ferrocene ligands were easily prepared from 1, 1'-ferrocenedicarboxylic acid chloride and the corresponding amines (eq. 1 and 2, Tables 1, and 2).

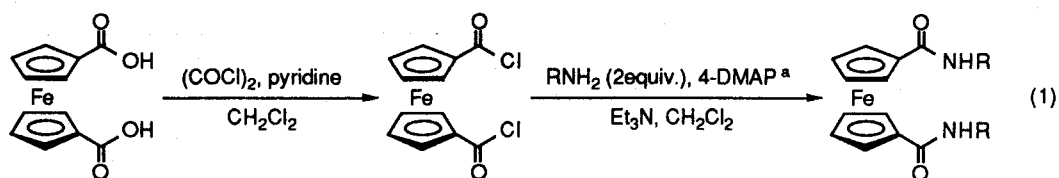


Table 1. Synthesis of Ferrocene Ligand

R		Yield (%)	R		Yield (%)
	2-BPEFA	85		BMEIFA	63
	4-BPEFA	80		2-BPMFA	79
	BPHEFA	84		BBFA	82

^a 4-DMAP = 4-Dimethylaminopyridine.

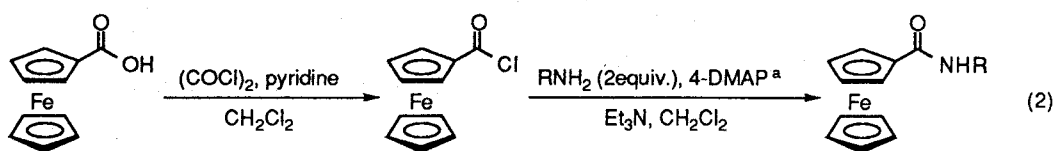


Table 2. Synthesis of Ferrocene Ligand

R		Yield (%)	R		Yield (%)
	2-PEFA	96		2-PMFA	93
	4-PEFA	86			

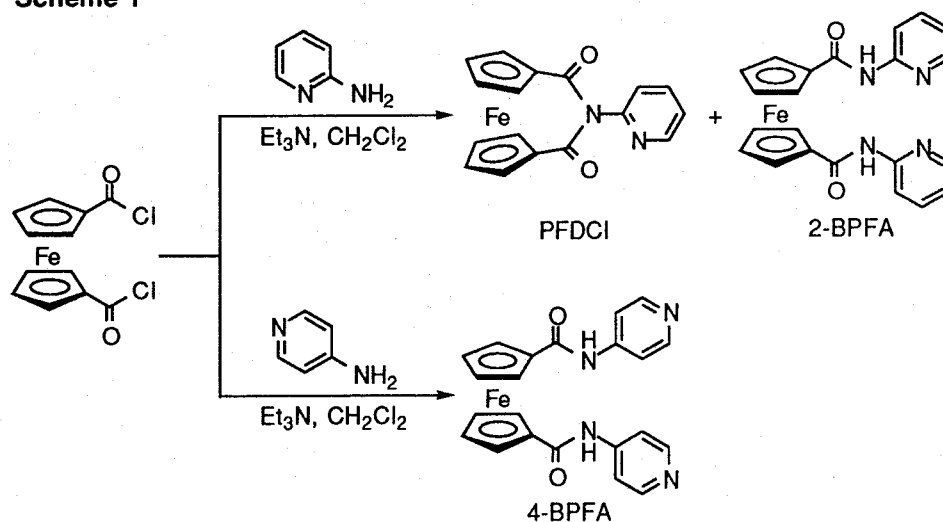
^a 4-DMAP = 4-Dimethylaminopyridine.

It should be noted that in the case 2-aminopyridine, the imide-bridged [3]ferrocenophane, 2-pyridyl-1,1'-ferrocenedicarboximide (PFDCI), was synthesized directly and predominantly in one stage in 57% yield (Scheme 1). The diamide, 2-BPFA, was obtained in only 4% yield. PFDCI appears to be the first example for the imide-bridged [3]ferrocenophanes to our best knowledge. This result is in sharp contrast with the finding that *N,N'*-bis(4-pyridyl)-1,1'-ferrocenedicarboxamide (4-BPFA) was produced exclusively in 74% yield

in the case of 4-aminopyridine. No intramolecular imide formation was observed. This difference is referred to the site of the pyridyl nitrogens, suggesting the involvement of an acylpyridinium intermediate in the cyclization step to PFDCI.

Metallocenophanes are structurally interesting aromatics and redox of transition metals permits potential utilization as materials and catalysts.³ Synthesis of [n]metallocenophanes has been addressed from these points of view.⁴ The internal strain is a key factor to design [n]metallocenophanes. A bridging unit containing heteroatoms expands the scope of metallocenophane chemistry.

Scheme 1



The X-ray crystal structure determination of PFDCI indicated the distortion of the ferrocenophane ring (Figure 1 and Table 3). The important bond distances and angles are listed in Table 4. The dihedral angle (16.4°) between the least-squares planes of two cyclopentadienyl rings is unexpectedly large as compared with those of the known [3]ferrocenophanes;⁴⁻⁷ the rings of [3]ferrocenophane-1,3-dione and cationic 2-*N,N*-dimethylammonium-[3]ferrocenophane iodide are tilted by 9.8° and 12.2°, respectively, with respect to each other.⁶

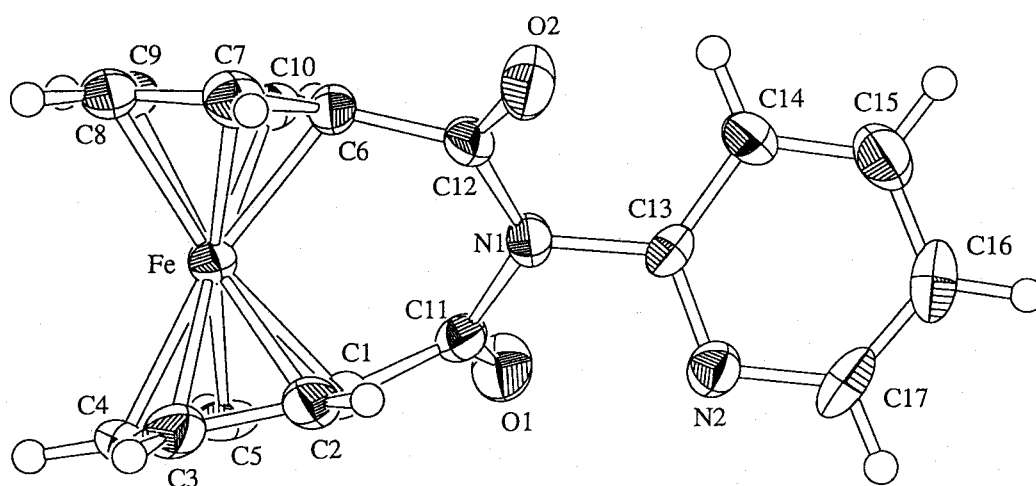


Figure 1. ORTEP view of the X-ray crystal structure of PFDCI (50% probability ellipsoids).

Table 3. Crystallographic Data for PFDCI

formula	$C_{17}H_{12}N_2O_2Fe$	$V, \text{\AA}^3$	1350.2(5)
mol wt	332.14	Z	4
cryst system	monoclinic	$D_{\text{calcd}}, \text{g cm}^{-3}$	1.634
space group	$P2_1/c$	$\mu(\text{Mo K}\alpha), \text{cm}^{-1}$	11.24
$a, \text{\AA}$	9.708(3)	$T, ^\circ\text{C}$	23
$b, \text{\AA}$	8.697(3)	$\lambda(\text{Mo K}\alpha), \text{\AA}$	0.71069
$c, \text{\AA}$	16.641(2)	R	0.063
β, deg	106.07(1)	R_w	0.073

Table 4. Selected Bond Distances (Å) and Bond Angles (deg) for PFDCI

Bond Distances			
Fe–C(1)	1.971(6)	Fe–C(10)	2.014(7)
Fe–C(2)	2.011(7)	C(1)–C(11)	1.482(9)
Fe–C(3)	2.069(7)	C(6)–C(12)	1.493(9)
Fe–C(4)	2.085(6)	C(11)–O(1)	1.217(8)
Fe–C(5)	2.037(6)	C(12)–O(2)	1.214(8)
Fe–C(6)	1.974(6)	C(11)–N(1)	1.446(8)
Fe–C(7)	2.043(7)	C(12)–N(1)	1.408(8)
Fe–C(8)	2.079(6)	C(13)–N(1)	1.446(8)
Fe–C(9)	2.080(7)		
Bond Angles			
C(1)–C(11)–N(1)	117.0(5)	O(2)–C(12)–N(1)	120.9(6)
C(1)–C(11)–O(1)	123.5(6)	C(11)–N(1)–C(12)	124.8(5)
O(1)–C(11)–N(1)	119.5(6)	C(11)–N(1)–C(13)	115.8(5)
C(6)–C(12)–N(1)	118.0(5)	C(12)–N(1)–C(13)	119.4(5)
C(6)–C(12)–O(2)	121.1(6)		

The β -angle defined as the angle between the plane of the cyclopentadienyl ring and C(ipso)-CO(bridging) bond is 34.6° for C(1)-C(2)-C(3)-C(4)-C(5) and C(1)-C(11)O(1) and 45.7° for C(6)-C(7)-C(8)-C(9)-C(10) and C(6)-C(12)O(2). The β -angle effect was supported by the ^{13}C -NMR spectrum that the up-field chemical shift for the C(ipso) atom and the down-field shift for the C(α) and C(β) atoms of the cyclopentadienyl rings were observed in comparison with those of 2-BPFA.

Another interesting feature is that the staggered orientation of the two cyclopentadienyl rings is accompanied by the twisting of the bridge in the imide system. The staggering degree 35.5° was defined here as the angle between the mean planes through the atoms Fe-C(1)-C(11) and Fe-C(6)-C(12). The two rings are approximately staggered, being in contrast

with the eclipsed ones of the known [3]ferrocenophanes.²⁻⁵ This unique distorted structure including the above-mentioned larger tilt angle is considered to be attributed to the imide linkage.

It should be also noted that the calculated position of the hydrogen atom on the cyclopentadienyl C(α) atom is almost located to face π -electrons of the pyridyl ring of the neighboring molecule in the crystal packing of PFDCI (Figure 2). The distance between the hydrogen and the center of the pyridyl ring is 2.97 Å, suggesting a π hydrogen bond⁸ in the crystal structure (edge-to-face interaction). The dihedral angle between the least-square planes of the cyclopentadienyl and pyridyl rings is 90.4°, which is reasonable for the edge-to-face interaction.

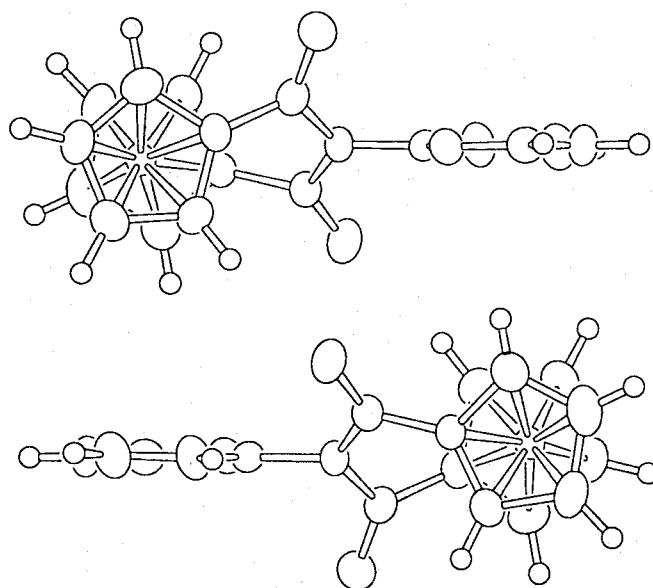


Figure 2. Molecular packing of PFDCI.

The preferred orientation of the imide linkage would seem to be perpendicular to the cyclopentadienyl ring planes leading to an eclipsed orientation of the rings. Because of steric interactions between the oxygen atoms, O(1) and O(2), and the pyridyl nitrogen atom and hydrogen atom at C(14) of the pyridyl ring, the orientation of the pyridyl ring would be within a limited range of parallel to the cyclopentadienyl ring. The

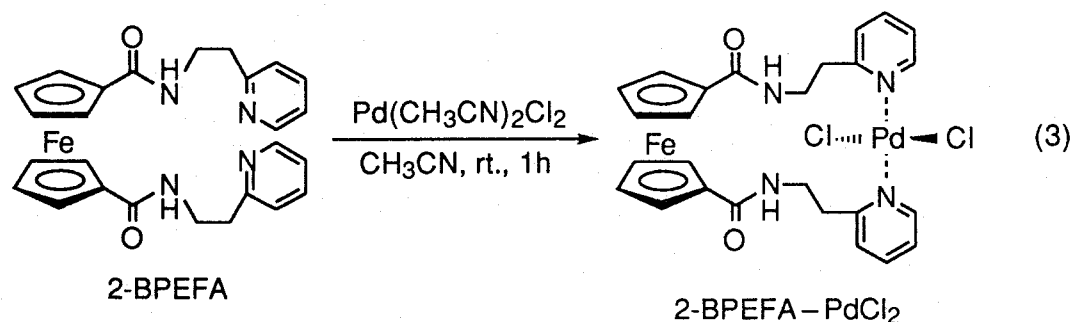
packing interaction, however, requires a rotation of the pyridyl ring away from this orientation, which is considered to induce a twist in the imide bridge, resulting in the observed staggered conformation and the tilted rings at the bridgehead carbon atoms to set the observed dihedral angle.

An alternative explanation might involve the larger angle at the bridging nitrogen atom, which would lead to the two cyclopentadienyl rings being further apart in a favored eclipsed orientation. The most likely explanation might be based on a combination of these two effects.

The strained imide bridge is predicted to effect the electronic state. The electrochemical properties of the above-obtained ferrocene derivatives were studied by cyclic voltammetry. A reversible oxidation wave of the Fc^+/Fc couple was observed at $E_{1/2}$ 1018 (PFDCI), 947 (2-BPFA), or 904 (4-BPFA) mV *vs.* SCE, respectively. PFDCI showed the large anodic shift of 71 mV in comparison with 2-BPFA. The difference is probably due to the distortion of the [3]ferrocenophane with the electron-withdrawing imide linkage.

3-2-2. Complexation with Palladium(II) Chloride

We investigated the complexation behavior of ferrocene derivatives. Although a wide range of relative orientations of the podand ligand, 2-BPEFA, is possible, a specific coordinating behavior was observed. 2-BPEFA formed a 1:1 complex with an equimolar amount of dichlorobis(acetonitrile)palladium(II) (eq. 3).



The structure of the isolated 2-BPEFA-PdCl₂ complex was elucidated by ¹H-NMR. The down-field shift of the pyridyl protons implies the coordination of the pyridyl nitrogens to palladium.

The single-crystal X-ray structure determination indicated C₂ symmetry of 2-BPEFA-PdCl₂ complex, being consistent with two equivalent pyridyl groups in ¹H-NMR (Figure 3 and Table 5). The two intramolecular pyridyl nitrogens coordinate *trans* to palladium. The coordination geometry is a nearly square planar with the palladium-bonded chloride.

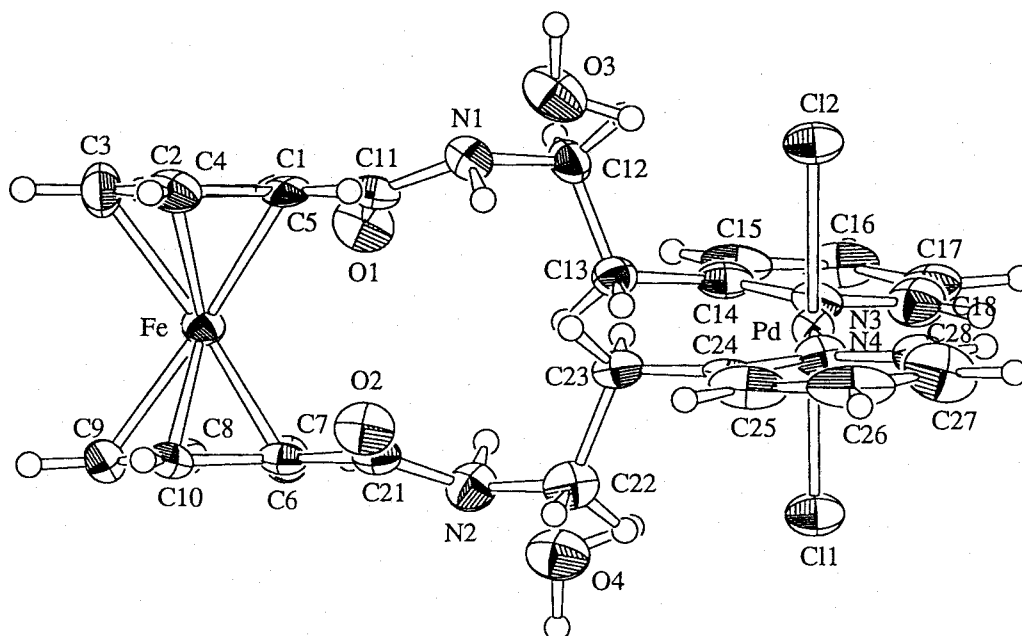
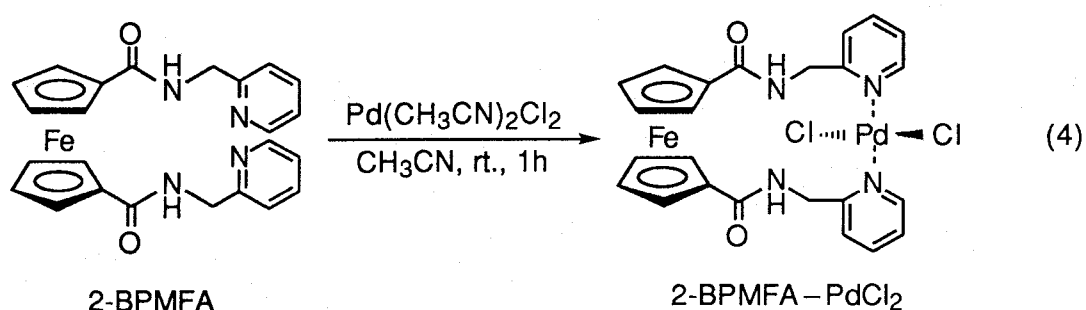


Figure 3. ORTEP view of the X-ray crystal structure of 2-BPEFA-PdCl₂ (40% probability ellipsoids).

Table 5. Crystallographic Data for 2-BPMFA, 2-BPMFA–PdCl₂, and 2-BPEFA–PdCl₂

	2-BPMFA	2-BPMFA–PdCl ₂	2-BPEFA–PdCl ₂
formula	C ₂₅ H ₂₃ N ₄ O ₂ Cl ₃	C ₂₄ H ₂₆ N ₄ O ₄ Cl ₂ FePd	C ₂₆ H ₃₀ N ₄ O ₄ Cl ₂ FePd
mol wt	573.69	667.65	695.70
cryst system	monoclinic	triclinic	triclinic
space group	<i>P</i> 2 ₁ / <i>c</i>	<i>P</i> $\bar{1}$	<i>P</i> $\bar{1}$
<i>a</i> , Å	10.132(3)	11.691(3)	12.333(4)
<i>b</i> , Å	23.907(3)	13.980(3)	12.390(5)
<i>c</i> , Å	10.399(3)	8.329(2)	11.880(6)
α , deg		100.01(2)	111.09(4)
β , deg	91.03(3)	109.06(2)	118.31(3)
γ , deg		88.17(2)	97.21(3)
<i>V</i> , Å ³	2518(1)	1266.4(6)	1390(1)
<i>Z</i>	4	2	2
<i>D</i> _{calcd} , g cm ^{−3}	1.513	1.751	1.661
μ (Mo K α), cm ^{−1}	9.47	15.32	13.99
<i>T</i> , °C	23	23	23
λ (Mo K α), Å	0.71069	0.71069	0.71069
<i>R</i>	0.071	0.048	0.076
<i>R</i> _w	0.078	0.058	0.088

2-BPMFA bearing the 2-pyridylmethyl group instead of the 2-pyridylethyl one also formed a 1:1 complex with an equimolar amount of dichloro-bis(acetonitrile)palladium(II) (eq. 4).



The pyridyl protons were down-field shifted and the two pyridyl groups were equivalent in ¹H-NMR as observed in 2-BPEFA–PdCl₂ complex. X-ray crystal structure determination of 2-BPMFA–PdCl₂ complex also showed the same coordination as 2-BPEFA (Figure 4 and

Table 5) and the two intramolecular pyridyl nitrogens coordinate *trans* to palladium. The two cyclopentadienyl rings of 2-BPMFA-PdCl₂ are staggered, being in contrast with the eclipsed conformation of 2-BPMFA (Figure 5).

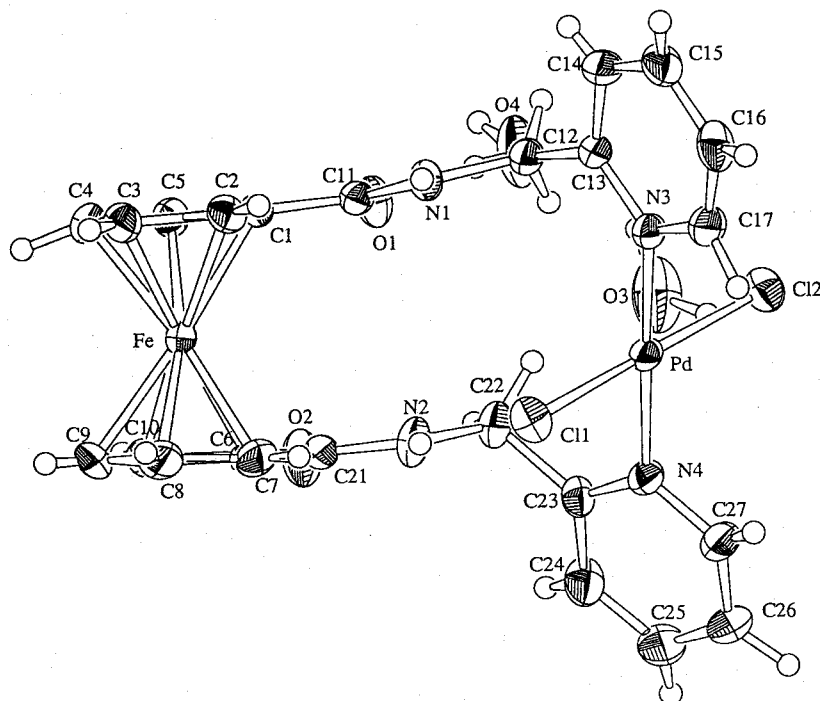


Figure 4. ORTEP view of the X-ray crystal structure of 2-BPMFA-PdCl₂ (40% probability ellipsoids).

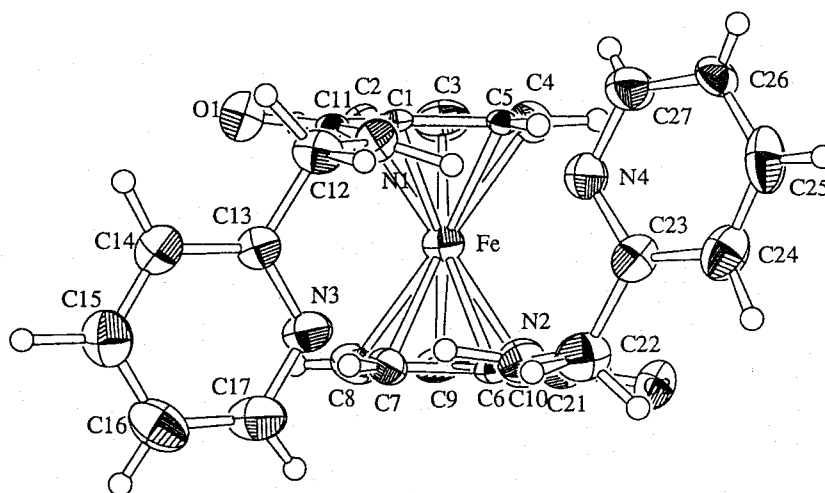


Figure 5. ORTEP view of the X-ray crystal structure of 2-BPMFA (40% probability ellipsoids). CHCl₃ is omitted for clarity,

2-BPMFA-PdCl₂ was found to be the strained complex based on distortion of the molecule. The extent of the strain is evaluated by deviation of the X-ray structural parameters. The dihedral angle (θ) of tilt

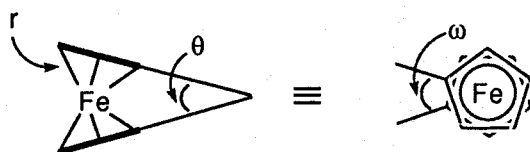


Figure 6. Notation of structural parameters in molecular geometry.

Table 6. Selected Bond Distances (Å), Bond Angles (deg), and Structural Parameters

	2-BPMFA	2-BPMFA-PdCl ₂	2-BPEFA-PdCl ₂
Bond Distances			
Pd-N(3)	-----	2.013(5)	2.02(1)
Pd-N(4)	-----	2.027(5)	2.03(1)
Pd-Cl(1)	-----	2.298(2)	2.307(4)
Pd-Cl(2)	-----	2.304(2)	2.303(4)
Fe-Pd	-----	6.35	7.42
Bond Angles			
N(3)-Pd-N(4)	-----	178.7(2)	176.1(5)
N(3)-Pd-Cl(1)	-----	89.4(2)	89.9(3)
N(3)-Pd-Cl(2)	-----	90.3(2)	90.2(3)
N(4)-Pd-Cl(1)	-----	91.6(2)	90.3(3)
N(4)-Pd-Cl(2)	-----	88.6(2)	89.5(3)
Cl(1)-Pd-Cl(2)	-----	178.31(7)	179.5(2)
Structural Parameters			
r (Å)	2.039	2.045	2.036
θ (°)	1.3	3.4	0.9
ω (°)	0.5	24.7	3.9

between the two cyclopentadienyl rings, the average distance (r) of the metal from the ring carbons, and the rotation (ω) of the two cyclopentadienyl rings about the Cp-Fe-Cp axis are shown in Figure 6. The selected bond distances, bond angles, and structural parameters of 2-BPMFA, 2-BPMFA-PdCl₂ complex, and 2-BPEFA-PdCl₂ complex are summarized in Table 6. The length of methylene chain affects the

complexation. The two cyclopentadienyl rings of 2-BPEFA-PdCl₂ are eclipsed, being in contrast with the staggered conformation of 2-BPMFA-PdCl₂ complex. The redox interaction between the palladium and iron does not exist since the distance between them is longer than 6 Å.

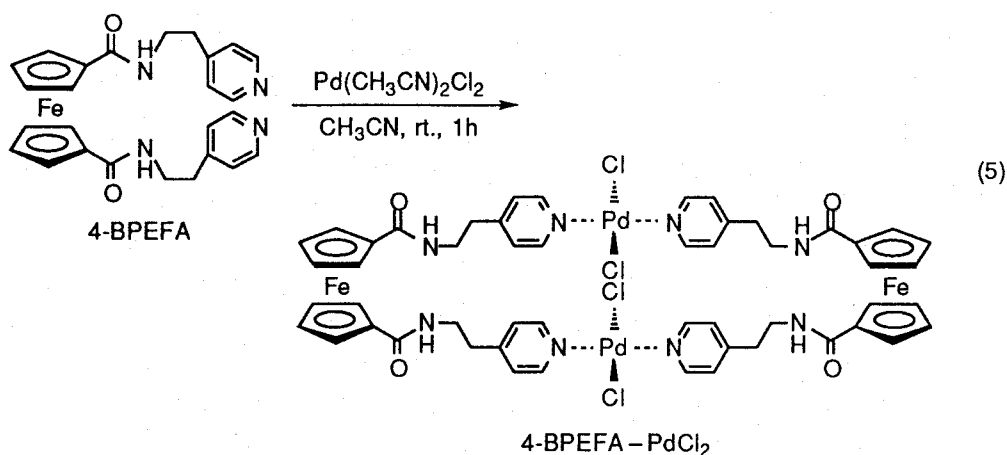
The redox properties of the ferrocene ligands and corresponding palladium complexes were investigated by cyclic voltammetry using 0.1 M Bu₄NClO₄ as a supporting electrolyte in acetonitrile at a 50 mVs⁻¹ scan rate (Table 7). Cyclic voltammetry verified that the redox of ferrocene was not affected even if the palladium coordinates to the pyridyl moieties.

Table 7. Redox Potential

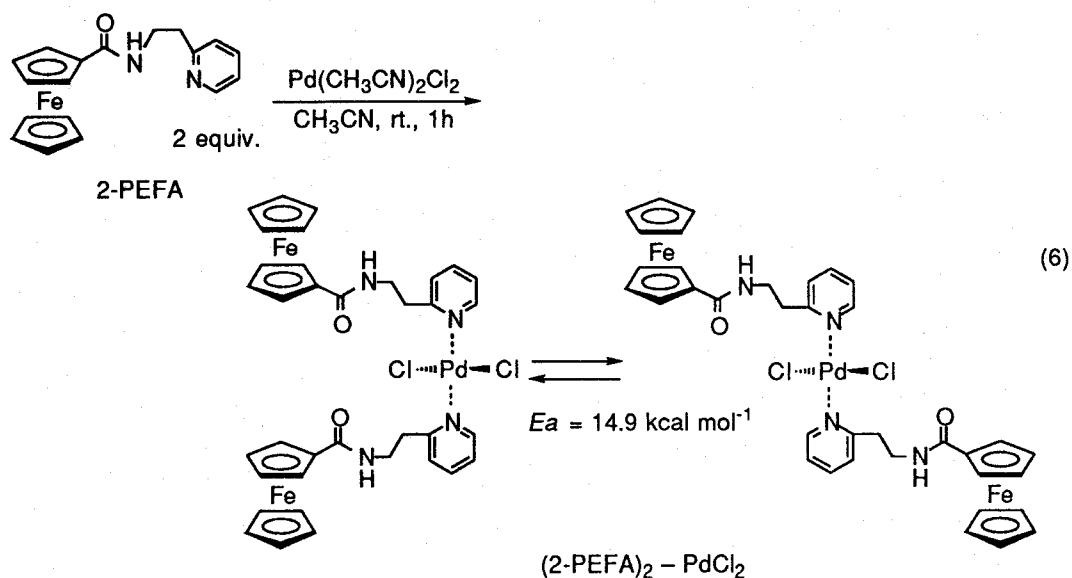
Ligand and complex	E _{1/2} ^a	Ligand and complex	E _{1/2} ^a
Ferrocene	0.330	BMEIFA	0.788
2-BPEFA	0.770	2-BPMFA	0.743
2-BPEFA – PdCl ₂	0.772	2-BPMFA – PdCl ₂	0.754
4-BPEFA	0.734	2-PEFA	0.556
BPHEFA	0.716	4-PEFA	0.564
BBFA	0.705	2-PMFA	0.569

^a V vs SCE.

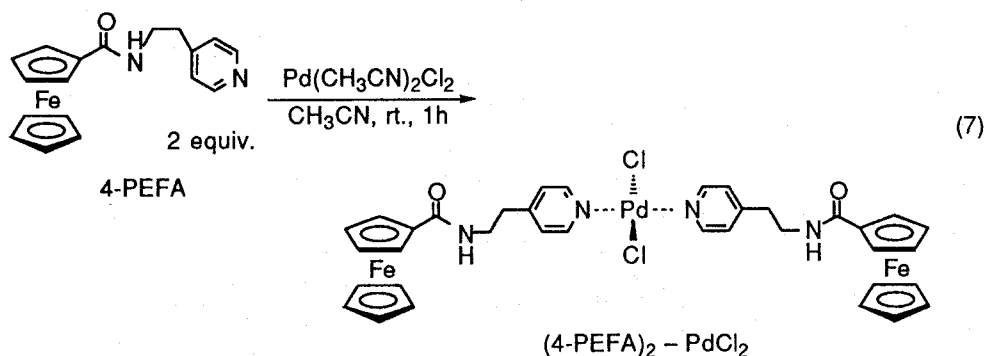
On the basis of these observations, the effect of the position of pyridyl nitrogen was examined. Interestingly, 4-BPEFA bearing the 4-pyridylethyl group was found to form the 2:2 macrocyclic complex maybe due to the difficulty in the intramolecular coordination as shown in eq. 5. All pyridyl protons were equivalent in ¹H-NMR.



To clear the character of complexation behavior of ferrocene ligands, then, 2-PEFA bearing only one pendant group was investigated. 2-PEFA was found to form the 2:1 complex with dichlorobis(acetonitrile)palladium(II) as shown in eq. 6. Two different kinds of peaks due to *cis* and *trans*-isomers were observed in ^1H -NMR. The rotational barrier of isomer, E_a , was calculated as $14.9 \text{ kcal mol}^{-1}$.



In the case of 4-PEFA bearing the 4-pyridyl group instead of the 2-pyridyl one, only one isomeric 2:1 complex was obtained as shown in eq. 7. The barrier of rotation of the pyridyl groups was not detected under the conditions employed here.



3-2-3. Interaction with *p*-Quinones

Ferrocene ligands bearing *N*-heterocyclic coordination sites were found to afford the specific coordination site. These complexation behaviors are characteristic of the pendant pyridyl coordination sites. The interaction with *p*-quinones was examined.

The CT complex was observed in UV-vis. spectra by irradiation (>490 nm) of a mixture of 2-BPEFA and *p*-chloranil as shown in Figure 7. Such a complexation was not observed in the dark. The efficient interaction between the pyridyl moieties and *p*-chloranil is considered to contribute to the complexation since the down-field shift of the pyridyl protons and no remarkable shift of the others were observed in ^1H -NMR.

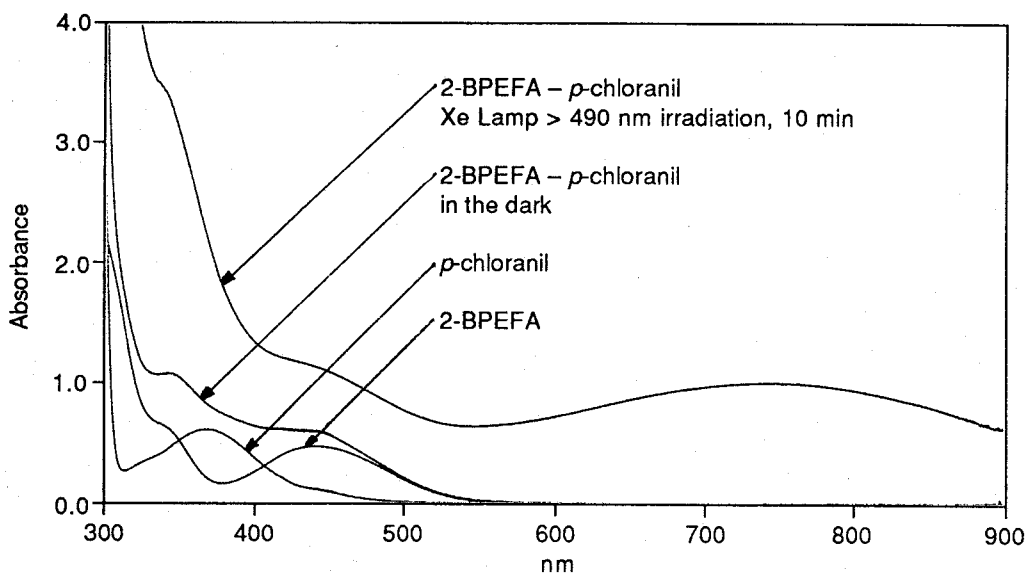


Figure 7. UV - vis. spectra of ligand and complex.
[2-BPEFA] = $1 \times 10^{-3}\text{M}$; [*p*-chloranil] = $1 \times 10^{-3}\text{M}$;
[2-BPEFA] = $1 \times 10^{-3}\text{M}$ - [*p*-chloranil] = $1 \times 10^{-3}\text{M}$;
solv. MeCN; under nitrogen.

Such a complexation was observed when 2,6-dichloro-*p*-quinone was employed instead of *p*-chloranil. 2-BPEFA interacts with 2,6-dichloro-*p*-quinone to result in a blue shift of the broad CT band as compared with *p*-chloranil (Figure 8). Such a spectral change might

support the charge transfer interaction. The similar down-field shift of the pyridyl protons was also observed in ^1H -NMR.

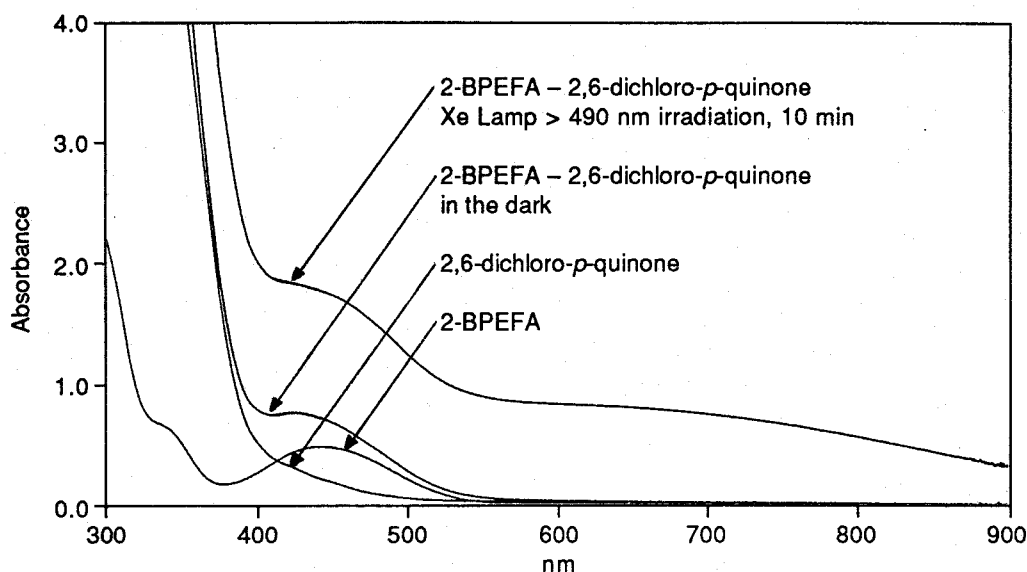


Figure 8. UV - vis. spectra of ligand and complex.
 $[2\text{-BPEFA}] = 1 \times 10^{-3} \text{M}$; $[2,6\text{-dichloro-}p\text{-quinone}] = 5 \times 10^{-3} \text{M}$;
 $[2\text{-BPEFA}] = 1 \times 10^{-3} \text{M} - [2,6\text{-dichloro-}p\text{-quinone}] = 5 \times 10^{-3} \text{M}$;
 solv.MeCN; under nitrogen.

Furthermore, BBFA which has no π -system did not form a CT complex even after irradiation. Although the CT complex has not been isolated yet, a combination of the ferrocene and aromatic π -system is considered to be a key factor for the novel photoinduced CT complexation. Since 2-PEFA bearing only one pendant group did not show such an interaction, two pendant group is also essential for the present interaction.

3-3. Conclusion

Synthesis and characterization of the complexation behavior of the ferrocene ligands bearing *N*-heterocyclic coordination sites are presented here. It has been disclosed that the imide-bridged [3]ferrocenophane, 2-pyridyl-1,1'-ferrocenedicarboximide, is synthesized directly in one stage and the ferrocene ligands afford the specific coordination sites based on two rotatory coplanar cyclopentadienyl rings.

3-4. Experimental

General

Melting points were measured using Yanagimoto micromelting point apparatus and are uncorrected. Infrared spectra were recorded on a Perkin-Elmer FT-IR 1605 infrared. ¹H-NMR spectra were recorded on a Bruker AM-600 (600MHz) spectrometer, a JEOL JNM-GSX-400 (400MHz) spectrometer, and a JEOL JNM-EX-270 (270MHz) spectrometer with tetramethylsilane as an internal standard. ¹³C-NMR spectra were recorded on a Bruker AM-600 (600MHz) spectrometer. UV-vis. spectra were recorded using a Hitachi U-3000. The X-ray crystallography was made on Rigaku AFC5R diffractometer. The fast atom bombardment mass spectra were run on a JEOL JMS-DX303HF spectrometer. Recycling preparative HPLC analysis was performed on a JAI LC-908. The standard electrochemical instrumentation consisted of a Hokuto Denko potentiostat / galvanostat HA-301S and a Hokuto Denko function generator HB-104S with a three-electrode system consisting of a glassy carbon working electrode, a platinum auxiliary electrode, and a KCl-

saturated calomel reference electrode. Cyclic voltammograms were recorded with Graphtec WX 1000.

Synthesis of *N,N'*-Bis{2-(2-pyridyl)ethyl}-1,1'-ferrocenedicarboxamide (2-BPEFA). To a stirred mixture of 2-(2-aminoethyl)pyridine (1.4 mL, 12 mmol), 4-dimethylaminopyridine (0.0369 g, 0.3 mmol), and triethylamine (8.6 mL, 60 mmol) in dichloromethane (20 mL) was dropwise added 1,1'-ferrocenedicarboxylic acid chloride (1.87 g, 6.0 mmol) in dichloromethane (40 mL) under nitrogen at 0 °C. The mixture was stirred at 0 °C for 7 h and at room temperature for 17 h. The resulting mixture was diluted with dichloromethane (30 mL), washed with saturated NaHCO₃ aqueous solution and brine, and dried over MgSO₄. The solvent was evaporated in vacuo, and the residue was chromatographed over alumina and eluted with dichloromethane. Orange solid, 2-BPEFA, was isolated in 85 % yield and purified as an orange prism by recrystallization from dichloromethane.

2-BPEFA. Mp 132-134 °C (uncorrected); IR (KBr, cm⁻¹) 3264 (NH), 1644 (C=O), 1554 (C=C); ¹H NMR (270 MHz, CDCl₃) δ 8.59 (ddd, 2H, *J* = 5.0, 1.7, 1.0 Hz, Py), 7.65 (dt, 2H, *J* = 7.6, 1.7 Hz, Py), 7.46 (br, 2H, NH), 7.26 (dt, 2H, *J* = 7.6, 1.0 Hz, Py), 7.18 (ddd, 2H, *J* = 7.6, 5.0, 1.0 Hz, Py), 4.49 (t, 4H, *J* = 2.0 Hz, Cp), 4.28 (t, 4H, *J* = 2.0 Hz, Cp), 3.81 (q, 4H, *J* = 6.6 Hz, CH₂), 3.13 (t, 4H, *J* = 6.6 Hz, CH₂); MS (FAB) *m/z* 483 (M⁺+1). Anal. Calcd for C₂₆H₂₆N₄O₂Fe: C, 64.74; H, 5.43; N, 11.62. Found: C, 64.52; H, 5.47; N, 11.63.

Synthesis of *N,N'*-Bis{2-(4-pyridyl)ethyl}-1,1'-ferrocenedicarboxamide (4-BPEFA). To a stirred mixture of 4-(2-aminoethyl)pyridine (1.2 mL, 10 mmol), 4-dimethylaminopyridine (0.0305 g, 0.25 mmol), and triethylamine (7.0 mL, 50 mmol) in dichloromethane (20 mL) was dropwise added 1,1'-ferrocenedicarboxylic acid chloride (1.56 g, 5.0 mmol) in dichloromethane (40 mL) under nitrogen at 0 °C. The

mixture was stirred at 0 °C for 7 h and at room temperature for 17 h. The resulting mixture was diluted with dichloromethane (30 mL), washed with saturated NaHCO₃ aqueous solution and brine, and dried over MgSO₄. The solvent was evaporated in vacuo, and the residue was chromatographed over alumina and eluted with dichloromethane. Orange solid, 4-BPEFA, was isolated in 80 % yield and purified as a microcrystalline orange solid by recrystallization from dichloromethane.

4-BPEFA. Mp 169-170 °C (decomp); IR (KBr, cm⁻¹) 3232 (NH), 1650 (C=O), 1548 (C=C); ¹H NMR (270 MHz, CD₃CN) δ 8.49 (d, 4H, *J* = 5.9 Hz, Py), 7.29 (d, 4H, *J* = 5.9 Hz, Py), 7.11 (br, 2H, NH), 4.40 (t, 4H, *J* = 2.0 Hz, Cp), 4.26 (t, 4H, *J* = 2.0 Hz, Cp), 3.58 (q, 4H, *J* = 6.9 Hz, CH₂), 2.92 (t, 4H, *J* = 6.9 Hz, CH₂); MS (FAB) *m/z* 483 (M⁺⁺1). Anal. Calcd for C₂₆H₂₆N₄O₂Fe: C, 64.74; H, 5.43; N, 11.62. Found: C, 64.61; H, 5.50; N, 11.74.

Synthesis of *N,N'*-Bis(2-phenethyl)-1,1'-ferrocenedicarboxamide (BPHEFA). To a stirred mixture of phenethylamine (1.1 mL, 9 mmol), 4-dimethylaminopyridine (0.0306 g, 0.25 mmol), and triethylamine (6.5 mL, 45 mmol) in dichloromethane (20 mL) was dropwise added 1,1'-ferrocenedicarboxylic acid chloride (1.40 g, 4.5 mmol) in dichloromethane (30 mL) under nitrogen at 0 °C. The mixture was stirred at 0 °C for 7 h and at room temperature for 17 h. The resulting mixture was diluted with dichloromethane (30 mL), washed with saturated NaHCO₃ aqueous solution and brine, and dried over MgSO₄. The solvent was evaporated in vacuo, and the residue was chromatographed over alumina and eluted with dichloromethane. Orange solid, BPHEFA, was isolated in 84 % yield and purified as an orange prism by recrystallization from dichloromethane.

BPHEFA. Mp 176-177 °C (uncorrected); IR (KBr, cm⁻¹) 3236 (NH), 1628 (C=O), 1554 (C=C); ¹H NMR (400 MHz, CDCl₃) δ 7.37-7.23 (m, 12H, Ph), 6.68 (br, 2H, NH), 4.37 (t, 4H, *J* = 1.8 Hz, Cp), 4.30 (t, 4H, *J* = 1.8 Hz, Cp),

3.69 (q, 4H, $J = 7.0$ Hz, CH₂), 2.98 (t, 4H, $J = 7.0$ Hz, CH₂); MS (FAB) m/z 481 ($M^{+}+1$). Anal. Calcd for C₂₈H₂₈N₂O₂Fe: C, 70.01; H, 5.88; N, 5.83. Found: C, 69.95; H, 5.91; N, 5.87.

Synthesis of *N,N'*-Bis(*n*-butyl)-1,1'-ferrocenedicarboxamide (BBFA).

To a stirred mixture of butylamine (0.395 mL, 4.0 mmol), 4-dimethylaminopyridine (0.0121 g, 0.1 mmol), and triethylamine (2.8 mL, 20 mmol) in dichloromethane (10 mL) was dropwise added 1,1'-ferrocenedicarboxylic acid chloride (0.62 g, 2.0 mmol) in dichloromethane (20 mL) under nitrogen at 0 °C. The mixture was stirred at 0 °C for 7 h and at room temperature for 17 h. The resulting mixture was diluted with dichloromethane (20 mL), washed with saturated NaHCO₃ aqueous solution and brine, and dried over MgSO₄. The solvent was evaporated in vacuo, and the residue was chromatographed over alumina and eluted with dichloromethane. Orange solid, BBFA, was isolated in 82 % yield and purified as a microcrystalline orange solid by recrystallization from dichloromethane.

BBFA. Mp 156-158 °C (uncorrected); IR (KBr, cm⁻¹) 3328 (NH), 1634 (C=O), 1554 (C=C); ¹H NMR (600 MHz, CD₃CN) δ 7.04 (br, 2H, NH), 4.52 (t, 4H, $J = 1.8$ Hz, Cp), 4.35 (t, 4H, $J = 1.8$ Hz, Cp), 3.28 (q, 4H, $J = 7.2$ Hz, CH₂), 1.57 (quit, 4H, $J = 7.2$ Hz, CH₂), 1.42 (sext, 4H, $J = 7.2$ Hz, CH₂), 0.96 (t, 6H, $J = 7.2$ Hz, CH₃); MS (FAB) m/z 385 ($M^{+}+1$). Anal. Calcd for C₂₀H₂₈N₂O₂Fe: C, 62.51; H, 7.34; N, 7.29. Found: C, 62.50; H, 7.40; N, 7.29.

Synthesis of *N,N'*-Bis{1-methoxycarbonyl-2-(4-imidazolyl)ethyl}-1,1'-ferrocenedicarboxamide (BMEIFA). To a stirred mixture of L-histidine methyl ester dihydrochloride (2.4212 g, 10 mmol), 4-dimethylaminopyridine (0.0304 g, 0.25 mmol), and triethylamine (10.5 mL, 75 mmol) in dichloromethane (20 mL) was dropwise added 1,1'-ferrocenedicarboxylic acid chloride (1.55 g, 5.0 mmol) in dichloromethane (40 mL) under nitrogen at 0 °C. The mixture was stirred at 0 °C for 7 h

and at room temperature for 17 h. The resulting mixture was diluted with dichloromethane (30 mL), washed with saturated NaHCO₃ aqueous solution and brine, and dried over MgSO₄. The solvent was evaporated in vacuo, and the residue was chromatographed over alumina and eluted with dichloromethane. Orange solid, BMEIFA, was isolated in 63 % yield and purified as an orange prism by recrystallization from dichloromethane.

BMEIFA. $[\alpha]_D = -64.8^\circ$; Mp 107-109 °C (uncorrected); IR (KBr, cm⁻¹) 3248 (NH), 1742, 1642 (C=O), 1540 (C=C); ¹H NMR (600 MHz, CDCl₃) δ 7.79 (br, 2H, NH), 7.62 (s, 2H, Im), 6.90 (s, 2H, Im), 4.93 (q, 2H, $J = 7.1$ Hz, CH), 4.75 (s, 2H, Cp), 4.71 (s, 2H, Cp), 4.42 (s, 4H, Cp), 3.74 (s, 6H, CH₃), 3.27-3.19 (m, CH₂); MS (FAB) m/z 577 (M⁺+1). Anal. Calcd for C₂₆H₂₈N₆O₆Fe·H₂O: C, 52.54; H, 5.09; N, 14.14. Found: C, 52.22; H, 4.92; N, 13.76.

Synthesis of *N,N'*-Bis((2-pyridyl)methyl)-1,1'-ferrocenedicarboxamide (2-BPMFA). To a stirred mixture of 2-(aminomethyl)pyridine (0.722 mL, 7 mmol), 4-dimethylaminopyridine (0.0429 g, 0.35 mmol), and triethylamine (4.9 mL, 35 mmol) in dichloromethane (20 mL) was dropwise added 1,1'-ferrocenedicarboxylic acid chloride (1.09 g, 3.5 mmol) in dichloromethane (30 mL) under nitrogen at 0 °C. The mixture was stirred at 0 °C for 7 h and at room temperature for 17 h. The resulting mixture was diluted with dichloromethane (30 mL), washed with saturated NaHCO₃ aqueous solution and brine, and dried over MgSO₄. The solvent was evaporated in vacuo, and the residue was chromatographed over alumina and eluted with dichloromethane. Orange solid, 2-BPMFA, was isolated in 79 % yield and purified as an orange prism by recrystallization from dichloromethane.

2-BPMFA. Mp 236-237 °C (decomp); IR (KBr, cm⁻¹) 3280 (NH), 1650 (C=O), 1554 (C=C); ¹H NMR (400 MHz, CD₃CN) δ 9.39 (br, 2H, NH), 8.59 (ddd, 2H,

$J = 4.9, 1.7, 0.7$ Hz, Py), 7.78 (dt, 2H, $J = 7.8, 1.7$ Hz, Py), 7.40 (ddd, 2H, $J = 7.8, 1.0, 0.7$ Hz, Py), 7.30 (ddd, 2H, $J = 7.8, 4.9, 1.0$ Hz, Py), 4.69 (t, 4H, $J = 2.0$ Hz, Cp), 4.45 (d, 4H, $J = 6.1$ Hz, CH₂), 4.37 (t, 4H, $J = 2.0$ Hz, Cp); MS (FAB) m/z 455 (M^{++1}). Anal. Calcd for C₂₄H₂₂N₄O₂Fe: C, 63.45; H, 4.88; N, 12.33. Found: C, 63.22; H, 4.92; N, 12.28.

Synthesis of 2-(2-Pyridyl)ethylferrocenecarboxamide (2-PEFA). To a stirred mixture of 2-(2-aminoethyl)pyridine (0.24 mL, 2 mmol), 4-dimethylaminopyridine (0.0060 g, 0.05 mmol), and triethylamine (1.4 mL, 10 mmol) in dichloromethane (10 mL) was dropwise added ferrocenecarboxylic acid chloride (0.50 g, 2.0 mmol) in dichloromethane (20 mL) under nitrogen at 0 °C. The mixture was stirred at 0 °C for 7 h and at room temperature for 17 h. The resulting mixture was diluted with dichloromethane (20 mL), washed with saturated NaHCO₃ aqueous solution and brine, and dried over MgSO₄. The solvent was evaporated in vacuo, and the residue was chromatographed over alumina and eluted with dichloromethane. Orange solid, 2-PEFA, was isolated in 85 % yield and purified as an orange needle by recrystallization from dichloromethane.

2-PEFA. Mp 143-144 °C (uncorrected); IR (KBr, cm⁻¹) 3300 (NH), 1628 (C=O), 1556 (C=C); ¹H NMR (400 MHz, CDCl₃) δ 8.63 (ddd, 1H, $J = 4.9, 1.8, 0.7$ Hz, Py), 7.86 (dt, 1H, $J = 7.7, 1.8$ Hz, Py), 7.24 (ddd, 1H, $J = 7.7, 1.1, 0.7$ Hz, Py), 7.20 (ddd, 1H, $J = 7.7, 4.9, 1.1$ Hz, Py), 6.91 (br, 1H, NH), 4.65 (t, 2H, $J = 1.8$ Hz, Cp), 4.31 (t, 2H, $J = 1.8$ Hz, Cp), 4.11 (s, 5H, Cp), 3.81 (q, 2H, $J = 6.0$ Hz, CH₂), 3.10 (t, 2H, $J = 6.0$ Hz, CH₂); MS (FAB) m/z 335 (M^{++1}). Anal. Calcd for C₁₈H₁₈N₂OFe: C, 64.69; H, 5.43; N, 8.38. Found: C, 64.52; H, 5.47; N, 8.44.

Synthesis of 2-(4-Pyridyl)ethylferrocenecarboxamide (4-PEFA). To a stirred mixture of 4-(2-aminoethyl)pyridine (0.35 mL, 3 mmol), 4-dimethylaminopyridine (0.0092 g, 0.075 mmol), and triethylamine (2.1

mL, 15 mmol) in dichloromethane (10 mL) was dropwise added ferrocenecarboxylic acid chloride (0.75 g, 3.0 mmol) in dichloromethane (20 mL) under nitrogen at 0 °C. The mixture was stirred at 0 °C for 7 h and at room temperature for 17 h. The resulting mixture was diluted with dichloromethane (20 mL), washed with saturated NaHCO₃ aqueous solution and brine, and dried over MgSO₄. The solvent was evaporated in vacuo, and the residue was chromatographed over alumina and eluted with dichloromethane. Orange solid, 4-PEFA, was isolated in 86 % yield and purified as an orange plate by recrystallization from dichloromethane.

4-PEFA. Mp 153-155 °C (uncorrected); IR (KBr, cm⁻¹) 3300 (NH), 1632 (C=O), 1544 (C=C); ¹H NMR (400 MHz, CDCl₃) δ 8.58 (dd, 2H, *J* = 4.6, 1.7 Hz, Py), 7.21 (dd, 2H, *J* = 4.6, 1.6 Hz, Py), 5.68 (br, 1H, NH), 4.60 (t, 2H, *J* = 2.0 Hz, Cp), 4.34 (t, 2H, *J* = 2.0 Hz, Cp), 4.15 (s, 5H, Cp), 3.69 (q, 2H, *J* = 7.0 Hz, CH₂), 2.94 (t, 2H, *J* = 7.0 Hz, CH₂); MS (FAB) *m/z* 335 (M⁺+1). Anal. Calcd for C₁₈H₁₈N₂OFe·0.25H₂O: C, 63.83; H, 5.51; N, 8.27. Found: C, 63.61; H, 5.51; N, 8.30.

Synthesis of (2-Pyridyl)methylferrocenecarboxamide (2-PMFA). To a stirred mixture of 2-(aminomethyl)pyridine (0.206 mL, 2 mmol), 4-dimethylaminopyridine (0.0060 g, 0.05 mmol), and triethylamine (1.4 mL, 10 mmol) in dichloromethane (10 mL) was dropwise added ferrocenecarboxylic acid chloride (0.50 g, 2.0 mmol) in dichloromethane (20 mL) under nitrogen at 0 °C. The mixture was stirred at 0 °C for 7 h and at room temperature for 17 h. The resulting mixture was diluted with dichloromethane (20 mL), washed with saturated NaHCO₃ aqueous solution and brine, and dried over MgSO₄. The solvent was evaporated in vacuo, and the residue was chromatographed over alumina and eluted with dichloromethane. Orange solid, 2-PMFA, was isolated in 93 % yield

and purified as an orange needle by recrystallization from dichloromethane.

2-PMFA. Mp 144-145 °C (uncorrected); IR (KBr, cm^{-1}) 3332 (NH), 1638 (C=O), 1548 (C=C); ^1H NMR (400 MHz, CDCl_3) δ 8.61 (ddd, 1H, J = 4.9, 1.8, 0.6 Hz, Py), 7.70 (dt, 1H, J = 7.8, 1.8 Hz, Py), 7.37 (dt, 1H, J = 7.8, 0.6 Hz, Py), 7.23 (ddd, 1H, J = 7.8, 4.9, 0.6 Hz, Py), 6.98 (br, 1H, NH), 4.75 (t, 2H, J = 1.8 Hz, Cp), 4.69 (d, 2H, J = 5.3 Hz, CH_2), 4.36 (t, 2H, J = 1.8 Hz, Cp), 4.18 (s, 5H, Cp); MS (FAB) m/z 321 ($\text{M}^+ + 1$). Anal. Calcd for $\text{C}_{17}\text{H}_{16}\text{N}_2\text{OFe} \cdot 0.5\text{H}_2\text{O}$: C, 62.03; H, 5.21; N, 8.51. Found: C, 62.06; H, 5.26; N, 8.53.

Synthesis of 2-Pyridyl-1,1'-ferrocenedicarboximide (PFDCI) and N,N' -Bis(2-pyridyl)-1,1'-ferrocenedicarboxamide (2-BPFA). To a stirred mixture of 2-aminopyridine (0.377g, 4.0 mmol), 4-dimethylaminopyridine (0.0122g, 0.1 mmol), and triethylamine (2.8 mL, 20 mmol) in dichloromethane (10 mL) was dropwise added 1,1'-ferrocenedicarboxylic acid chloride (0.62 g, 2.0 mmol) in dichloromethane (30 mL) under nitrogen at 0 °C. The mixture was stirred at 0 °C for 7 h and at room temperature for 17 h. The resulting mixture was diluted with dichloromethane (20 mL), washed with saturated NaHCO_3 aqueous solution and brine, and dried over MgSO_4 . Orange solid was obtained by evaporation of the dichloromethane solution in vacuo. PFDCI and 2-BPFA were isolated by recycling preparative HPLC and recrystallized from dichloromethane.

PFDCI. Orange prisms; yield, 57%; mp 215-219 °C (decomp); IR (KBr, cm^{-1}) 1702, 1655 (C=O), 1587 (C=C); ^1H NMR (400 MHz, CDCl_3) δ 8.62 (ddd, 1H, J = 4.9, 2.0, 0.7 Hz, Py), 7.86 (dt, 1H, J = 7.7, 2.0 Hz, Py), 7.38 (ddd, 1H, J = 7.7, 1.0, 0.7 Hz, Py), 7.33 (ddd, 1H, J = 7.7, 4.9, 1.0 Hz, Py), 4.82 (t, 4H, J = 2.0 Hz, Cp), 4.58 (t, 4H, J = 2.0 Hz, Cp); ^{13}C NMR (150 MHz, CDCl_3) δ 171.4 (C=O), 153.2 (Py), 149.7 (Py), 138.4 (Py), 123.1 (Py), 122.9 (Py), 76.9 (ipso Cp),

75.3 (Cp), 72.8 (Cp); MS (FAB) m/z 333 (M^{++1}). Anal. Calcd for $C_{17}H_{12}N_2O_2Fe$: C, 61.48; H, 3.64; N, 8.43. Found: C, 61.27; H, 3.67; N, 8.38.

2-BPFA. Orange prisms; yield, 4%; mp 158-161 °C (decomp); IR (KBr, cm^{-1}) 3362 (NH), 1664 (C=O), 1576 (C=C); 1H NMR (400 MHz, $CDCl_3$) δ 8.66 (bs, 2H, NH), 8.26 (ddd, 2H, $J = 4.9, 2.1, 1.1$ Hz, Py), 8.24 (dt, 2H, $J = 8.3, 1.1$ Hz, Py), 7.65 (ddd, 2H, $J = 8.3, 7.3, 2.1$ Hz, Py), 7.02 (ddd, 2H, $J = 7.3, 4.9, 1.1$ Hz, Py), 4.91 (t, 4H, $J = 2.0$ Hz, Cp), 4.53 (t, 4H, $J = 2.0$ Hz, Cp); ^{13}C NMR (150 MHz, $CDCl_3$) δ 168.1 (C=O), 151.5 (Py), 147.6 (Py), 138.4 (Py), 119.5 (Py), 114.2 (Py), 77.7 (ipso Cp), 72.7 (Cp), 70.4 (Cp); MS (FAB) m/z 427 (M^{++1}). Anal. Calcd for $C_{22}H_{18}N_4O_2Fe \cdot 0.25H_2O$: C, 61.34; H, 4.33; N, 13.01. Found: C, 61.27; H, 4.42; N, 12.54.

Synthesis of N,N' -Bis(4-pyridyl)-1,1'-ferrocenedicarboxamide (4-BPFA). To a stirred mixture of 4-aminopyridine (0.847g, 9.0 mmol), 4-dimethylaminopyridine (0.0274g, 0.23 mmol), and triethylamine (6.5 mL, 45 mmol) in dichloromethane (20 mL) was dropwise added 1,1'-ferrocenedicarboxylic acid chloride (1.40 g, 4.5 mmol) in dichloromethane (60 mL) under nitrogen at 0 °C. The mixture was stirred at 0 °C for 7 h and at room temperature for 17 h. The resulting mixture was diluted with dichloromethane (30 mL), washed with saturated $NaHCO_3$ aqueous solution and brine, and dried over $MgSO_4$. The solvent was evaporated in vacuo, and the residue was chromatographed over alumina and eluted with dichloromethane. Orange solid, 4-BPFA, was isolated in 74 % yield and purified as a microcrystalline orange solid by recrystallization from dichloromethane.

4-BPFA. Mp 174-177 °C (decomp); IR (KBr, cm^{-1}) 3234(NH), 1675(C=O), 1581(C=C); 1H NMR (400 MHz, $CDCl_3$) δ 8.88 (bs, 2H, NH), 8.58 (dd, 4H, $J = 4.9, 1.6$ Hz, Py), 7.73 (dd, 4H, $J = 4.9, 1.6$ Hz, Py), 4.69 (t, 4H, $J = 1.8$ Hz, Cp), 4.56 (t, 4H, $J = 1.8$ Hz, Cp); ^{13}C NMR (150 MHz, $CDCl_3$) δ 170.0 (C=O), 150.9 (Py), 145.2 (Py), 113.7 (Py), 78.4 (ipso Cp), 71.9 (Cp), 71.5 (Cp); MS (FAB)

m/z 427 (M^++1). Anal. Calcd for $C_{22}H_{18}N_4O_2Fe \cdot H_2O$: C, 59.48; H, 4.54; N, 12.61. Found: C, 59.73; H, 4.41; N, 12.46.

Preparation of 2-BPEFA-PdCl₂. A mixture of 2-BPEFA (0.0242 g, 0.05 mmol) and dichloro-bis(acetonitrile)palladium(II) (0.0130 g, 0.05 mmol) was stirred in acetonitrile (3.0 mL) under nitrogen atmosphere at room temperature for 1 h. The reaction mixture was filtered to remove impurities. After evaporation of the solution, orange solid, 2-BPEFA-PdCl₂, was isolated in 80 % yield and purified as an orange prism by recrystallization from a chloroform/acetonitrile (1:1 v/v).

2-BPEFA-PdCl₂: Mp 215-217 °C (decomp.); IR (KBr, cm⁻¹) 3312 (NH), 1634 (C=O), 1548 (C=C); ¹H-NMR (400 MHz, CD₃CN) δ 9.01 (ddd, 2H, J = 5.7, 1.6, 0.7 Hz, Py), 7.88 (dt, 2H, J = 7.7, 1.6 Hz, Py), 7.52 (dt, 2H, J = 7.7, 1.6, 0.7 Hz, Py), 7.39 (ddd, 2H, J = 7.7, 5.7, 1.6 Hz, Py), 7.10 (br, 2H, NH), 4.70 (t, 4H, J = 2.0 Hz, Cp), 4.45 (t, 4H, J = 2.0 Hz, Cp), 4.37-4.32 (m, 4H, CH₂), 3.94-3.88 (m, 4H, CH₂); MS (FAB) m/z 660 (M^++1). Anal. Calcd for $C_{26}H_{26}N_4O_2FePdCl_2 \cdot 2H_2O$: C, 44.89; H, 4.35; N, 8.05; Cl, 10.19. Found: C, 44.70; H, 4.37; N, 8.21; Cl, 10.44.

Preparation of 4-BPEFA-PdCl₂. A mixture of 4-BPEFA (0.0242 g, 0.05 mmol) and dichloro-bis(acetonitrile)palladium(II) (0.0130 g, 0.05 mmol) was stirred in acetonitrile (20 mL) under nitrogen atmosphere at room temperature for 1 h. The reaction mixture was filtered to remove impurities. After evaporation of the solution, orange solid, 4-BPEFA-PdCl₂, was isolated in 58 % yield and purified as a microcrystalline orange solid by recrystallization from acetonitrile.

4-BPEFA-PdCl₂: Mp >300 °C (decomp.); IR (KBr, cm⁻¹) 3308 (NH), 1622 (C=O), 1534 (C=C); ¹H-NMR (600 MHz, d₆-DMSO) δ 8.66 (d, 8H, J = 6.5 Hz, Py), 7.99 (t, 4H, J = 6.8 Hz, NH), 7.45 (d, 8H, J = 6.6 Hz, Py), 4.63 (t, 8H, J = 1.7 Hz, Cp), 4.25 (t, 8H, J = 1.7 Hz, Cp), 3.48 (q, 8H, J = 6.8 Hz, CH₂), 2.95 (t, 8H, J = 6.8 Hz, CH₂); MS (FAB) m/z 1320 (M^++1).

Preparation of 2-BPMFA-PdCl₂. A mixture of 2-BPMFA (0.0226 g, 0.05 mmol) and dichloro-bis(acetonitrile)palladium(II) (0.0131 g, 0.05 mmol) was stirred in acetonitrile (3.0 mL) under nitrogen atmosphere at room temperature for 1 h. The reaction mixture was filtered to remove impurities. After evaporation of the solution, orange solid, 2-BPMFA-PdCl₂, was isolated in 83 % yield and purified as an orange prism by recrystallization from acetonitrile.

2-BPMFA-PdCl₂: Mp 194-196 °C (decomp.); IR (KBr, cm⁻¹) 3332 (NH), 1648 (C=O), 1534 (C=C); ¹H-NMR (400 MHz, CD₃CN) δ 9.10 (ddd, 2H, *J* = 5.7, 1.6, 0.7 Hz, Py), 7.93 (dt, 2H, *J* = 7.7, 1.6 Hz, Py), 7.59 (ddd, 2H, *J* = 7.7, 1.6, 0.7 Hz, Py), 7.38 (br, 2H, NH), 5.58 (d, 4H, *J* = 5.0 Hz, CH₂), 4.81 (t, 4H, *J* = 2.0 Hz, Cp), 4.37 (t, 4H, *J* = 2.0 Hz, Cp); MS (FAB) *m/z* 1264 (2M⁺⁺+1). Anal. Calcd for C₂₄H₂₂N₄O₂FePdCl₂·2H₂O: C, 43.18; H, 3.93; N, 8.39; Cl, 10.62. Found: C, 43.47; H, 3.97; N, 8.49; Cl, 10.48.

Preparation of (2-PEFA)₂-PdCl₂. A mixture of 2-PEFA (0.0134 g, 0.04 mmol) and dichloro-bis(acetonitrile)palladium(II) (0.0052 g, 0.02 mmol) was stirred in acetonitrile (2.0 mL) under nitrogen atmosphere at room temperature for 1 h. The reaction mixture was filtered to remove impurities. After evaporation of the solution, yellow solid, (2-PEFA)₂-PdCl₂, was isolated in 84 % yield and purified as a yellow needle by recrystallization from a chloroform/acetonitrile (1:1 v/v).

(2-PEFA)₂-PdCl₂: Mp 158-161 °C (decomp.); IR (KBr, cm⁻¹) 3230 (NH), 1621 (C=O), 1544 (C=C); ¹H-NMR (600 MHz, CD₃CN) δ 9.29 (d, 2H, *J* = 5.6 Hz), 9.05 (d, 2H, *J* = 5.6 Hz), 7.90-7.84 (m, 4H), 7.60 (d, 2H, *J* = 7.8 Hz), 7.54 (d, 2H, *J* = 7.8 Hz), 7.42-7.36 (m, 6H), 6.90 (br, 2H), 4.78 (t, 4H, *J* = 1.7 Hz), 4.73 (t, 4H, *J* = 1.7 Hz), 4.32 (t, 8H, *J* = 1.7 Hz), 4.27-4.23 (m, 8H), 4.19-4.15 (m, 4H), 4.12-4.01 (m, 24H); MS (FAB) *m/z* 846 (M⁺⁺+1). Anal. Calcd for C₃₆H₃₆N₄O₂Fe₂PdCl₂·0.5CHCl₃: C, 48.42; H, 4.06; N, 6.19; Cl, 13.71. Found: C, 48.25; H, 4.10; N, 6.22; Cl, 13.80.

Preparation of (4-PEFA)₂-PdCl₂. A mixture of 4-PEFA (0.0133 g, 0.04 mmol) and dichloro-bis(acetonitrile)palladium(II) (0.0052 g, 0.02 mmol) was stirred in acetonitrile (2.0 mL) under nitrogen atmosphere at room temperature for 1 h. The reaction mixture was filtered to remove impurities. After evaporation of the solution, yellow solid, (4-PEFA)₂-PdCl₂, was isolated in 72 % yield and purified as a yellow needle by recrystallization from acetonitrile.

(4-PEFA)₂-PdCl₂: Mp 207-210 °C (decomp.); IR (KBr, cm⁻¹) 3259 (NH), 1619 (C=O), 1535 (C=C); ¹H-NMR (600 MHz, d₆-DMSO) δ 8.62 (d, 4H, *J* = 6.5 Hz, Py), 7.91 (t, 4H, *J* = 6.8 Hz, NH), 7.45 (d, 4H, *J* = 6.5 Hz, Py), 4.73 (t, 8H, *J* = 1.7 Hz, Cp), 4.32 (t, 8H, *J* = 1.7 Hz, Cp), 3.47 (q, 8H, *J* = 6.8 Hz, CH₂), 2.94 (t, 8H, *J* = 6.8 Hz, CH₂); MS (FAB) *m/z* 846 (M⁺+1). Anal. Calcd for C₃₆H₃₆N₄O₂Fe₂PdCl₂: C, 51.13; H, 4.29; N, 6.63; Cl, 8.38. Found: C, 51.05; H, 4.28; N, 6.66; Cl, 8.13.

UV-vis. Spectra Measurements. UV-vis. spectra were taken under nitrogen atmosphere at 30 °C after keeping the acetonitrile solutions of 2-BPEFA and *p*-quinone.

Electrochemical Experiments. All electrochemical measurements were carried out at 25 °C under an atmospheric pressure of nitrogen, which was previously passed through a solution of the same composition as the electrolysis solution. Cyclic voltammograms were obtained in the dichloromethane solutions containing 0.1 M Bu₄NClO₄ as a supporting electrolyte ([ferrocene derivatives] = 1 × 10⁻³ M). Potentials were determined with reference to a KCl saturated calomel electrode at 100 mVs⁻¹ scan rate.

X-ray Crystal Structure Determination of PFDCI. An orange crystal of PFDCI with approximate dimensions of 0.50 x 0.30 x 0.30 mm was mounted on a glass fiber. The measurement was made on Rigaku AFC5R diffractometer with graphite-monochromated Mo-Kα radiation

and a 12kW rotating anode generator. Cell constants and an orientation matrix for data collection were obtained from a least-square refinement using the setting angles of 25 carefully centered reflections in the range $27.15 < 2\theta < 27.43^\circ$ corresponded to a primitive monoclinic cell with dimensions. The data were collected at a temperature of $23 \pm 1^\circ\text{C}$ using the ω - 2θ scan technique to a maximum 2θ value of 55.1° . Totals of 3513 independent reflections were obtained and 3325 were unique ($R_{\text{int}} = 0.061$). The structure was solved by direct methods and expanded using Fourier techniques. The non-hydrogen atoms were refined anisotropically. The final cycle of full-matrix least-squares refinement was based on 2161 observed reflections ($I > 3.00\sigma(I)$) and 217 variable parameters. $R = 0.063$, $R_w = 0.073$. Crystallographic details are given in Table 3.

X-ray Crystal Structure Determination of 2-BPMFA. An orange crystal of 2-BPMFA with approximate dimensions of $0.30 \times 0.30 \times 0.30$ mm was mounted on a glass fiber. The measurement was made on Rigaku AFC5R diffractometer with graphite-monochromated Mo- $K\alpha$ radiation and a 12kW rotating anode generator. Cell constants and an orientation matrix for data collection were obtained from a least-square refinement using the setting angles of 24 carefully centered reflections in the range $27.00 < 2\theta < 27.40^\circ$ corresponded to a primitive monoclinic cell with dimensions. The data were collected at a temperature of $23 \pm 1^\circ\text{C}$ using the ω - 2θ scan technique to a maximum 2θ value of 55.0° . Totals of 6256 independent reflections were obtained and 5936 were unique ($R_{\text{int}} = 0.040$). The structure was solved by direct methods and expanded using Fourier techniques. The non-hydrogen atoms were refined anisotropically. The final cycle of full-matrix least-squares refinement was based on 3714 observed reflections ($I > 3.00\sigma(I)$) and 398 variable

parameters. $R = 0.071$, $R_w = 0.078$. Crystallographic details are given in Table 5.

X-ray Crystal Structure Determination of 2-BPMFA-PdCl₂. A n orange crystal of 2-BPMFA-PdCl₂ with approximate dimensions of 0.70 x 0.50 x 0.20 mm was mounted on a glass fiber. The measurement was made on Rigaku AFC5R diffractometer with graphite-monochromated Mo-K α radiation and a 12kW rotating anode generator. Cell constants and an orientation matrix for data collection were obtained from a least-square refinement using the setting angles of 25 carefully centered reflections in the range $27.10 < 2\theta < 27.45^\circ$ corresponded to a primitive monoclinic cell with dimensions. The data were collected at a temperature of $23 \pm 1^\circ\text{C}$ using the ω - 2θ scan technique to a maximum 2θ value of 55.0° . Totals of 6122 independent reflections were obtained and 5831 were unique ($R_{\text{int}} = 0.036$). The structure was solved by direct methods and expanded using Fourier techniques. The non-hydrogen atoms were refined anisotropically. The final cycle of full-matrix least-squares refinement was based on 4701 observed reflections ($I > 3.00\sigma(I)$) and 417 variable parameters. $R = 0.048$, $R_w = 0.058$. Crystallographic details are given in Table 5.

X-ray Crystal Structure Determination of 2-BPEFA-PdCl₂. A n orange crystal of 2-BPEFA-PdCl₂ with approximate dimensions of 0.10 x 0.20 x 0.30 mm was mounted on a glass fiber. The measurement was made on Rigaku AFC5R diffractometer with graphite-monochromated Mo-K α radiation and a 12kW rotating anode generator. Cell constants and an orientation matrix for data collection were obtained from a least-square refinement using the setting angles of 25 carefully centered reflections in the range $27.10 < 2\theta < 27.46^\circ$ corresponded to a primitive monoclinic cell with dimensions. The data were collected at a temperature of $23 \pm 1^\circ\text{C}$ using the ω - 2θ scan technique to a maximum 2θ

value of 55.0 °. Totals of 6661 independent reflections were obtained and 6364 were unique ($R_{\text{int}} = 0.048$). The structure was solved by direct methods and expanded using Fourier techniques. The non-hydrogen atoms were refined anisotropically. The final cycle of full-matrix least-squares refinement was based on 3438 observed reflections ($I > 3.00\sigma(I)$) and 343 variable parameters. $R = 0.076$, $R_w = 0.088$. Crystallographic details are given in Table 5.

3-5. References

1. (a) Medina, J. C.; Li, C.; Bott, S. G.; Atwood, J. L.; Gokel, G. W. *J. Am. Chem. Soc.* **1991**, *113*, 366. (b) Beer, P. D.; Chen, Z.; Goulden, A. J.; Graydon, A.; Stokes, S. E.; Wear, T. *J. Chem. Soc., Chem. Commun.* **1993**, 1834.
2. (a) Beer, P. D.; *Chem. Rev.* **1989**, *18*, 409. (b) Butler, I. R.; *Organometallics* **1992**, *11*, 74. (c) Medina, J. C.; Goodnow, T. T.; Rojas, M. T.; Atwood, J. L.; Lynn, B. C.; Kaifer, A. E.; Gokel, G. W. *J. Am. Chem. Soc.* **1992**, *114*, 10583. (d) Beer, P. D.; Chen, Z.; Drew, M. G. B.; Kingston, J.; Ogden, M.; Spencer, P. *J. Chem. Soc., Chem. Commun.* **1993**, 1046. (e) Yamamoto, Y.; Tanase, T.; Mori, I.; Nakamura, Y. *J. Chem. Soc., Dalton Trans.* **1994**, 3191.
3. (a) Sinn, H.; Kaminsky, W. *Adv. Organomet. Chem.* **1980**, *18*, 99. (b) Kaminsky, W.; Külper, K.; Brintzinger, H. H.; Wild, F. R. W. P. *Angew. Chem., Int. Ed. Engl.* **1985**, *24*, 507. (c) Röhl, W.; Brintzinger, H. H.; Rieger, B.; Zolk, R. *Angew. Chem., Int. Ed. Engl.* **1990**, *29*, 279. (d) Spaleck, W.; Antberg, M.; Rohrmann, J.; Winter, A.; Bachmann, B.; Kiprof, P.; Behm, J.; Herrmann, W. A. *Angew. Chem., Int. Ed. Engl.* **1992**, *31*, 1347 and references therein. (e) Erker,

- G.; Aulbach, M.; Wingbermühle, D.; Krüger, C.; Werner, S. *Chem. Ber.* **1993**, *126*, 755.
4. Hisatome, M. *Rev. Heteroat. Chem.* **1992**, *6*, 142 and references therein.
 5. (a) Jones, N. D.; Marsh, R. E.; Richards, J. H. *Acta Crystallogr., Sect. B* **1965**, *19*, 330. (b) Lecomte, P. C.; Dusausay, Y.; Protas, J.; Moise, C.; Tirouflet, J. *Acta Crystallogr., Sect. B* **1973**, *29*, 488. (c) Lecomte, P. C.; Dusausay, Y.; Protas, J.; Moise, C. *Acta Crystallogr., Sect. B* **1973**, *29*, 1127. (d) Batail, P.; Grandjean, D.; Astruc, D.; Dabard, R. *J. Organomet. Chem.* **1975**, *102*, 79.
 6. (a) Gyepes, E.; Glowiak, T.; Toma, S.; Soldánová, J. *J. Organomet. Chem.* **1984**, *276*, 209. (b) Plenio, H.; Yang, J.; Diodone, R.; Heinze, J. *Inorg. Chem.* **1994**, *33*, 4098.
 7. Ogino, H.; Tobita, H.; Habazaki, H.; Shimoi, M. *J. Chem. Soc., Chem. Commun.* **1989**, 828.
 8. (a) Burley, S. K.; Petsko, G. A. *Science* **1985**, *229*, 23. (b) Nishio, M.; Hirota, M. *Tetrahedron* **1989**, *45*, 7201. (c) Jorgensen, W. L.; Severance, D. L. *J. Am. Chem. Soc.* **1990**, *112*, 4768. (d) Atwood, J. L.; Hamada, F.; Robinson, K. D.; Orr, G. W.; Vincent, R. L. *Nature* **1991**, *349*, 683. (e) Suzuki, S.; Green, P. G.; Bumgarner, R. E.; Dasgupta, S.; Goddard III, W. A.; Blake, G. A. *Science* **1992**, *257*, 942. (f) Cochran, J. E.; Parrott, T. J.; Whitlock, H. W. *J. Am. Chem. Soc.* **1992**, *114*, 2269. (g) Subramanian, S.; Wang, L.; Zaworotko, M. J. *Organometallics* **1993**, *12*, 310. (h) Sakaki, S.; Kato, K.; Miyazaki, T.; Musashi, Y.; Ohkubo, K.; Ihara, H.; Hirayama, C. *J. Chem. Soc., Faraday Trans.* **1993**, *89*, 659.

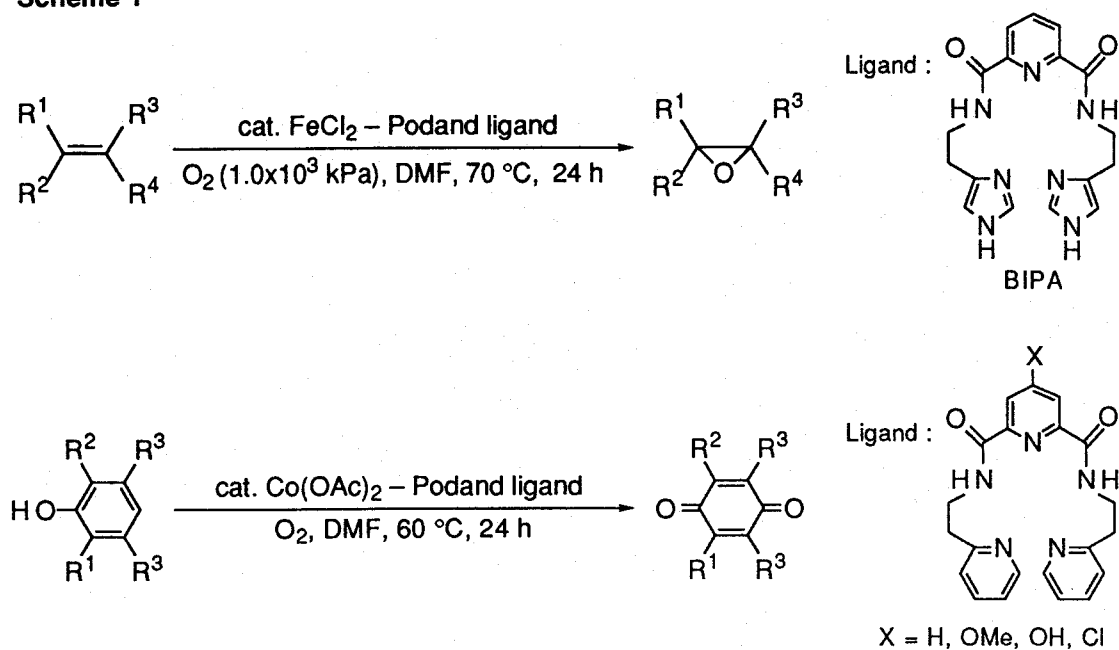
Conclusion

In this thesis, novel transition metal complexes with *N*-heterocyclic multidentate ligands for efficient redox systems are studied. The complexation of transition metals with the flexible multidentate podand ligands is revealed to permit the construction of efficient non-heme systems of oxygenation. It has been disclosed that the multidentate *N*-heterocyclic ligands with the redox center afford the specific coordination sites.

In Chapter 1, the complexation of FeCl_2 with the flexible multidentate podand ligand, BIPA, is revealed to permit the epoxidation reaction with molecular oxygen even in the absence of a co-reductant. Furthermore, the addition of 4-ethoxycarbonyl-3-methyl-2-cyclohexen-1-one leads to the facile epoxidation reaction with molecular oxygen under the milder conditions. The cobalt(II) complex with 2-BPEPA serves as an efficient catalyst for the selective oxygenation of phenols to the corresponding quinones. A combination of podand ligands and transition metals is a key factor for the construction of efficient non-heme systems of oxygenation, possibly due to the difference of the multidentate coordination interaction (Scheme 1).

In Chapter 2, the complexation behavior of quinone ligands is disclosed to depend on the coordination sites or gegen ions. In the case of palladium(II) complexes in which the quinone oxygen coordinates to palladium, four separate reversible redox couples based on the smooth redox interaction between palladium and quinone are observed.

Scheme 1



In Chapter 3, it is disclosed that the imide-bridged [3]ferrocenophane, 2-pyridyl-1,1'-ferrocenedicarboximide, is synthesized directly in one stage and the ferrocene ligands afford the specific coordination sites based on two rotatory coplanar cyclopentadienyl rings.

Ligand coordination greatly contributes to redox process, and the ligand design is a key factor for the construction of a versatile catalytic system.

List of Publications

1. A Novel System for Oxygenation. Effect of Multidentate Podand Ligand in Transition Metal Catalyzed Epoxidation with Molecular Oxygen
Toshikazu Hirao, Toshiyuki Moriuchi, Satoshi Mikami, Isao Ikeda, and Yoshiki Ohshiro
Tetrahedron Lett. **1993**, 34, 1031.
2. An Efficient Epoxidation with Molecular Oxygen Catalyzed by Iron Complex of Multidentate *N*-Heterocyclic Podand Ligand. Additive Effect of 4-Ethoxycarbonyl-3-methyl-2-cyclohexen-1-one
Toshiyuki Moriuchi, Toshikazu Hirao, Yoshiki Ohshiro, and Isao Ikeda
Chem. Lett. **1994**, 915.
3. Multidentate *N*-Heterocyclic Podand Ligand. Efficient Oxygenation of Phenols Catalyzed by Novel Cobalt Complex
Toshiyuki Moriuchi, Toshikazu Hirao, Takuji Ishikawa, Yoshiki Ohshiro, and Isao Ikeda
J. Mol. Catal. **1994**, 95, L1.
4. Synthesis and Molecular Structure of the Novel Imide-Bridged [3]Ferrocenophane
Toshiyuki Moriuchi, Toshikazu Hirao, and Isao Ikeda
Organometallics, in press.

5. Synthesis and Characterization of Novel Palladium(II) Complexes with Quinones Bearing an *N*-Heterocyclic Pendant Functional Group
Toshiyuki Moriuchi, Toshikazu Hirao, Takuo Watanabe, and Isao Ikeda
Inorg. Chem., in contribution.
6. Novel Catalytic System for Oxygenation with Molecular Oxygen Induced by Transition Metal Complex with *N*-Heterocyclic Multidentate Podand Ligand
Toshiyuki Moriuchi, Toshikazu Hirao, Takuji Ishikawa, Kouichirou Nishimura, Satoshi Mikami, Yoshiki Ohshiro, and Isao Ikeda
J. Mol. Catal., in contribution.
7. Synthesis and Characterization of Novel Palladium(II) Complexes of Ferrocene Derivatives Bearing *N*-Heterocyclic Coordination Sites
Toshiyuki Moriuchi, Toshikazu Hirao, and Isao Ikeda
In preparation.
8. Photoinduced Complexation of Ferrocene Receptor Bearing *N*-Heterocyclic Coordination Sites
Toshikazu Hirao, Toshiyuki Moriuchi, and Isao Ikeda
In preparation.

Acknowledgement

I would like to express my sincerest gratitude to Professor Isao Ikeda for his continuous guidance, helpful suggestions, fruitful discussions, and hearty encouragement throughout this work.

I would also like to express my sincerest thanks to Professor Yoshiki Ohshiro for his continuous guidance and hearty encouragement.

It is a great pleasure to express that I am much obliged to Professor Toshikazu Hirao for his invaluable suggestions, stimulating discussion, and hearty encouragement.

I wish to thank Professor Mitsuo Komatsu, Associate Professor Akiya Ogawa, and Associate Professor Shinobu Itoh for their kind suggestions and constant encouragement. Grateful acknowledgements are made to Mr. Satoshi Mikami, Mr. Takuo Watanabe, Mr. Takuji Ishikawa, and Mr. Kouichirou Nishimura for their helpful collaboration in the course of experiments. Further, I also wish to thank all the members of the research group of Professor Isao Ikeda and Professor Yoshiki Ohshiro, and my friends for their hearty supports, helpful advices, and friendship.

I am grateful to Professor Yasushi Kai and Dr. Nobuko Kanehisa for their comments and advice on X-ray crystallographic determination of complexes.

I wish to express my special gratitude to Mrs. Yoko Miyaji and Mrs. Toshiko Muneishi at the Analytical Center, Faculty of Engineering, Osaka University for their valuable advice and assistance.

Finally I would like to acknowledge my parents, brother and sister for their encouragement.